Local Hydroelectric Energy Storage

A feasibility study about a small scale energy storage system combining hydropower, gravity power, spring power and air pressure

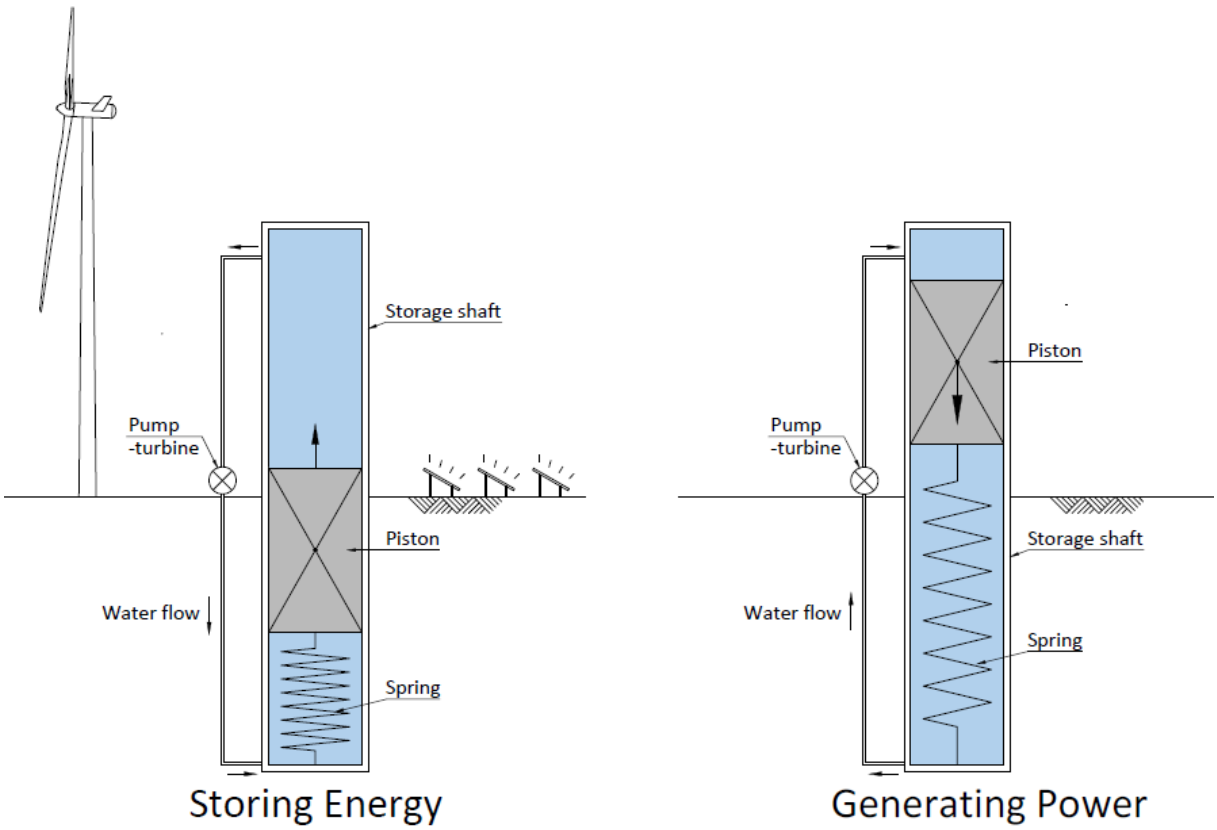

Master Thesis – TU Delft

Marius Hendriks

TU Delft

anteagroup

Local Hydroelectric Energy Storage

A feasibility study about a small scale energy storage system combining hydropower, gravity power, spring power and air pressure

This research has been performed to fulfil the requirements of the Master of Science degree in Civil Engineering as set forth by Delft University of Technology, Faculty of Civil Engineering and Geosciences, Section of Hydraulic Engineering, to be defended publicly on Friday October 14th 2016 at 15.30 AM.

Thesis committee:

Prof. dr. ir. Bas Jonkman	TU Delft, section Hydraulic Engineering
Ir. Kristina Reinders	TU Delft, section Hydraulic Engineering
Ir. Ad van der Toorn	TU Delft, section Hydraulic Engineering
Ir. Peter de Vries	TU Delft, section Structural and Building Engineering
Ir. Jordy Hornschuh	Antea Group
Ir. George Bitter	Antea Group

Written by Marius Hendriks
Student number: 4242602
E-mail: marius.t.hendriks@gmail.com

An electronic version of this thesis is available at http://repository.tudelft.nl/.

Preface

This graduation thesis is written as part of the Master specialisation Hydraulic Structures at the Faculty of Civil Engineering and Geosciences of the Delft University of Technology in the Netherlands. The project was executed at the office of Antea Group in cooperation with the TU Delft.

This thesis contains a feasibility study about a local hydroelectric energy storage system from the first conceptual ideas up to a preliminary design. The focus lies mostly on the technical part of such a system. An estimation of the economic consequences and the possible risks is made to get a feeling about the feasibility of the system.

I would like to thank my graduation committee for their extensive support and feedback during my graduation project. In the first place my mentors Ad van der Toorn and Kristina Reinders from the TU Delft and Jordy Hornschuh from Antea Group for being my first point of contact whenever I needed any help. Peter de Vries and George Bitter for brainstorming about the design with me. And lastly Bas Jonkman for keeping a broad view of my research, but still paying attention for details.

I wish you a pleasant reading.

Marius Hendriks
Delft, October 2016

Table of contents

Acronyms

ALP-CAES	Adiabatic Liquid Piston Compressed Air Energy Storage
CAES	Compressed Air Energy Storage
CAPHES	Compressed Air Pumped Hydro Energy Storage
LHES	Local Hydroelectric Energy Storage
PHS	Pumped Hydro Storage
PSP	Pumped Storage Plant
MCA	Multi Criteria Analysis

List of symbols

Symbol	Quantity	Unit
A	Surface area	[m^2]
c	Corrosion allowance	[mm]
d	Wire thickness	[mm]
D	Diameter	[mm]
D_e	Outside diameter	[mm]
D_i	Inside diameter	[mm]
D_m	Mean diameter	[mm]
e	Wall thickness	[mm]
e_n	Nominal wall thickness	[mm]
e_{min}	Minimum possible fabrication thickness	[mm]
e_a	Analysis thickness	[mm]
E	Energy	[J]
f	Nominal design stress	[MPa]
f	Friction factor	[-]
F_{max}	Maximum reachable force	[N]
g	Gravitational acceleration	[m/s^2]
G	Shear modulus	[N/mm^2]
h_L	Head loss	[m]
H	Water head	[m]
k	Spring constant	[N/mm]
L_n	Neutral length	[mm]
N	Number of active coils	[-]
p	Pressure	[MPa]*
P	Power	[W]
Q	Water discharge	[m^3/s]
Re	Reynolds number	[-]
R_m	Tensile strength	[MPa]
T	Time	[s]
u	Change of length/displacement	[mm]
u_0	Initial displacement	[mm]
u_{max}	Maximum displacement	[mm]
v	Water velocity	[m/s]
V	Volume	[m^3]
z	Joint coefficient	[-]
ρ	Density	[kg/m^3]
σ	Stress	[N/mm^2]
τ_w	Allowable torsional stress	[N/mm^2]
η	Efficiency constant	[-]
ε	Absolute roughness coefficient	[-]
v	Kinematic coefficient of viscosity	[-]

* MPa for calculation purpose only, otherwise the unit may be bar (1 MPa = 10 bar).

Definitions

Energy and power units

Energy can be measured in joules [J] or kilowatt hour [kWh]. Where one joule [J] is equal to the work done by a force of one newton [N] when its point of application moves one meter [m] in the direction of action of the force, so [J] = [N] * [m].

Power can be explained as the rate at which electrical energy is transmitted and can be measured in watts [W] or joule [J] per second [s], so [W] = [J] / [s]. Which also makes: [J] = [W] * [s].

*Example: A vacuum cleaner has a power input of 2 kW. During the week, it is used for 1 hour. The total energy consumed is now 2 kW * 1 hour = 2 kWh.*

Energy units	Power units
1000 Wh = 1 kWh (kilowatt hour) 1000 kWh = 1 MWh (megawatt hours) 1000 MWh = 1 GWh (gigawatt hours) $\mathbf{1\ kWh = 1\ [kW] * 3600\ [s] = 1\left[\frac{kJ}{s}\right] * 3600\ [s]}$ $\mathbf{= 3,6\ MJ = 3,6\ MNm}$	1000 W = 1 kW (kilowatt) 1000 kW = 1 MW (Megawatt) 1000 MW = 1 GW (Gigawatt)

Pressure

Pressure can be measured in Pascal [Pa] where one Pascal [Pa] is defined as one Newton [N] per square meter [m^2], so [Pa] = [N]/[m^2].

Pressure units
1000 Pa = 1 kPa (kilopascal) 1000 kPa = 1 MPa (megapascal) 1000 MPa = 1 GPa (gigapascal)

Pascal is used for calculation purposes only, otherwise the unit may be bar where 1 [MPa] = 10 [bar].

Efficiency

The efficiency of an energy storage system is defined as:

$$\eta = \frac{E_{output}}{E_{input}}$$

in which:

$\eta \quad = efficiency$
$E_{output} = Electricity\ output$
$E_{input} \ = Electricity\ input$

Summary

Renewable energy sources, like wind- and solar power, are expected to generate a greater part of the electricity production in the Netherlands each upcoming year. Besides all the advantages, the energy supply of these renewable energy sources fluctuates heavily as they mainly depend on the amount of wind and sun. Therefore, the electricity market is in need of a solution to mitigate supply fluctuations and deliver sustainable electricity even during dark and low-wind periods.

This research focusses on the feasibility of a Local Hydroelectric Energy Storage (LHES) system which can be applied in the built environment. The use of proven technology from Pumped Hydro Storage plants combined with measures which increase the water pressure result in an energy dense storage solution which would be well suitable for flat countries such as the Netherlands. One way to increase the water pressure is to combine hydro-, gravity- and spring power by equipping a water tower with a heavy piston and attaching a spring. This basic principle, shown in the figure below, is the starting point of this research.

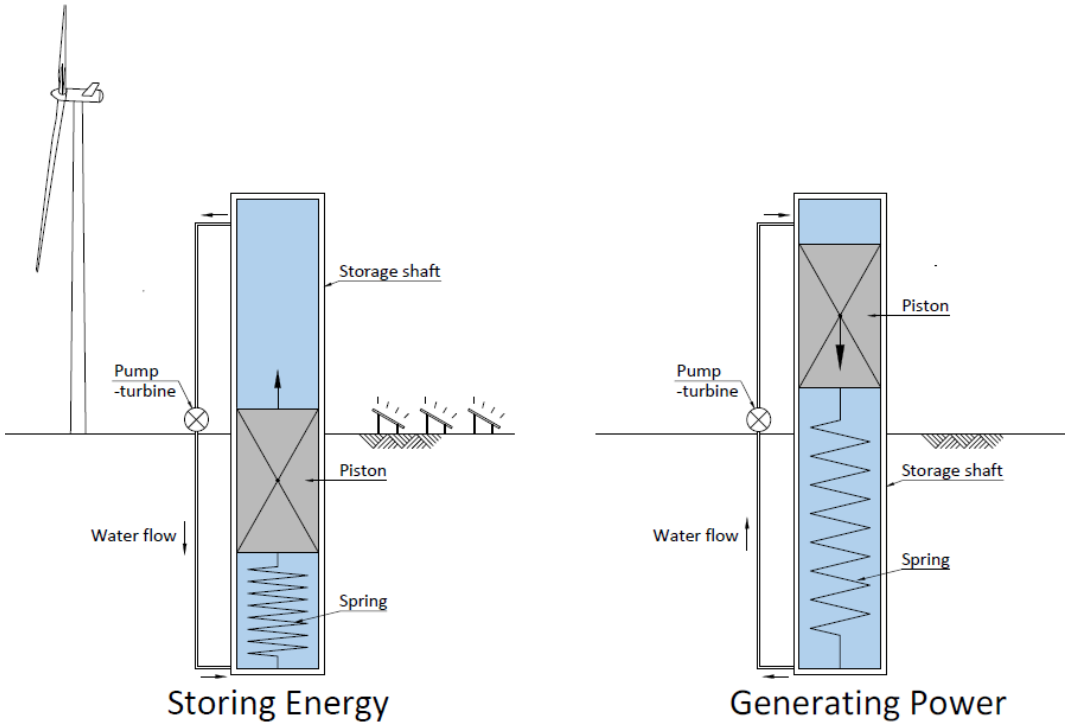

Figure 0-1 A schematic view of a Local Hydroelectric Energy Storage system

In the storing stage, the water in the upper chamber is pumped toward the lower chamber, rising the heavy piston and extending the spring. The potential energy, which is now stored, can be released when the piston moves down. The water in the lower chamber will run through a turbine which generates power, after which it comes back into the upper chamber. This cycle can be repeated over and over. The amount of potential energy which could be stored in such a system will mainly depend on the size and weight of the piston and the strength and displacement of the spring. The mechanical springs, however, store a very small amount of energy, making it hard for any investment to be worthwhile. The piston suffers the same problem for small diameter shafts, making a gravity power storage facility only interesting for larger diameters (>10 [m]).

An alternative storage solution may be the use of an air spring. Compressed air can be stored in a pressure vessel, which is connected to a water pump/turbine unit and a reservoir. The compressed air functions like a cushion, while the incompressible water is used as moving material to store energy or generate power by moving in and out of the pressure vessel. This so called Compressed Air Pumped Hydro Energy Storage (CAPHES) principle is shown in the figure below.

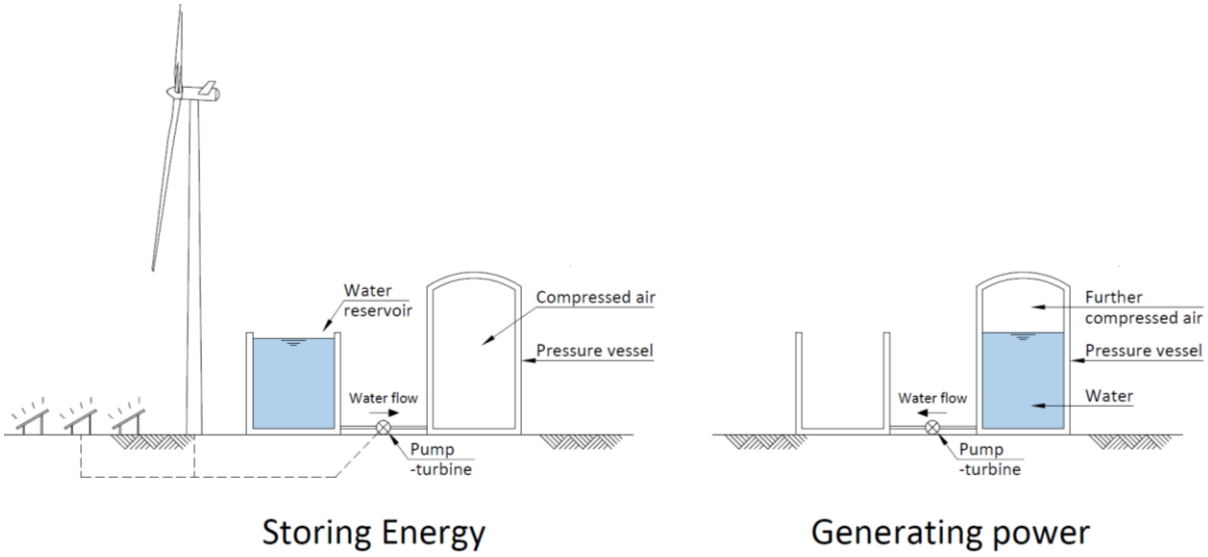

Figure 0-2 Schematic view of a Compressed Air Pumped Hydro Energy Storage system

In the pressure vessel, air can be compressed up to a certain pressure. When water is pumped into the pressure vessel, the volume of the air decreases. This makes the air compressed even further and 'wants' to press the water back out. That way, the CAPHES system stores a large amount of potential energy in a small amount of space, making it perfectly suitable to function as a local storage system. In order to apply the system in the built environment, an application as foundation of a street of eight houses is chosen. A part of the hollow steel piles will then function as a water reservoir while the other part will function as storage shafts, as shown in Figure 0-3.

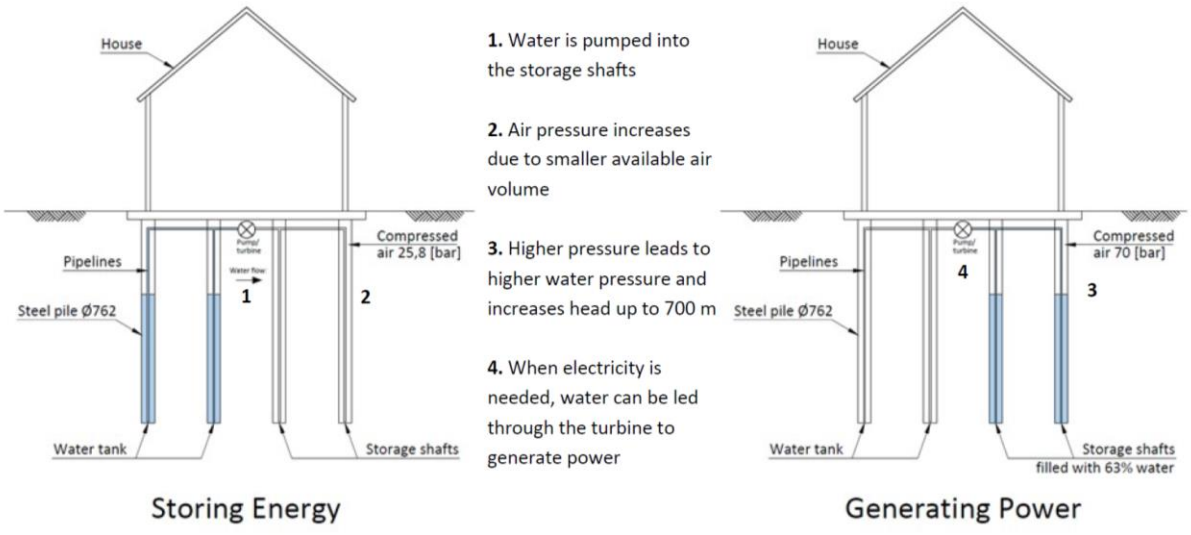

Figure 0-3 A Local Hydroelectric Energy Storage system applied in the hollow pile foundation of a house while storing energy (left) and while generating power (right)

The first advantage of this application is that no additional land is needed. Secondly, money can be saved upon the construction costs, as no further foundation is needed. However, the potential risks which come with large pressure equipment are now implemented in an urban area, which is a drawback of this application. The results of the Local Hydroelectric Energy Storage system are shown in Table 0-1:

Table 0-1 Main characteristics of the LHES system

Characteristics	Value	[unit]
Amount of water stored	82,7	[m^3]
Maximum pump capacity	5	[l/s]
Maximum turbine flow rate	5	[l/s]
Storage capacity	93	[kWh]
Maximum power output	29,8 – 10,9	[kW]
Minimum power output*	9,9 – 3,6	[kW]
Running time	4,5 – 13,5	[hours]
Roundtrip efficiency	76	%

* Approximately ⅓ of the maximum power output can be delivered by the Pelton turbine with the same efficiency.

With estimated storage costs per [MWh] between € 384 and € 768, the LHES system can be considered economically feasible and even competitive with respect to other storage systems such as batteries or thermal storage. Several other points of the system are still unknown and need further research. However, the preliminary research done in this thesis shows that the concept has a lot of potential to become a widely used storage system, mitigate supply fluctuations and deliver sustainable electricity even during dark and low-wind periods.

Figure 0-4 Impression of a street of houses equipped with a LHES system

1 Introduction

1.1 Background

The need for clean energy continues to grow. Solar panels and wind turbines are increasingly used in order to meet this need. Besides all the advantages, these renewable energy sources have a large variability of energy supply. The supply lowers at times when the sun does not shine or when the wind intensity drops. However, the demand of energy does not drop at the same rhythm. Large fluctuations and differences between supply and demand cause inefficiencies and cost money. The market is in need of an efficient, sustainable solution that can absorb these fluctuations and differences.

One way to absorb these fluctuations is to use an energy storage system. With such a system, the energy produced in peak producing hours can be temporary stored and then used when the demand goes up. The most common way to do this, is by using a Pumped Hydro Storage (PHS) system. However, such a system usually needs large height differences and especially in flat countries, this is not always possible. Furthermore, these systems are commonly engineered as large or even mega scale projects, which due to lack of finance, environmental impact, or other reasons do not seem to come off the ground.

A potential alternative may be a smaller scale energy storage system which combines hydropower with gravity power, spring power and compressed air. Such a system can be made as a standalone energy tower, but also integrated into a foundation of a house or as a core of an apartment building for instance. Weather such a system may be technologically and economically feasible needs yet to be investigated.

1.2 Goal

The goal of this research is to investigate the technological and economic feasibility of such a local, small scale energy storage system which combines hydropower, gravity power, spring power and compressed air.

1.3 Research questions

The aim of this research is to answer the following main question:

- *What is technologically and economically the most feasible way to apply a local energy storage system by combining hydropower, gravity power, spring power and compressed air?*

The main research question is supported by the following sub questions:

- *What is the current state of local, national and international hydro power energy storage, gravity power storage, spring energy storage and compressed air energy storage?*
- *How can these four techniques of hydro-, gravity-, spring- and compressed air power be combined?*
- *How can such a system be technically designed?*
- *Where can such a system be locally applied or implemented?*
- *What challenges appear when combining such a local storage system with normal structural elements?*
- *Will the use of the most promising local energy storage system be economically feasible?*

1.4 Approach

In order to find the current state of energy storage systems, a literature study is done. A quick sketch design of a hydropower, gravity power, spring and compressed air energy storage system is made, after which these four systems are combined to a Local Hydroelectric Energy Storage system. Dimensions are estimated and a rough idea about the materials used is represented. With this rough sketch design, a first estimate of the costs and storage capacity is made after which an application could be found and the feasibility could be estimated.

Possible optimizations for the rough sketch design are found and then applied to the system. Multiple variants are presented and the most promising one is chosen by using a multi criteria analysis. A preliminary design of this chosen system is then made and the total corresponding storage capacity is found. The construction and operating costs as well as the benefits are calculated and by using a simplified cost-benefit analysis, the economic feasibility is checked.

1.5 Scope boundaries

One way to apply hydro-, gravity- and spring power into an energy storage system is by equipping a water tower with a heavy piston and attaching a spring. This basic principle is the starting point of this research (Figure 1-1). The dashed line around the water tower shows the boundaries of the scope of this research. A quick look, but no comprehensive analysis, about the pump/turbine unit, its efficiency and the energy supply and demand in the Netherlands is taken. With this, the economic feasibility of the system could be estimated.

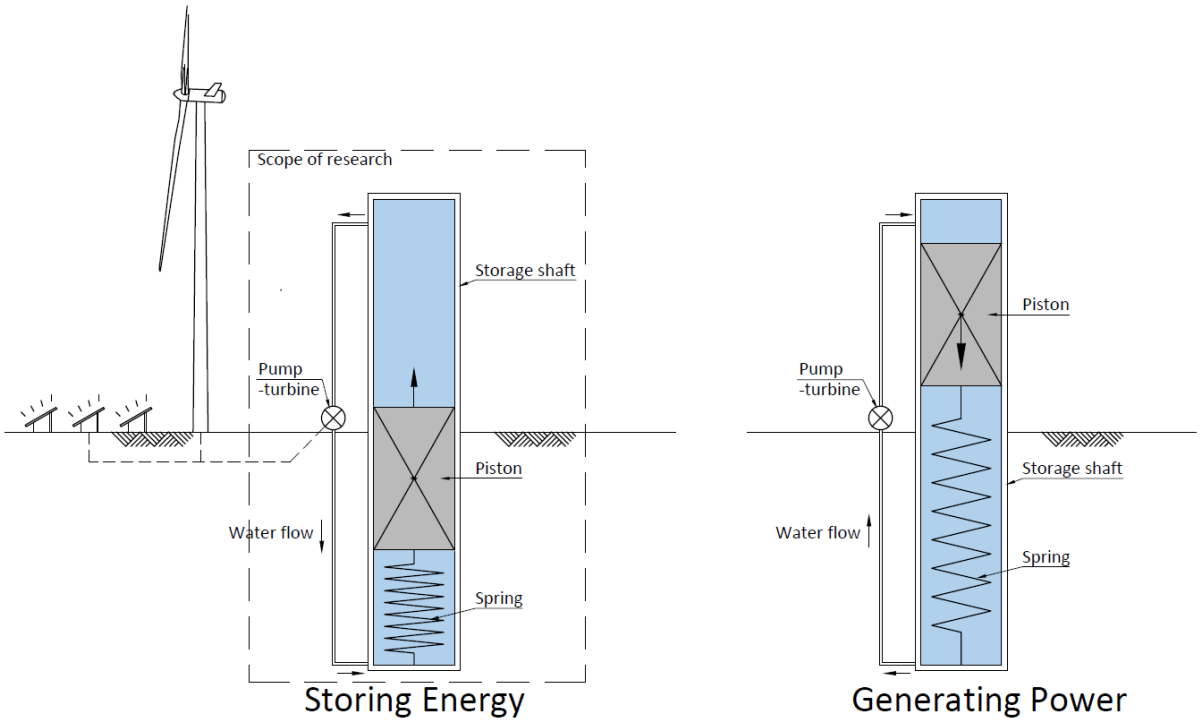

Figure 1-1 A schematic view of a LHES system with the scope boundaries of this research

1.6 Structure of the report

The report elaborates about the energy market, known energy storage technologies and previous studies in Chapter 2. In Chapter 3, a principle analysis of Hydropower-, Gravity power-, Spring power- and Compressed air energy storage is made and the most promising method is chosen. Multiple variants and possible applications for a Local Hydroelectric Energy Storage (LHES) system are summed up in Chapter 4. The best system is elaborated to a preliminary design in Chapter 5 by making use of a Multi Criteria Analysis. This preliminary design focusses on the main parts of the LHES system and gives an idea about how such a system could look like in reality. The risks which come with the system are then mapped after which the economic feasibility is checked.

2 Energy Storage

The previous chapter introduced the problem and the need for a solution that can absorb fluctuations in energy supply and demand. In this chapter, the energy market is explained further. In particular the electricity market in the Netherlands, where this research focuses on. The current way electricity is produced and demanded is explained in order to understand the way energy storage can improve the stability of the grid. Furthermore, as a thought experiment, a situation where all electricity production is done by solar panels is sketched, to demonstrate the potential of energy storage. Subsequently, previous researches about Pumped Hydro Storage (PHS) technologies are shown and the position of this research is made clear.

2.1 The energy market

In 2009, European countries have agreed to commit themselves to renewable energy targets for the year 2020. The target for the Netherlands is set at 14 percent, where the target for the entire EU is set at an average of 20 percent renewable energy in the year 2020. The average of the European countries only have 4 percentage points to go to meet their target. The Netherlands is, with 8,5 percentage points to go at the end of 2014, however still lacking behind (CBS, 2016). In the beginning of 2014 a policy guideline for climate and energy for the period from 2020 to 2030 was released by the European Commission, foreseeing even further sustainability and reduction of CO^2 emission (European Commission, 2014). In order for the Netherlands to meet their targets, a large increase in production of renewable energy is needed.

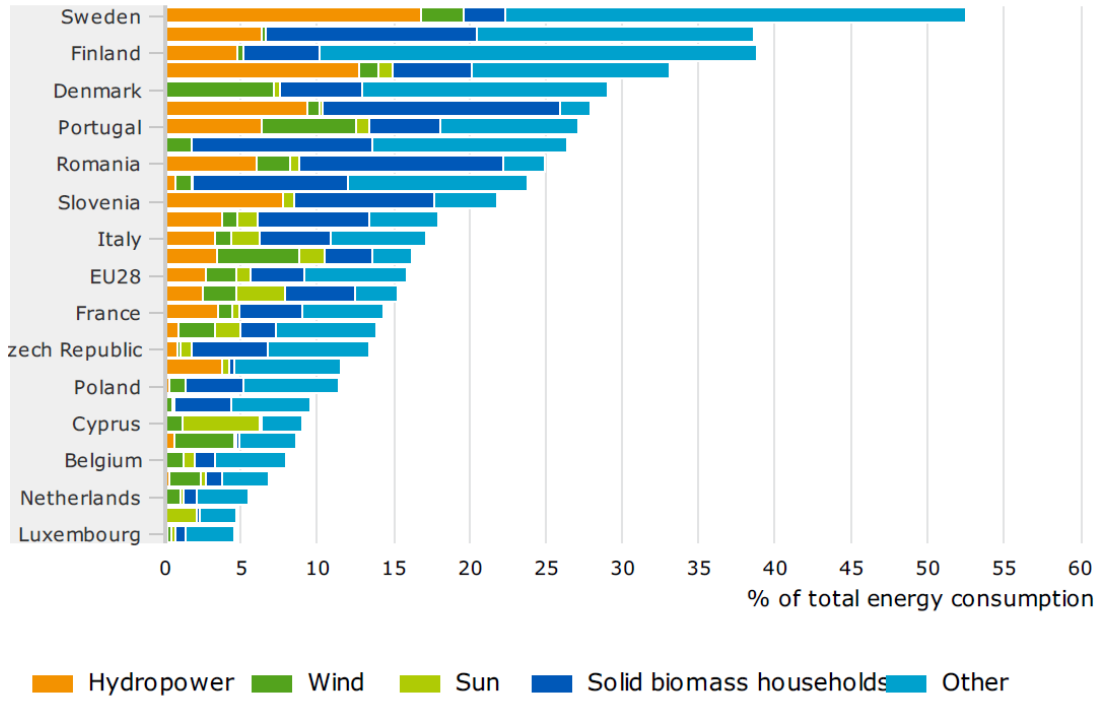

Figure 2-1 Renewable energy consumption of European countries in 2014 (CBS, 2016)

The energy market can roughly be subdivided into three separate markets, namely the Transport- (on fuel), the electricity- and the heating & cooling market. These markets are changing rapidly. Gas prices

are high while electricity prices have dropped. As a consequence, the decrease in natural gas consumption in households in the Netherlands has continued from about 1900 [m^3] in 1995 to 1340 [m^3] in 2012 (ECN, 2014). The market which will be considered in this research is the electricity market. This market reacts with fluctuating prices, which partly come forward from the fluctuating supply of wind turbines and solar panels. But since these production methods are unpredictable, the capacity of controllable power plants remains necessary to absorb fluctuations. In the future, these fluctuations could also be absorbed by energy storage systems. In order to design a good working storage system, one must first understand how the electricity market works.

2.2 The electricity market in the Netherlands

The electricity market in the Netherlands has connections with Belgium, Germany, Norway and the United Kingdom. In the annually published 'Energy Trends Netherlands' the amount of import and export of electricity is shown, which has a large variety during the years. One trend that is clearly visible is that on windy or sunny days, a large amount of electricity is imported from Germany (ECN, 2014). This is caused by the heavily subsided renewable electricity production, which Germany itself does not totally utilize on those days. This 'left over' electricity is then offered to bordering countries for a very low rate, which make that the Netherlands is still importing cheaper German electricity while the Dutch power companies cannot fully utilize their own capacity. Another trend is the growing wind and solar energy production. Table 2-1 shows the absolute and relative amounts of electricity production by energy source in the Netherlands for the years 2013 and 2014. An interesting development is the sudden drop in the total renewable energy production. This is mainly caused by the lower amount of biomass that is used in 2014.

Table 2-1 Electricity production by energy source in the Netherlands (CBS, 2016)

Subjects	Gross production electricity and heat			
	Electricity			
	Electricity (MWh)		Electricity (%)	
Central/decentral production	Total central/decentral production		Total central/decentral production	
Periods	2013	2014	2013	2014
Energy commodities	*MWh*		%	
Total energy commodities	100 875 336	103 417 851	100.0	100.0
Total fossil fuels	82 699 007	84 292 092	82.0	81.5
Natural gas	54 028 719	50 991 982	53.6	49.3
Hard coal	24 560 150	28 760 067	24.3	27.8
Fuel oil	89 993	342 284	0.1	0.3
Other fossil fuels	4 020 145	4 197 758	4.0	4.1
Total renewable energy	12 211 360	11 707 203	12.1	11.3
Solar energy	515 900	784 762	0.5	0.8
Wind energy	5 627 148	5 797 334	5.6	5.6
Hydro power	114 312	111 925	0.1	0.1
Biomass	5 954 000	5 013 182	5.9	4.8
Nuclear energy	2 890 859	4 091 306	2.9	4.0
Other energy commodities	3 074 110	3 327 250	3.0	3.2

The production of electricity in the Netherlands is mainly happening in a number of larger production facilities. The locations of these facilities are shown in Figure 2-2. This map shows the power plants and wind farms with more than 60 MW power output.

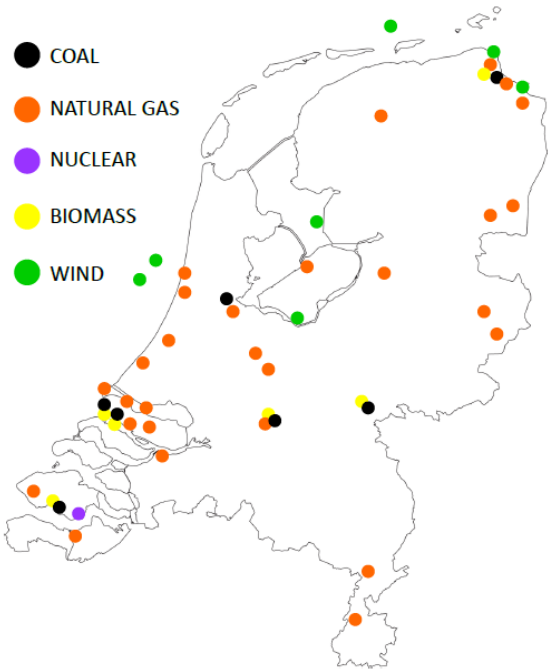

Figure 2-2 Map of power plants in the Netherlands with more than 60 MW capacity (ECN, 2014)

The electricity demand in the Netherlands is for a large part determined by the behaviour of people. During the night, when most people are asleep, up to half the amount of power is demanded compared to the day. The power demand data are gathered by the European Network of Transmission System Operators for Electricity (ENTSO-E, 2015), and shown for a particular Wednesday in all four seasons of 2015 in Figure 2-3.

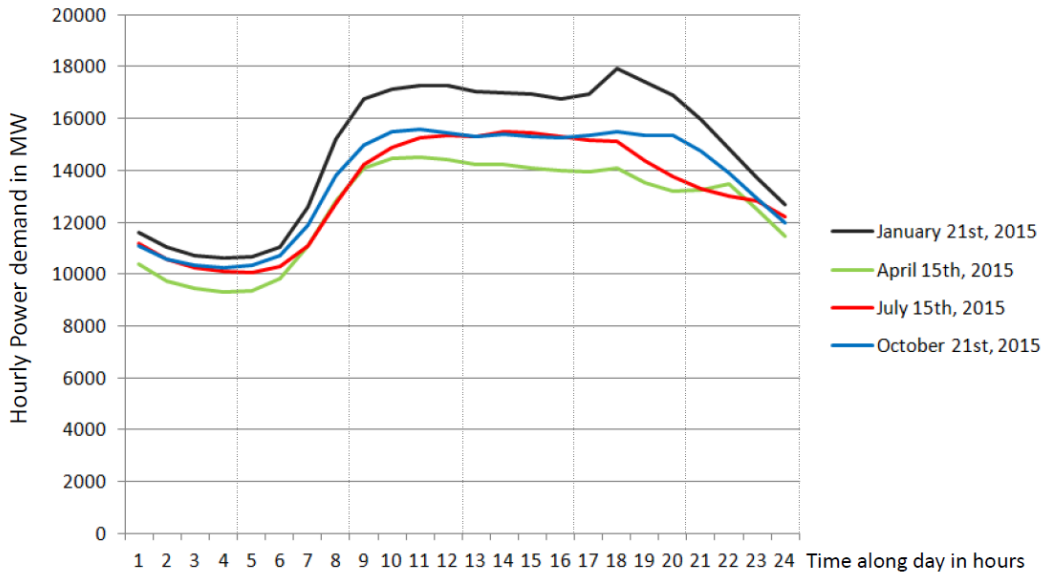

Figure 2-3 Hourly electricity demand curve for the Netherlands on a particular Wednesday in all four seasons of 2015 (ENTSO-E, 2015)

These data clearly show a larger energy demand during the winter. This can be explained by the lower temperature and shorter days, which cause people to use more (electrical) heating and lighting. Furthermore, we see a sharp peak between 17.30 and 19.30 due to the fact that people come home after work and turn on their applications. Throughout the week, this behaviour continues, as can be seen in Figure 2-4. During the weekend however, the electricity demand lowers. This can be explained do to the fact that most people do not work during the weekend and offices and factories are not in operation. The variation throughout the seasons mainly depends on the temperature and the length of the day, as can be seen in Figure 2-5.

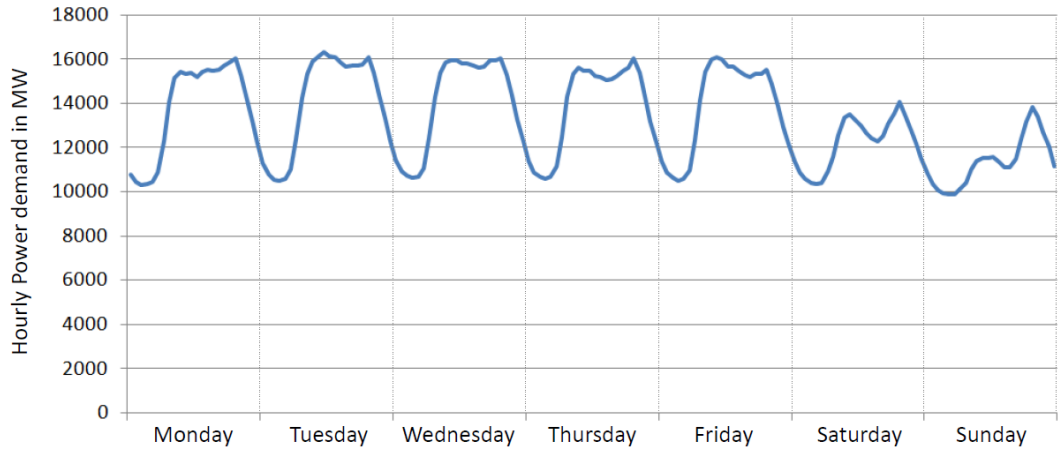

Figure 2-4 Hourly electricity demand curve for the Netherlands in Week 10, 2015 (ENTSO-E, 2015)

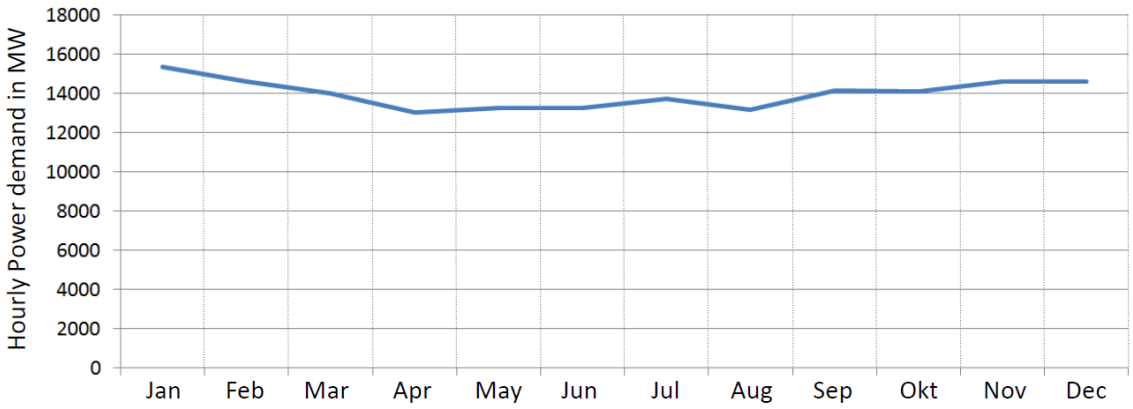

Figure 2-5 Hourly electricity demand curve for the Netherlands for the 3rd Wednesday of every month in 2015 (ENTSO-E, 2015)

A large disadvantage of renewable energy sources, like solar panels or wind turbines, is that their production is unpredictable and does not follow the same curve as the demand of electricity. This is one of the reasons electricity companies still use a lot of reliable power plants, which work on fossil fuels like coals and natural gas.

But suppose all the electricity in the Netherlands would be supplied by solar panels. The yield of a solar panel depends mostly on the amount of light which can be absorbed. This can be direct sunlight, but also indirect as can be expected on a cloudy day. For the Netherlands, an average solar panel could provide roughly 130 [kWh/m^2] per year (Nuon, 2016). Taking this into account, the total amount of electricity demand of 103,4 *10^6 [MWh] in 2014 (Table 2-1) could theoretically be supplied by 800*10^6 [m2] of solar panels. To give an idea of dimensions, this area is sketched in the form of a blue square of approximately 28 by 28 [km] in Figure 2-6.

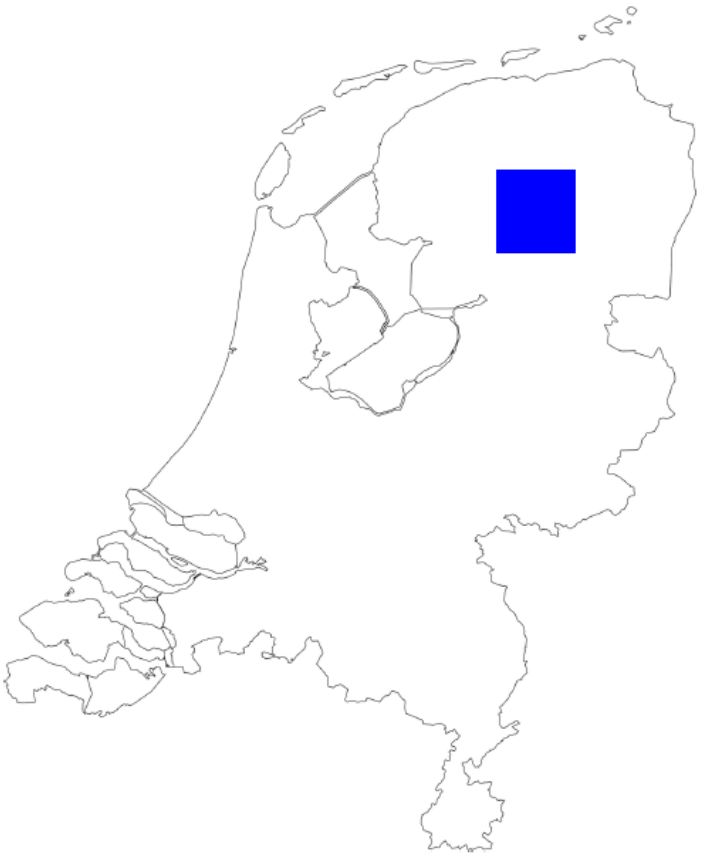

Figure 2-6 Surface area used by solar panels in case of full electricity coverage (based on Table 2-1)

This area may look rather large. But one should take into account that most of the solar panels could be installed on the roofs of houses, apartments and other utility buildings and will therefore not take up any additional land. However, the solar panels will produce electricity only during the day. Taking the estimated supply of the solar panels on a sunny day in March and projecting it to the average of the hourly power demand during a single day (Figure 2-3), we find the following figure:

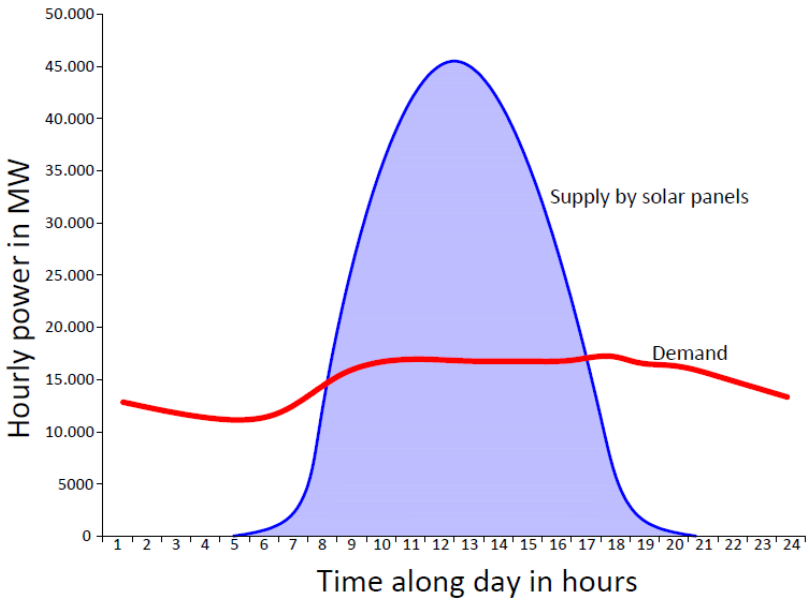

Figure 2-7 Estimated hourly electricity supply by $800*10^6$ [m2] solar panels on a sunny day in March with respect to the average hourly electricity demand curve in the Netherlands (based on Figure 2-3)

Where the blue line represents the theoretical power supply by the solar panels and the red line represents the average power demand during a single day. Figure 2-7 clearly shows the potential value of energy storage. If the leftover power supply could be stored during the day, it could be used to meet the energy demand during the night. In this figure, the seasonal difference in power supply and demand has not been taken into account. Additional seasonal storage could be used to store extra energy during the summer, which could be used during winter when the demand is higher and the supply is lower. Further elaboration about seasonal energy storage is considered outside the scope of this research.

Now that the potential benefits of energy storage are made clear, we have a closer look at the different storage technologies which could be used.

2.3 Pumped Hydro Storage technologies

Pumped Hydroelectric Storage, in short PHS, facilities store energy in the form of water. Typically, water is pumped from a lower reservoir into an upper reservoir during periods of low energy demand or when the energy else way would be lost. During periods of high electricity demand, power is generated by releasing the stored water back to the lower reservoir by letting it run through turbines. A large height difference or head between the two reservoirs is preferred as the storage capacity will largely depend the water pressure when generating power. Figure 2-8 shows a typical PHS facility with its aspects. Besides the upper and lower reservoir, the facility has a discharge pipe or penstock which lead the water to the turbine, where the power is produced using the generator. A transformer then transforms the power and delivers it to the grid.

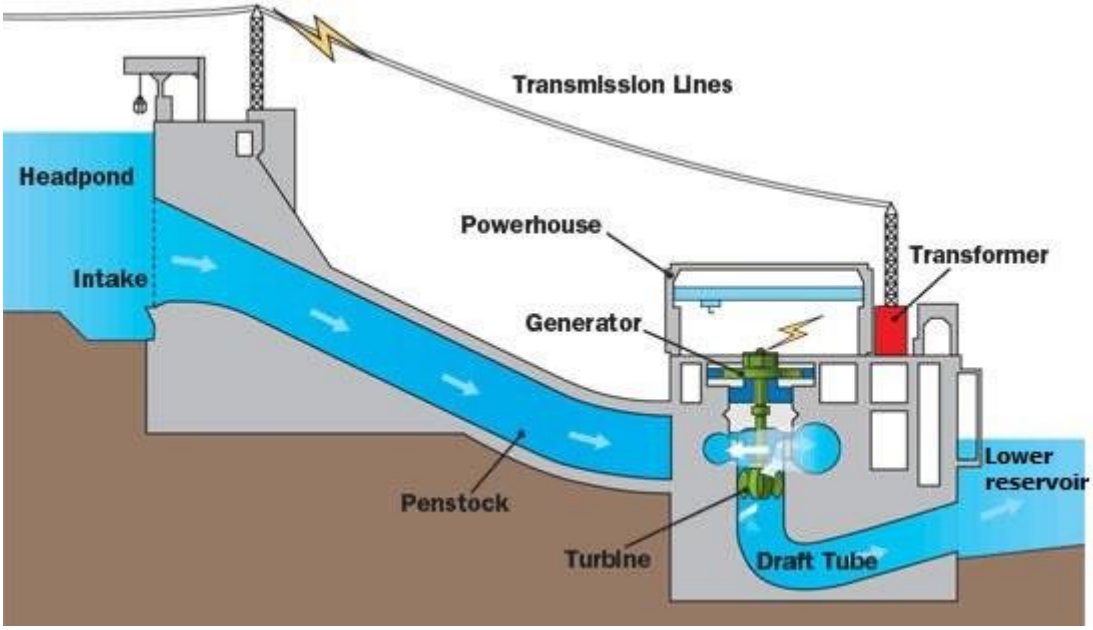

Figure 2-8 A typical Pumped Hydro Storage facility (Waterturbines, 2016)

For flat countries like the Netherlands, creating a large height difference is hard or otherwise very costly. But fortunately, there are other ways to increase the water pressure in order to increase the storage capacity. An overview of previous studies about Pumped Hydro Storage technologies in the Netherlands can be found in the figure below. An elaborated overview of these different energy storage technologies is included in Appendix A.

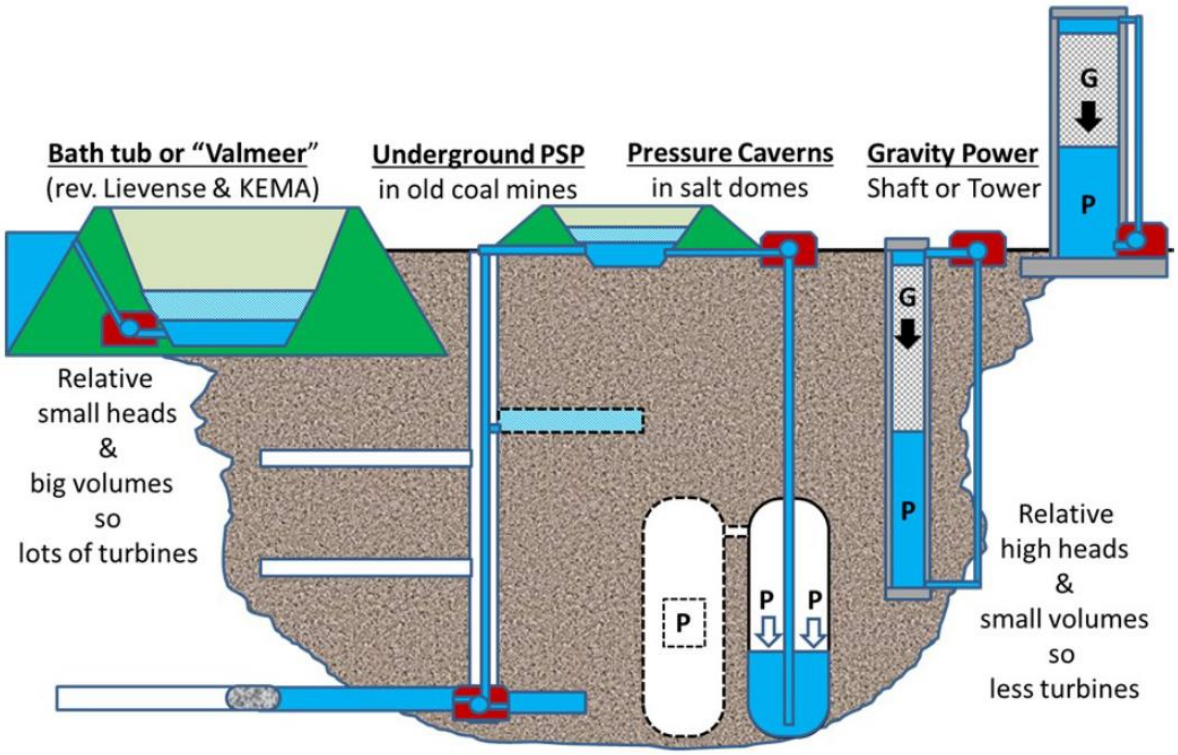

Figure 2-9 Overview of the previous studies about Pumped Hydro Storage Technologies in the Netherlands (van der Toorn)

Figure 2-8 includes the following researches:

- **Energy Island**; describes a ring of dikes built in the middle of the North Sea. The dikes create a reservoir which can be used to store energy by letting a large volume of water run into it (Boer, 2007). **Properties**: 30 [GWh] installed capacity, 2500 [MW] power output.
- **Pumped hydro storage the Slufter**; describes the transformation of the Slufter from a silt depot into a pumped hydro-electricity storage system where large amounts of water can be stored (Kibrit, 2013). **Properties**: 2,16 [GWh] installed capacity, 350 [MW] power output.
- **Underground pumped storage plant in old coal mines**; describes an open space in the form of an abandoned coal mine or drilled pipes at a very large depth (usually more than 1000 [m]), which is connected to the surface. The open space underground creates a lower reservoir which can be used to store energy by letting water run into it (O-PAC, 2009). **Properties**: 8 [GWh] installed capacity, 1400 [MW] power output.
- **Pressure Caverns in salt domes**; uses the underground space left by salt mining to store energy. The salt water is pushed out of the domes, which are put under pressure with air to prevent the dome from collapsing, into a shaft all the way to the surface where a pump turbine is placed (Bergum, 2014). **Properties**: 156 [MWh] installed capacity, 65 [MW] power output.
- **Gravity Power**; describes a storage tank which can store energy by moving a heavy piston up with a pressurized fluid. When the piston falls down under its gravity power, the fluid can be used to power a turbine. The shaft can be executed underground (Tarigheh, 2014) or as a standalone tower (Imambaks, 2013). **Properties**: 80 [MWh] installed capacity, power output unknown.

2.3.1 The position of this research

The different studies shown above are all focusing on a large scale, centralized storage facility. These facilities often require a rather large investment which may be one of the main reasons why they don't seem to come off the ground. Furthermore, renewable energy sources are producing more and more energy on a local scale. Solar panels build on the roof of a house are a perfect example of this for instance. Creating a centralized storage facility for locally produced energy requires a lot of electricity transport back and forward which may cause even more inefficiencies. This research is therefore focusing on the technical and economic feasibility of a small scale, local energy storage system with a capacity in the range of 6 to 60 [kWh] and a power output in the range of 3 to 30 [kW].

Why local?

Applying local energy storage systems on a wide range will have a great impact on the Dutch power grid. A couple of main issues where local energy storage may be the solution are listed below:

- Transporting electricity causes losses. When the electricity which is produced by solar panels of a private home owner is delivered back to the grid, this potential transport loss could be as much as doubled. When storing the produced electricity on a local scale, the transport and thereby the transport losses are brought to a minimum.

- When the number of solar panels in the Netherlands increases further, problems in the electricity distribution networks can be expected. These have been dimensioned as such that they are sufficient to meet the maximum demand for electricity (which, in general, occurs on winter days). With a further expansion of solar panels, the supply peak of electricity on a local level (which, in general occurs on sunny summer days), will become larger than the peak demand and will thus become determinative for dimensioning the grid network. Study by (J. Lemmens, 2014) shows that for a total solar panel capacity in the Netherlands of 4 [GWp], which may be realized by 2020, measures have to be taken in order not to lose a lot of solar powered energy. These measures can be taken by enlarging the power grid, or installing local energy storage.

- Private home owners with solar panels on their roof can benefit from supplying power to the grid when the sun shines and the power produced is not used up by themselves. When the sun does not shine but power is needed, electricity from the grid is used. At the end of the year the electricity produced by the solar panels may be extracted from the amount of electricity which was required from the grid, leaving a bill for the private owner with only the net demanded electricity cost. This 'balancing of electricity' legislation will remain functioning until 2020 (Schoenmakers, 2015) but for the period after it, it remains unclear if this will still be possible. Extracting the self-powered electricity from the demanded power from the grid is very advantageous for private solar panel owners. It stimulates private investors to buy solar panels since it reduces the payback time drastically. If the legislation does not hold, applying a local energy storage system may be lucrative instead.

3 Principle analysis of Hydropower, Gravity power, Spring power and Compressed air energy storage

Now that the benefits of local energy storage are known, the techniques which could be used to make a local hydroelectric energy storage are explained. First, the principle of energy density of water is explained after which the principle analysis of a hydropower, gravity power, spring power and compressed air energy storage system are elaborated. In order to compare the different systems with each other and to see where the optimal energy storage dimensions lie, friction losses or other losses are not taken into account yet. In other words, the efficiency is assumed to be 100%. We have to keep in mind however that there are always efficiency losses in reality.

3.1 Energy density of water

The water pressure below a water column roughly increases with 10 [kPa] when an extra meter of water is added. One way to increase the pressure and thereby the energy density of water is to add a heavy weight on top of the water, as described in the Gravity Power studies from (Tarigheh, 2014) and (Imambaks, 2013). The pressure 'p' can be calculated using $p = \rho*g*h$ in which the density of water ρ_{water} = 1000 [kg/m^3], for the piston ρ_{piston} = 4000 [kg/m^3] is assumed, the gravitational acceleration g = 9,81 [m/s^2] and the height is expressed in 'h'. The weight of a 7,5 [m] piston adds an additional pressure that is equal to a water column of 30 [m] as is shown in the figure below. In other words, the shaft that holds the water column without the piston needs to be 30 – 7,5 = 22,5 [m] higher to store the same amount of potential energy.

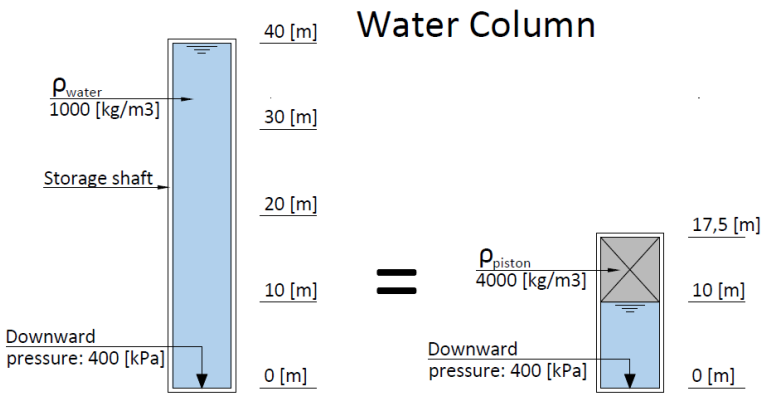

Figure 3-1 Downward pressure in a 40 [m] water column compared with a column equipped with a piston (round of pressures are used)

To increase the water pressure and thus the energy density even further, a spring could be attached to the heavy weighing piston. In the next figure, a spring with a tension force equal to 1 [m] piston weight is assumed. Another way to increase the water pressure is to add compressed air on top of the water column as can be seen in the following figure:

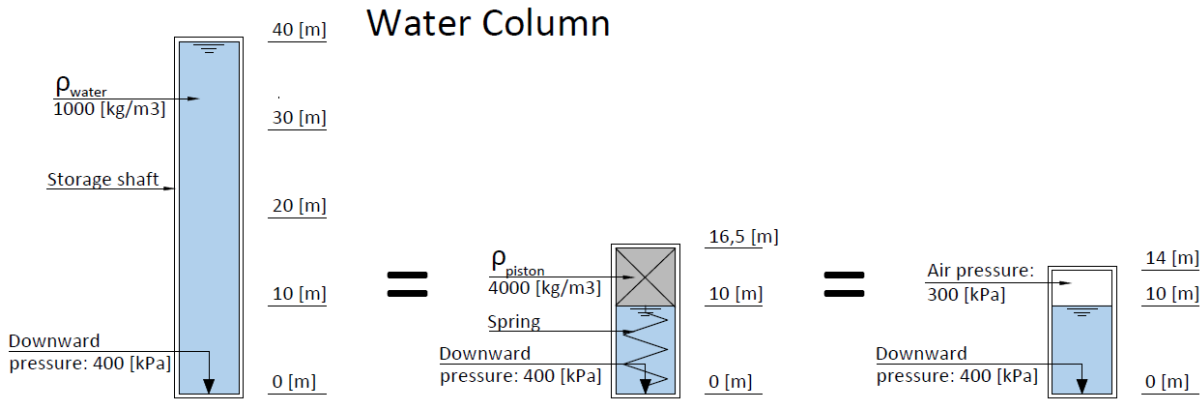

Figure 3-2 Downward pressure in a 40 [m] water column, a column with piston and spring and a column with compressed air added.

These different techniques that increase the energy density of the water could be used when designing an energy storage system. A small system with a relatively large storage capacity has advantages compared to a larger system with the same storage capacity, as a smaller system might be cheaper and easier to integrate in a building.

3.2 Hydropower

When water is elevated to a certain height, potential energy is stored. When this water is running down with a discharge 'Q' [m^3/s] over a head difference 'H', the energy could be gained again. Using (Duivendijk, 2007) we find that the resulting (gross) energy will then be:

$$E = \rho * g * Q * H * T$$

Where:

E *is the total amount of energy that can be stored* $[J]$
ρ *is the density of water* $[kg/m^3]$
g *is the gravitational acceleration* $[m/s^2]$
Q *is the water discharge* $[m^3/s]$
H *is the water head* $[m]$
T *is the time the power can be delivered* $[s]$

The density 'ρ' and the gravitational acceleration 'g' are constants in this formula. The water discharge 'Q' and the running time of the system 'T' have a relationship since they both depend on the Volume of the upper basin V [m^3]: V = Q * T. With this relation, we can simplify the energy equation to E = ρ*g*V*H. Where increasing either of the variables 'V' and 'H' would have the same linear increasing effect with respect to the energy generated. The relationship curves between E and H, and E and V are shown in Figure 3-3:

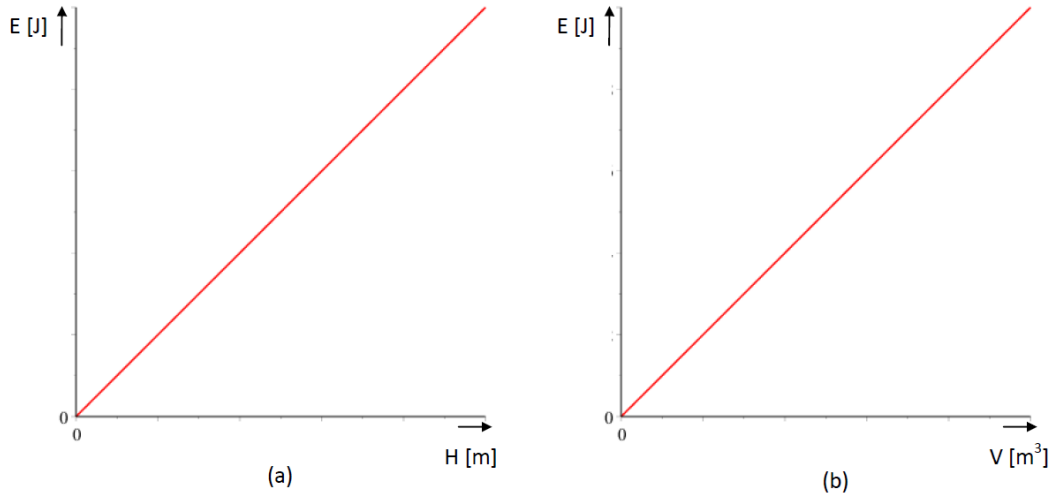

Figure 3-3 The relationship curves between the amount of energy storage 'E' and the water head 'H' (left) and 'E' and the volume of the upper basin 'V' (right)

Example calculation

Assume a water tower (Figure 3-4) with an upper basin volume 'V' of 300 [m^3] (Ø=8[m], h_{basin}=6[m]) and a water head 'H' of 20 [m]. The water density ρ is 1000 [kg/m^3] and the gravitational acceleration g is 9,81 [m/s^2]. The water volume which is holding up in the shaft of the water tower is neglected. The resulting (gross) energy will then be: E = 1000 * 9,81 * 300 * 20 = 58,86 [MJ]. Assuming the power will be delivered for 4 hours, we find P = $(58{,}86*10^6)/(4*60*60)$ = 4,09 [kW]. This power can be delivered for 4 hours, which makes the capacity of one storage cycle 16,35 [kWh].

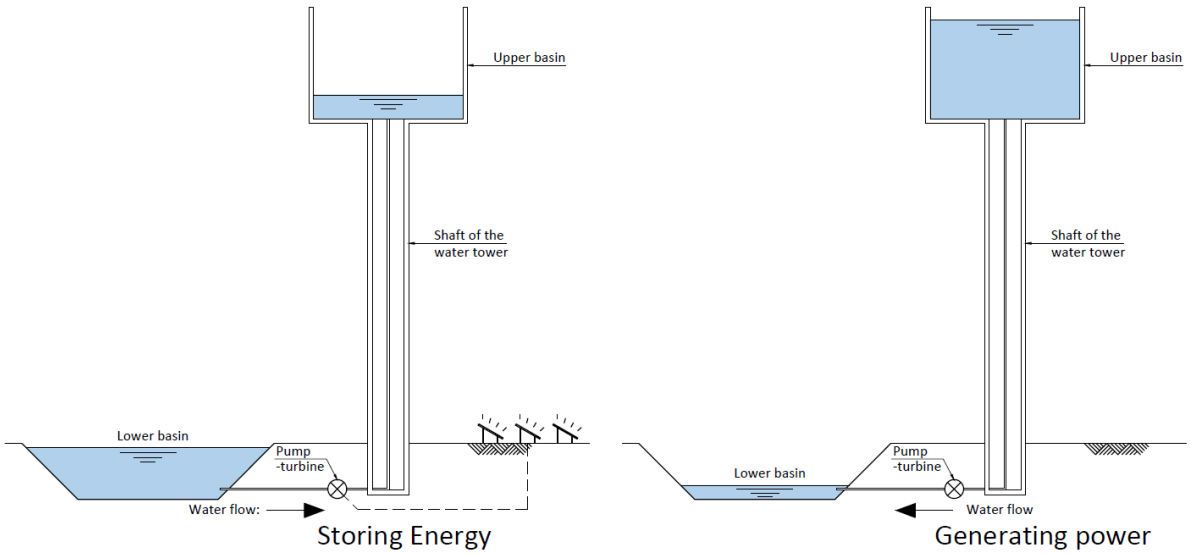

Figure 3-4 Schematic view of a Hydropower system

Conclusions

Hydropower storage systems are proven technology and therefore relatively easy to apply. It does, however, need a large volume or height difference in order for the system to work.

3.3 Gravity power

Instead of increasing the water height of a storage system, one could also increase the water pressure by adding a weight on top. This is called gravity power. In a gravity power storage system, a heavy weight rests on a column of water. This increases the pressure of which the water is pressed through a turbine and thereby increases the storage capacity. A design choice may be to make it a closed system. This can be done by looping the pressed water back up in the water tower. Although this will decrease the storage capacity, less space is needed for such a closed system, making it financially attractive in some cases. A research about gravity power done by (Imambaks, 2013) shows that we can use the following energy equation for a cylindrical gravity power storage system:

$$E = (\rho_{piston} - \rho_{water}) * \frac{1}{4}\pi D^2 * h * g * z$$

Where:

E *is the total amount of energy that can be stored* $[J]$
D *is the diameter of the piston* $[m]$
h *is the height of the piston* $[m]$
g *is the gravitational acceleration* $[m/s^2]$
z *is the potential elevation height of the piston* $[m]$
ρ_{piston} *is the density of the piston* $[kg/m^3]$
ρ_{water} *is the density of water* $[kg/m^3]$

Figure 3-5 Cylindrical piston on water (Tarigheh, 2014)

For this system, the height of the storage shaft 'H' is equal to the height of the piston plus the potential elevation height of the piston. Using H = h + z, we can rewrite above formula to:

$$\frac{E}{(\rho_{piston} - \rho_{water}) * \frac{1}{4}\pi D^2 * g} = h * (H - h)$$

For a given piston in a storage shaft, ρ_{piston}, ρ_{water} and g are constants and the diameter is known. To optimize the piston height compared to the total height of the storage shaft, we derive above equation to 'h', which gives:

$$\frac{d\left(\frac{E}{(\rho_{piston} - \rho_{water}) * \frac{1}{4}\pi D^2 * g}\right)}{dh} = \frac{d(h * H - h^2)}{dh}$$

And results in:

$$H - 2h = 0 \rightarrow H = 2h$$

This means that the piston height should be designed as half the height of the storage shaft in order to store the largest amount of energy. So when $h = z = H/2$, the optimal energy equation can be written as: $E = (\rho_{piston} - \rho_{water}) * \frac{1}{16}\pi D^2 * g * H^2$. This formula clearly shows that increasing the diameter 'D' has the same effect as increasing the height 'H' of the shaft in respect to the energy storage capacity.

The relationship curve between E and h is shown in Figure 3-6:

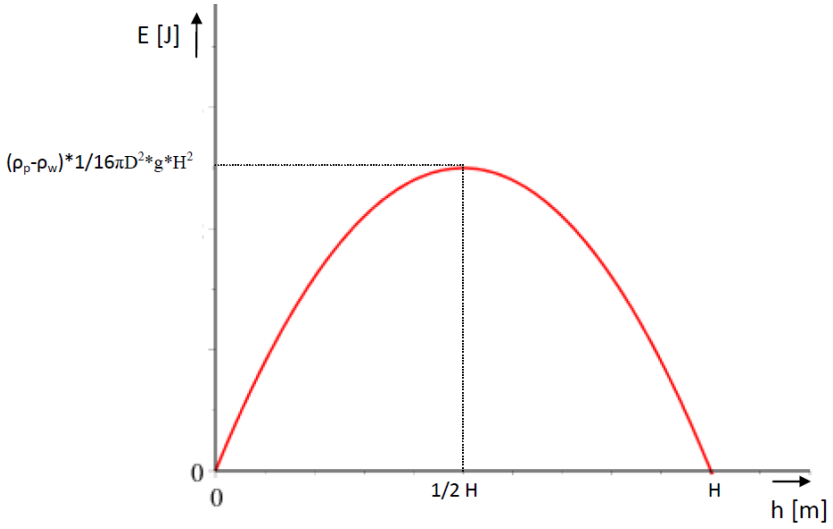

Figure 3-6 The relationship curve between the amount of energy storage 'E' and the height of the piston 'h'

Example calculation

Assume a storage shaft (Figure 3-7) with a diameter of 3 [m], a height of 20 [m] and a piston made out of composite steel and heavy concrete with an average piston density ρ_{piston}, of 4000 [kg/m^3]. The piston height is 10 [m] (half the height of the storage shaft), which makes the total volume of the piston $\frac{1}{4}\pi D^2*h=70,69$ [m^3]. Using the energy equation, we find $E=(4000-1000)*70,69*9,81*10 = 20,80$ [MJ]. Assuming the power will be delivered for 4 hours, we find $P = (20,80*10^6)/(4*60*60) = 1,45$ [kW]. This power can be delivered for 4 hours, which makes the capacity of one storage cycle 5,80 [kWh].

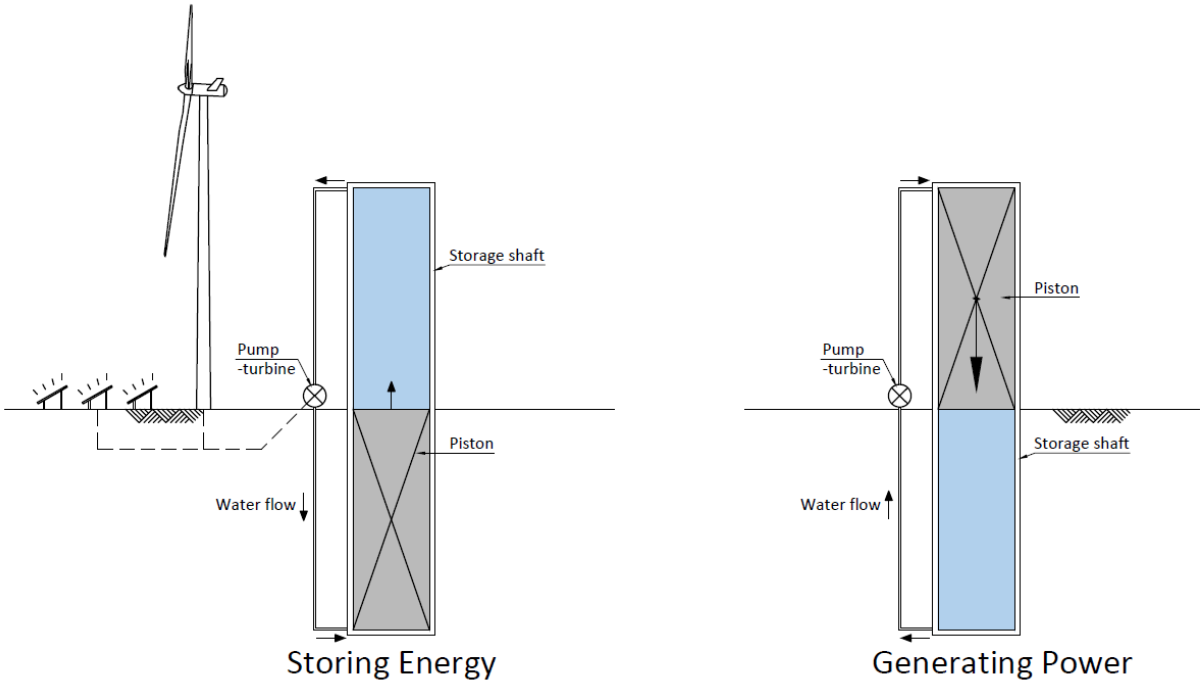

Figure 3-7 Schematic view of a Gravity Power energy storage system

The relationship curve between the amount of energy storage 'E' and the diameter of the shaft 'D is shown in figure 3.5. Here, the piston density and the shaft height are set as constants with ρ_{piston} = 4000 [kg/m^3] and H = 20 [m].

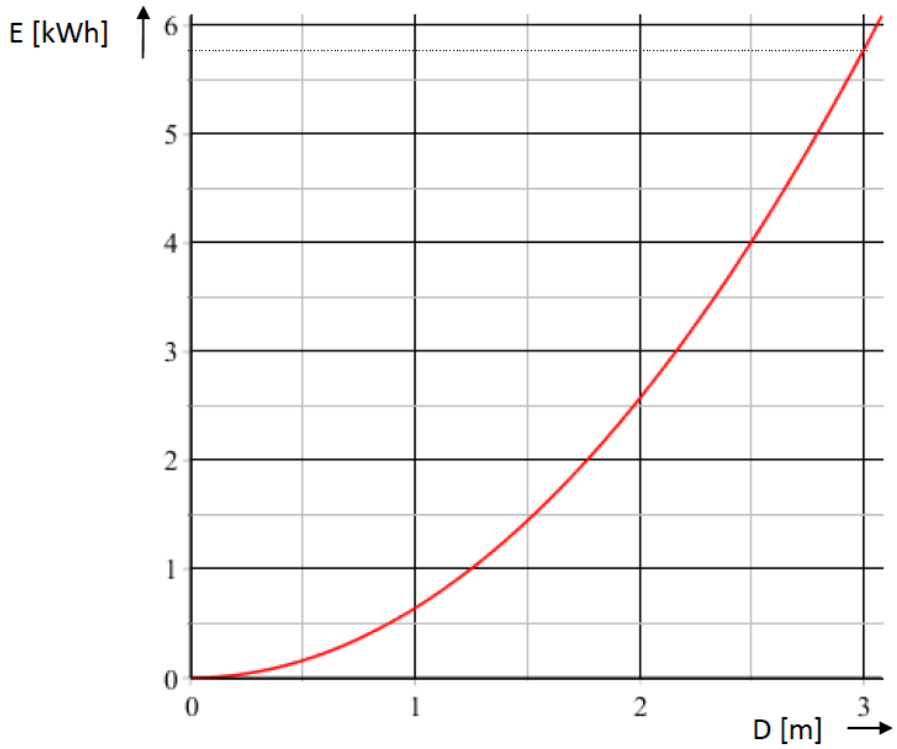

Figure 3-8 The relationship curve between the amount of energy storage 'E' and the diameter of the shaft 'D'

Conclusions

The gravity power storage system does show good potential as a feasible energy storage system. A larger shaft diameter will exponentially increase the storage capacity. Even when the optimal piston height to shaft height ratio is not met, the performance stays relatively high. In order to store the largest amount of energy in the smallest amount of space, a material with a very high density could be used.

3.4 Spring power

When a spring is extended to a certain position, it 'wants' to move back to its neutral position. With this principle, potential energy could be stored in the spring. In order to calculate this amount of potential energy, there are a couple of factors that need to be taken into account. First of all, for a steel wire to work as a spring, the following boundary condition concerning the mean diameter is taken into account:

$$D_m \geq D - d \geq 6 * d$$

Where:

D_m *is the mean diameter of the spring* $[mm]$
D *is the outside diameter of the spring* $[mm]$
d *is the wire thickness of the spring* $[mm]$

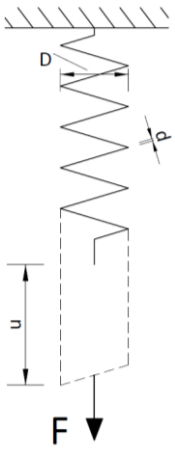

Figure 3-9 A spring with an acting force F

In other words, the mean diameter is the outside diameter minus the wire thickness, but this value has to be at least six times that same wire thickness.

Secondly, the length of the spring, as well as the number of active coils have to be determined. A maximum boundary of the amount of coils can be found by dividing the length of the spring in neutral position by the wire thickness.

When the wire material, thickness and outside diameter of the spring are known, the maximum reachable force can be calculated using:

$$F_{max} = \frac{\pi * d^3 * \tau_w}{8 * D}$$

Where:
F_{max} *is the maximum reachable force of the spring* $[N]$
τ_w *is the allowable torsional stress of the material* $[N/mm^2]$

When the amount of active coils 'N' is known, the maximum extension length needs to be found with:

$$u_{max} = \frac{8 * N * D_m^3 * F_{max}}{d^4 * G}$$

Where:
u_{max} *is the maximum change of length of the spring* $[mm]$
N *is the number of active coils of the spring* $[-]$
G *is the shear modulus of the material* $[N/mm^2]$

And the spring constant 'k' can then be determined:

$$k = \frac{G * d^4}{8 * D_m^3 * N}$$

Where:
$k\ is\ the\ spring\ constant\ [N/mm]$

If we now plot the amount of force needed to make the spring extend a certain amount (Figure 3-10), we find that the slope of this line is determined by the spring constant 'k'. Furthermore, we know that the work that is done to displace the spring is equal to the potential amount of energy that is stored. This potential energy can be visualized as the orange area underneath the spring constant line as can be seen in the following figure:

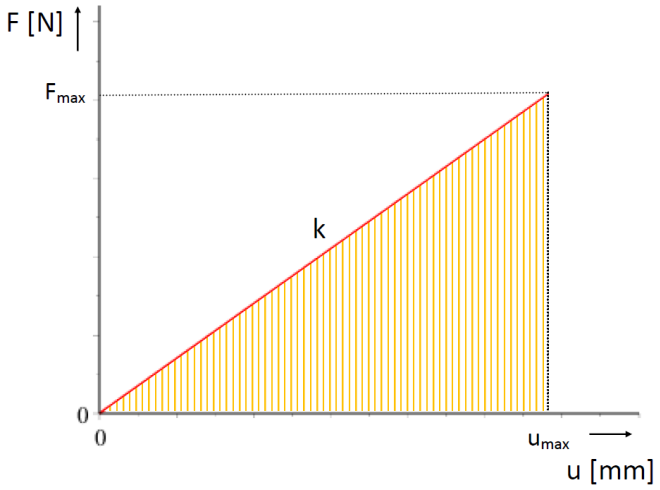

Figure 3-10 Plot of the force needed to extend the spring over a certain distance

In order to pre-stress a spring, an initial tensional displacement 'u_0' can be applied to it. This initial displacement ' u_0' plus the actual extension length 'u' which was foreseen in the design should not exceed the maximum displacement u_{max}, so $u_{max} = u + u_0$. If we now plot the potential energy of the spring, we find the following figure:

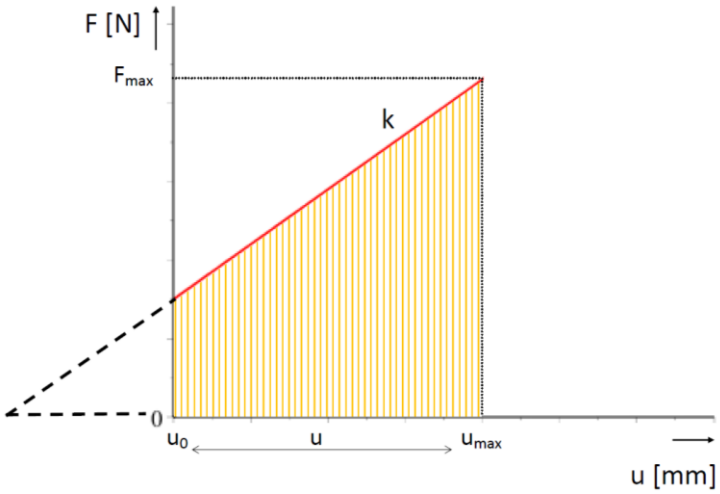

Figure 3-11 Plot of the force needed to extend the pre-stressed spring over a certain distance

To calculate the amount of stored energy, the surface of the hatched area, we find:

$$E = \int_0^{u_{max}} k * u_{max}\, du_{max} - \int_0^{u_0} k * u_0\, du_0 = \frac{1}{2} * k * u_{max}^2 - \frac{1}{2} * k * u_0^2 = \frac{1}{2} * k * (u_{max}^2 - u_0^2)$$

Using the fact that $u_0 = u_{max} - u$, we can rewrite this formula to:

$$E = k * u * (u_{max} - \frac{1}{2}u)$$

Where 'k' depends on 'u' with the following relation (Hook's law):

$$k = \frac{F_{max}}{u_{max}}$$

For a given spring the maximum allowable force F_{max} and maximum extension u_{max} are constants. In above formula, the amount of energy can therefore be determined by the only remaining variable u, the change of length of the spring. Deriving the energy equation to 'u' gives:

$$\frac{dE}{du} = \frac{d}{du}\left(k * u * \left(u_{max} - \frac{1}{2}u\right)\right)$$

$$0 = k * u_{max} - k * u$$

Which results in $u = u_{max}$. At this ratio, a maximum amount of potential energy $E = ½*k*u_{max}^2$ can be stored.

The relationship curve between E and u is shown in Figure 3-12.

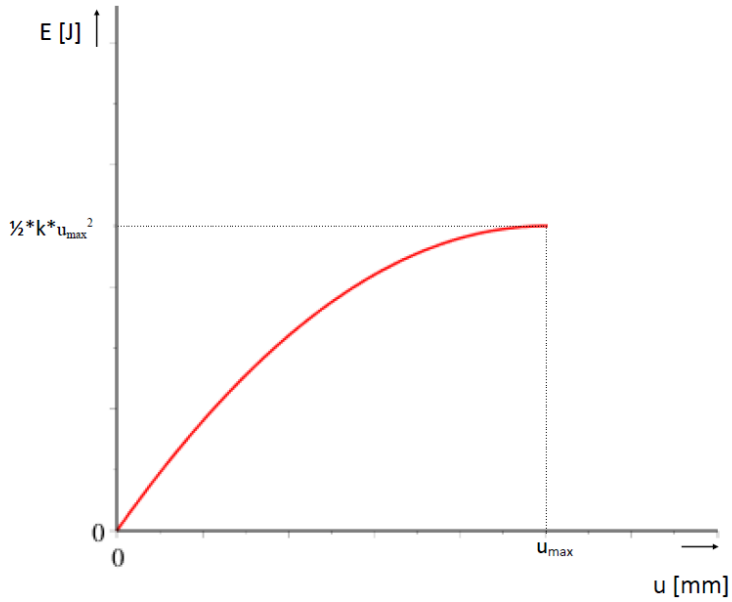

Figure 3-12 Relationship curve between the amount of energy storage 'E' and the change of length of the spring 'u'

Example calculation

Assume a storage shaft (Figure 3-13) with a diameter of 3 [m], a height of 20 [m] and a watertight piston with a negligible weight. Seven springs are connected to the piston, using the following pattern:

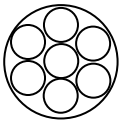

When the springs are in neutral position, their length L_n is 6000 [mm]. In extended position, their length L_e is 16.000 [mm], making the extension length 'u' to come to 10.000 [mm]. The number of active coils of the spring 'N' is 60. Furthermore, the springs have the following dimensional and material values:

Wire thickness	:	d = 75 [mm]
Outer diameter	:	D = 900 [mm]
Mean diameter	:	D_m = 900 – 75 = 825 [mm] ≥ 6*75 = 450
Material	:	Music Wire ASTM A228
Shear modulus	:	G = 80.000 [N/mm^2]
Allowable torsional stress	:	τ_w = 650 [N/mm^2]

The maximum reachable force then comes to F_{max} = (π*75^3*650)/(8*900) = 119,65 *10^3 [N]. The maximum extension length u_{max} = (8*60*825^3*119,65*10^3)/(75^4*80.000) = 12740 [mm] = 12,74 [m]. The spring constant k = (80.000*75^4)/(8*825^3*60) = 9,39 [N/mm] = 9,39 *10^3 [N/m]. Using the optimal energy equation, we find a total amount of potential energy storage for all 7 springs of E =7*½*9,39*10^3*12,74^2 = 5,33 [MJ]. Assuming the power will be delivered for four hours, we find P = (5,33*10^6)/(4*60*60) = 0,37 [kW] and the capacity of one storage cycle is 1,48 [kWh].

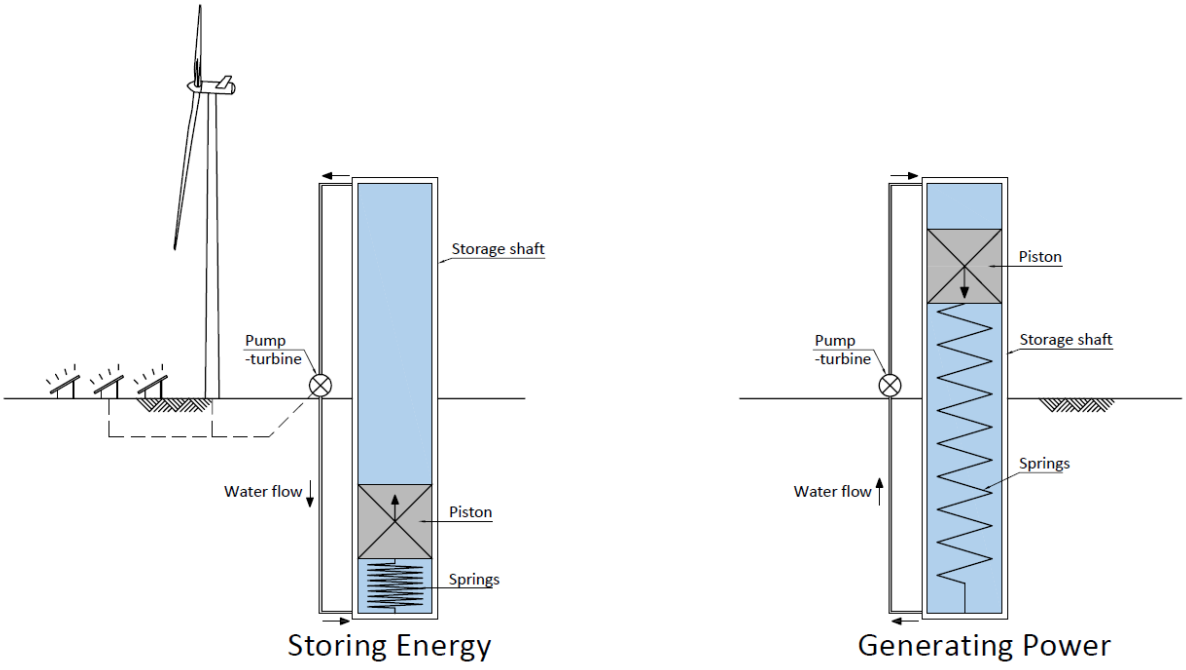

Figure 3-13 Schematic view of a Spring power system in a storage shaft

Conclusions:

In order to get the maximum amount of energy storage capacity of a spring, the extension length in the design should be set equal to the maximum extension length of the spring. In practise this means that there will be no possibility to pre-stress the spring any further. In other words: pre-stressing the spring should only be done when physical limitations limit the spring to reach its maximum extension length. The wire thickness does have a large influence on potential energy storage. An elaborated analysis of this relation can be found in Appendix B.

Taking above example calculation into account, we find that the total amount of potential energy storage of a spring with a realistic wire thickness is relatively low. Furthermore, the neutral length of the spring will make the total stroke of the piston and thereby the amount of movable water a lot smaller. We can therefore conclude that spring power energy storage by itself is not beneficial for this application.

3.5 Compressed air

When compressed air is added to a Pumped Hydro Storage system, it can function as an air cushion. This can best be explained using the schematic illustration shown in Figure 3-14. The system consists of a tank with air and water, an open water reservoir, a water pump/turbine and an air compressor which is used only once. Before the first storage cycle, air is compressed into the tank by the compressor. This makes that the tank has a pre-set pressure. During periods with low demand of energy, the water in the reservoir is pumped into the tank with air by the water pump. The water entering the tank will compress the air even further, storing even more energy. During periods with high demand of energy, the water is released under high pressure through the water turbine back into the reservoir. This can be repeated over again.

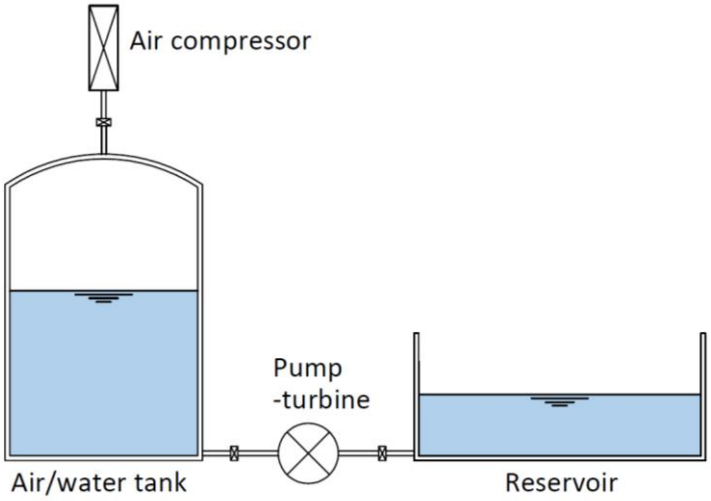

Figure 3-14, Schematic illustration of a Compressed Air Pumped Hydro Energy Storage system.

A great advantage of the added compressed air, is that the storage capacity of the system increases significantly. Furthermore, in contradiction to traditional Compressed Air Energy Storage (CAES) systems, this system uses water instead of air as transporting medium. Air may heat up when compressed rapidly, which usually happens in traditional CAES systems, causing inefficiencies. The pumped water of a Compressed Air Pumped Hydro Energy Storage (CAPHES) system can run through a highly efficient hydro turbine and does not heat up.

If the compression of air happens very slow and the container is a good heat conductor, the air does not heat up and the temperature of the whole remains a constant. This is called isothermal compression. However, if the container is perfectly insulated or the process happens very rapidly, so hardly any heat transfer takes place, the temperature of the air raises. This is called adiabatic compression. In this CAPHES system, the air is compressed by a compressor before the first storage cycle. Because this air compression is pre-setting the system only once at the start, the possible heat losses or other inefficiencies are not taken into account when studying the storage cycle efficiency of the system. At the start of the storage cycle, the air is compressed even further when water is pumped into the tank. Because this process happens very slowly in a tank which conducts heat very well, an isothermal compression is assumed.

A research about CAPHES systems done by (J. Bi, 2013) uses the following model (Figure 3-15) to find a relationship between the amount of energy storage and the compressed air volume in an isothermal compression.

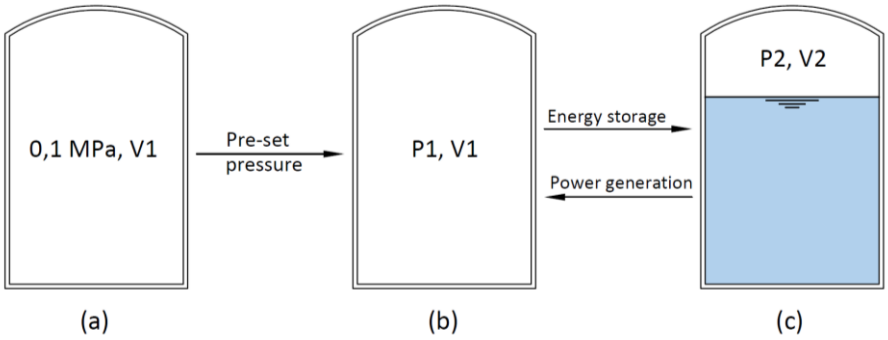

Figure 3-15, the model of the compressed air pumped hydro energy storage system.

Where V_1 is the total volume of the air-water tank and initially an atmospheric pressure of 0,1 [MPa] or $1*10^5$ [Pa] is assumed (shown in Figure 2(a)). Before the first storage cycle, the air inside the tank is compressed up to a certain pre-set pressure p_1 (Figure 2(b)). During the storage cycle, water is pumped inside the tank which will increase the air pressure inside. The maximum pressure of the compressed air is p_2, which can be kept equal to the withstand pressure value of the tank, in order to store the most energy. The corresponding volume of the air at that moment is V_2 (Figure 2(c)).

In the process of power generation, the volume of the air in the tank is V_x, and the pressure is p_x. In the isothermal process, the relationship between the volume and the pressure is:

$$p_2 * V_2 = p_x * V_x$$

At the end of the storage cycle when the water from the tank is discharged, all the stored energy is released. The converted energy in this process is:

$$E = \int_{V_2}^{V_1} p_x dV_x = \int_{V_2}^{V_1} \frac{p_2 * V_2}{V_x} dV_x = p_2 * V_2 * [\ln(V_x)]_{V_2}^{V_1} = p_2 * V_2 * \ln(\frac{V_1}{V_2})$$

For a given tank, its capacity V_1 and the maximum pressure it can withstand (value p_2) are constants. In the above formula, the amount of released energy is therefore determined by the only remaining variable V_2, the volume of the compressed air when the pressure is at its maximum. Deriving the energy equation to V_2 gives:

$$\frac{dE}{dV_2} = p_2 * \ln\left(\frac{V_1}{V_2}\right) - p_2$$

When this derivative equals 0, the volume of compressed air is $V_2 = V_1/e$ (with $e \approx 2{,}72$). At this ratio, the maximum amount of energy $E = P_2 * V_1/e$ can be can be released. The pre-set pressure $p_1 = p_2 * V_2/V_1$ at that moment is $p_1 = p_2/e$.

The relationship curve between E and V_2 is shown in Figure 3-16.

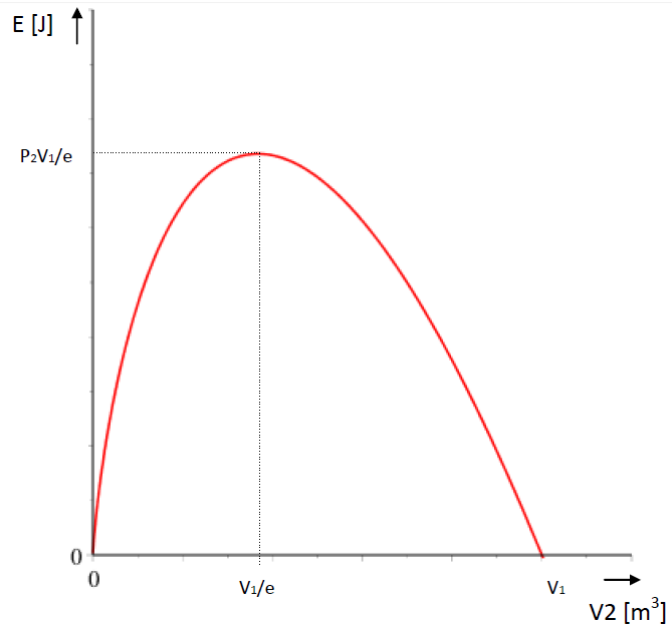

Figure 3-16, The relationship between the amount of energy storage 'E' and the volume of compressed air when the maximum pressure is reached 'V_2' in isothermal process.

Example calculation

Assume a storage shaft (Figure 3-17) with a diameter of 3 [m], a height of 20 [m] and a withstand pressure value p_2 of 2,5 [MPa]. The shaft has a total volume of 141,37 [m^3]. A water- and an air tank which is later put under pressure, are attached to the shaft. When energy is stored, the water fills up the entire shaft. Therefore, using above formula, we find $V_{tank} = (V_{tank} + V_{shaft})/e$. And with V_{shaft} = 141,37 [m^3] we find a V_{tank} of 82,27 [m3]. The pre-set pressure in this case should be set using $p_1 = p_2/e$. With p_2 = 2,5 [MPa] we find p_1 = 0,92 [Mpa]. Using the energy equation $E=p_2*V_1/e$ we find E = 2,5 * (141,37 + 82,27) / e = 205,68 [MJ]. Assuming the power will be delivered for 4 hours, the average P = $(205,68*10^6)/(4*60*60)$ = 14,28 [kW] and the capacity of one storage cycle is 57,13 [kWh].

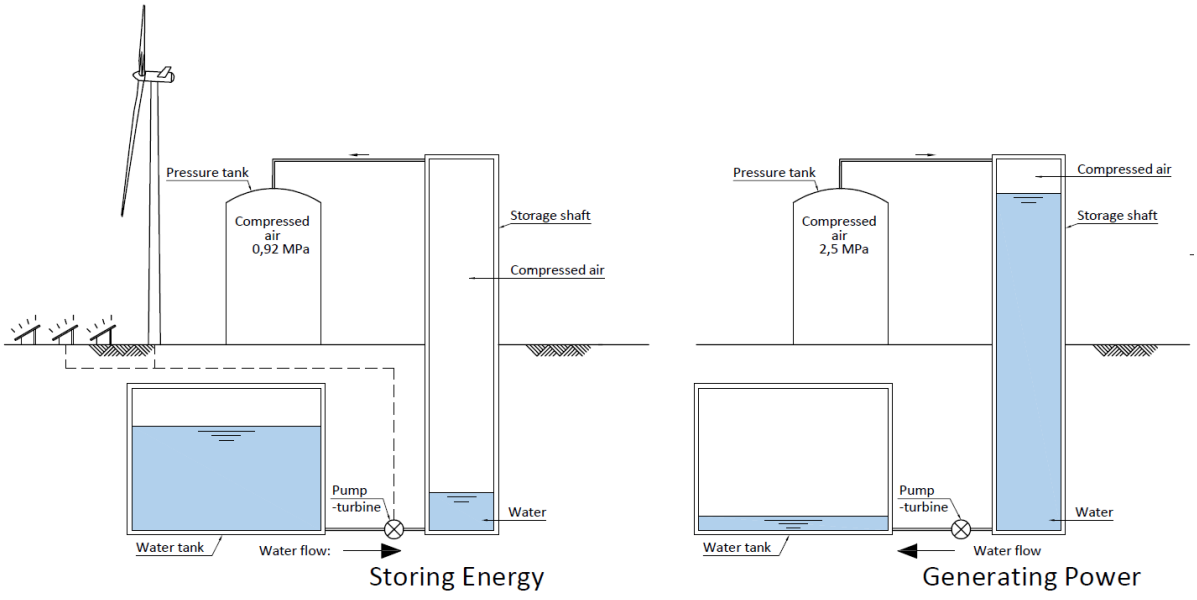

Figure 3-17 Schematic view of a Compressed Air system in a storage shaft

Conclusions

The compressed air pumped hydro energy storage system shows good prospects for the amount of potential storage capacity. Even in a rather small volume, a relatively large amount of energy could be stored. When the diameter and thus the volume of the shaft increases, the capacity will increase even further, as can be seen in Appendix C.

3.6 Result

If we combine any of the above systems, we find that none of the combinations add extra storage capacity. The following example calculation shows this for a combination of gravity power and compressed air energy storage.

Example calculation, compressed air combined with gravity power

Assume a storage shaft (Figure 3-18) with a diameter of 3 [m], a height of 20 [m], a withstand pressure value p_2 of 2,5 [MPa] and a piston of 10 [m] with a density of 7850 [kg/m^3]. The shaft has a total air volume of 70,69 [m^3]. A water- and an air tank which is later put under pressure, are attached to the shaft. When energy is stored, the water fills up the shaft, pressing the piston up. Using above formula, we find $V_{tank} = (V_{tank} + V_{shaft})/e$. And with V_{shaft} = 70,69 [m^3] we find a V_{tank} of 41,14 [m3]. The pre-set pressure in this case should be set using $p_1 = p_2/e$. With p_2 = 2,5 [MPa] we find p_1 = 0,92 [Mpa]. Using the energy equation $E=p_2*V_1/e +(\rho_{piston}-\rho_{water})*¼\pi D^2*h*g*z$ we find $E = 2,5*10^6 * (70,69 + 41,14) / e + (7850-1000)*¼\pi*3^2*10*9,81*10 = 150,30$ [MJ]. Assuming the power will be delivered for 4 hours, the average $P = (150,30*10^6)/(4*60*60) = 10,44$ [kW] and the capacity of one storage cycle is 41,75 [kWh]. This is less than the capacity of 57,13 [kWh] for a compressed air pumped hydro energy storage system with the same dimensions.

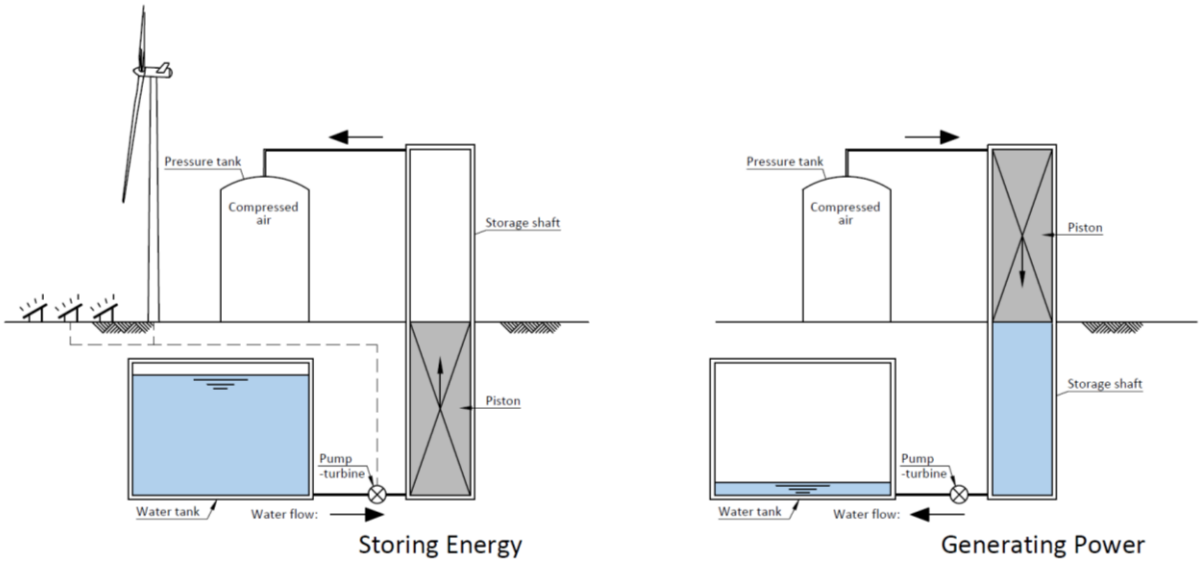

Figure 3-18 Schematic view of a Compressed Air system combined with gravity power

Combining a compressed air or gravity power system with spring power will also not result in a larger storage capacity, as is concluded in chapter 3.3. Comparing the storage capacity of a compressed air-, gravity power and spring power system, we find the following relations between the amount of potential energy storage 'E' and the diameter of the shaft 'D' as shown in the figure below. Here, the compressed air graph corresponds with Figure C-3 in Appendix C, the Gravity Power graph corresponds with Figure 3-5 and the Spring graph follows from Figure B-7 in Appendix B, calculated for different shaft diameters.

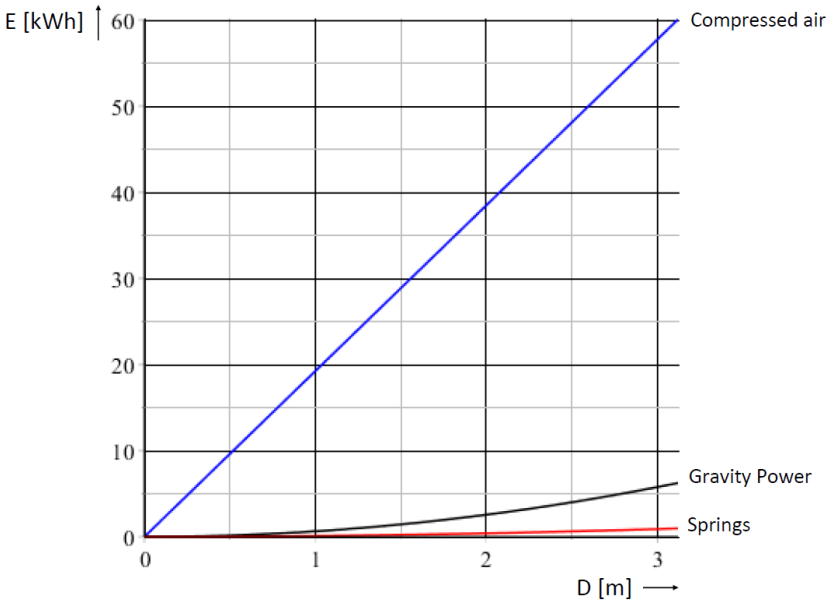

Figure 3-19 The relationship curves between the amount of energy storage 'E' and the diameter of the shaft 'D' for a compressed air-, gravity power and spring power system

If we compare above systems to each other, the following table results.

Table 3-1 Downsides and advantages of the three systems to be compared

	Energy storage capacity	Downsides	Advantages
Gravity Power	Low	The piston occupies half of the storage shaft, leaving little space for the water	Relatively simple structure. Storage capacity increases exponentially with the diameter
Spring Power	Very low	The spring decreases the stroke and thereby the amount of movable water	Up to a certain wire thickness, the springs are relatively easy to make
Compressed air	Good	For working with compressed air, rather strict safety requirements have to be met	Stores a lot of energy in a very compact amount of space

If we look at Table 3-1, it is clear that using a compressed air pumped hydro energy storage (CAPHES) system will result in the largest energy storage in the smallest amount of space. As a result, materials and spacing can be saved upon. The safety requirements that come with the use of compressed air are mapped in Chapter five and are considered challenging but executable. It is therefore that the CAPHES system is chosen as the most promising of the three systems.

4 Sketch design: Local Energy Storage system

In the previous chapter, the principles of the different systems were explained and the one with the best potential is chosen. In this chapter, a sketch design of a Local Hydroelectric Energy Storage (LHES) system is made. As the previous chapter has shown, a compressed air pumped hydro energy storage (CAPHES) system can be made using a water reservoir and an air/water compression tank. This latter can best be made in the form of a cylinder or a sphere for structural efficiency. Furthermore, we want this local energy storage system to be applicable in urban areas where the use of additional land should be limited as this is rather expensive. If the air/water compression tank is made of a steel pipe foundation pile, both these requirements are met. For this reason, we will consider the use of steel foundation piles as air/water compression tank in order to make a sketch design. An impression of steel pipe foundation piles is shown in Figure 4-1.

Figure 4-1 Impression of steel pipe foundation piles, equipped with a dill head

4.1 Rough economic analysis

In order to compare the construction costs of the system with respect to its diameter, we assume that the delivery and instalment of the steel piles are the largest construction expense. A closer look at the delivery and instalment of the steel piles is taken in Appendix D. The piles are divided by the ranges of diameter were a certain execution method can be applied.

Piles with a diameter from 168 to 762 [mm] can be installed as internally driven closed end steel piles or steel drilling piles. For internally driven piles a free-fall drop hammer inside the pile is used to install it to the desired depth. The hollow pile is provided with a welded base plate. During pile driving, a few buckets of gravel stones are often thrown to the bottom of the pile in order to drive it without punching through the base plate. A drilled pile is a pile with a drilling head attached to it. The pile is screwed into the ground by applying an axial pressure and a torque moment. After reaching the desired depth, the pile may be considered installed. This method is vibration free and can be applied in a various range of soil properties. Furthermore, in contrast with the internally driven piles, the drilled piles can be installed under a slope. The advantages of these execution methods are that it is relatively cheap, easy and the shaft does not need to be dug out afterwards.

Piles with a diameter >762 to roughly 1600 [mm] are open ended steel piles, installed using a vibration or a hydraulic hammer. The piles are usually vibrated into the soil as far as possible. Subsequently if needed, a hydraulic hammer can install the pile to its final position. Afterwards, the soil inside the pile needs to be excavated and a underwater concrete floor can be poured. A steel plate can then be welded to the pile in order to make it a 100 percent watertight and pressure resistant. Compared to the internally driven piles, this method is more expensive mainly due to the excavation and waterproofing afterwards.

Piles with a diameter >1600 to 3000 [mm] usually become too big and too heavy to be installed by standard equipment. Just for handling, a rather large crane is often needed. For instalment, a modified vibration or a hydraulic hammer can be used to position the piles into the soil to its desired level. Afterwards, the soil inside the pile needs to be excavated and a underwater concrete floor can be poured. A steel plate can then be welded to the pile in order to make it a 100 percent watertight and pressure resistant. The equipment which is needed for installing such a pile will increase the instalment costs drastically compared to the smaller piles.

Execution costs depend on a lot of factors and are therefore rather hard to estimate. What is clear is that the use of large and special equipment will increase the cost drastically. The estimated construction costs for above pile ranges can be found in the following graph shown in Figure 4-2. In this graph, the costs of a single pile are shown as if this is the only pile which is installed. When multiple piles are installed, the cost per pile will decrease since the mobilization and demobilization of the equipment is a rather large part of the total expenditure, but this will be the same for installing one of multiple piles.

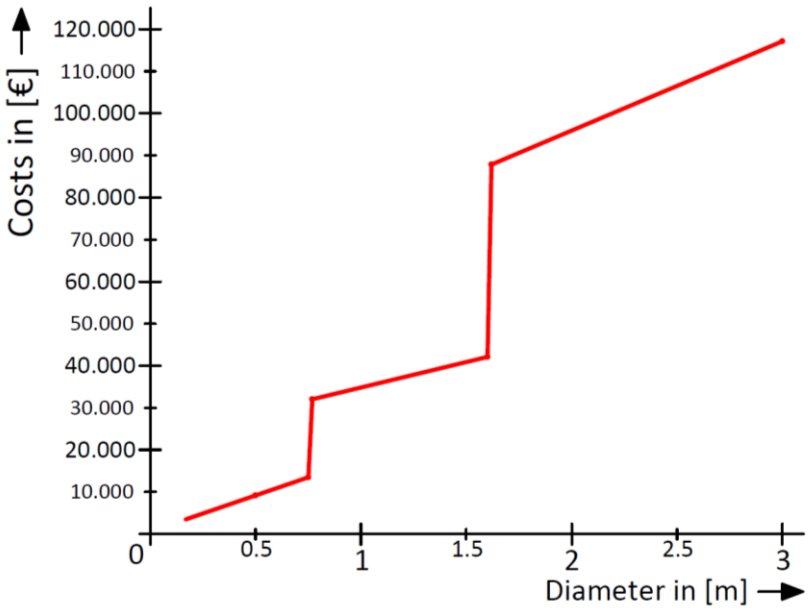

Figure 4-2 Estimated construction costs of a single steel pile with respect to its diameter

4.2 Possible variants

Keeping Figure 4-2 of the previous section in mind, three variants of compressed air pumped hydro storage systems with different pile dimensions are made.

4.2.1 Variant 1, small piles

For variant 1, fifteen piles with a diameter of 762 [mm] are foreseen. The piles can be installed using a drill machine. It is assumed that the steel piles have sufficient bearing capacity to function as a foundation without being filled with concrete afterwards. The Compressed Air Pumped Hydro Energy Storage (CAPHES) system further contains a single pump-turbine unit and a compressed air tank, which are connected to the piles by steel tubes. For economical and practical reasons, the pump-turbine and compressed air units are placed on ground level. A schematic drawing of this variant is shown in Figure 4-3.

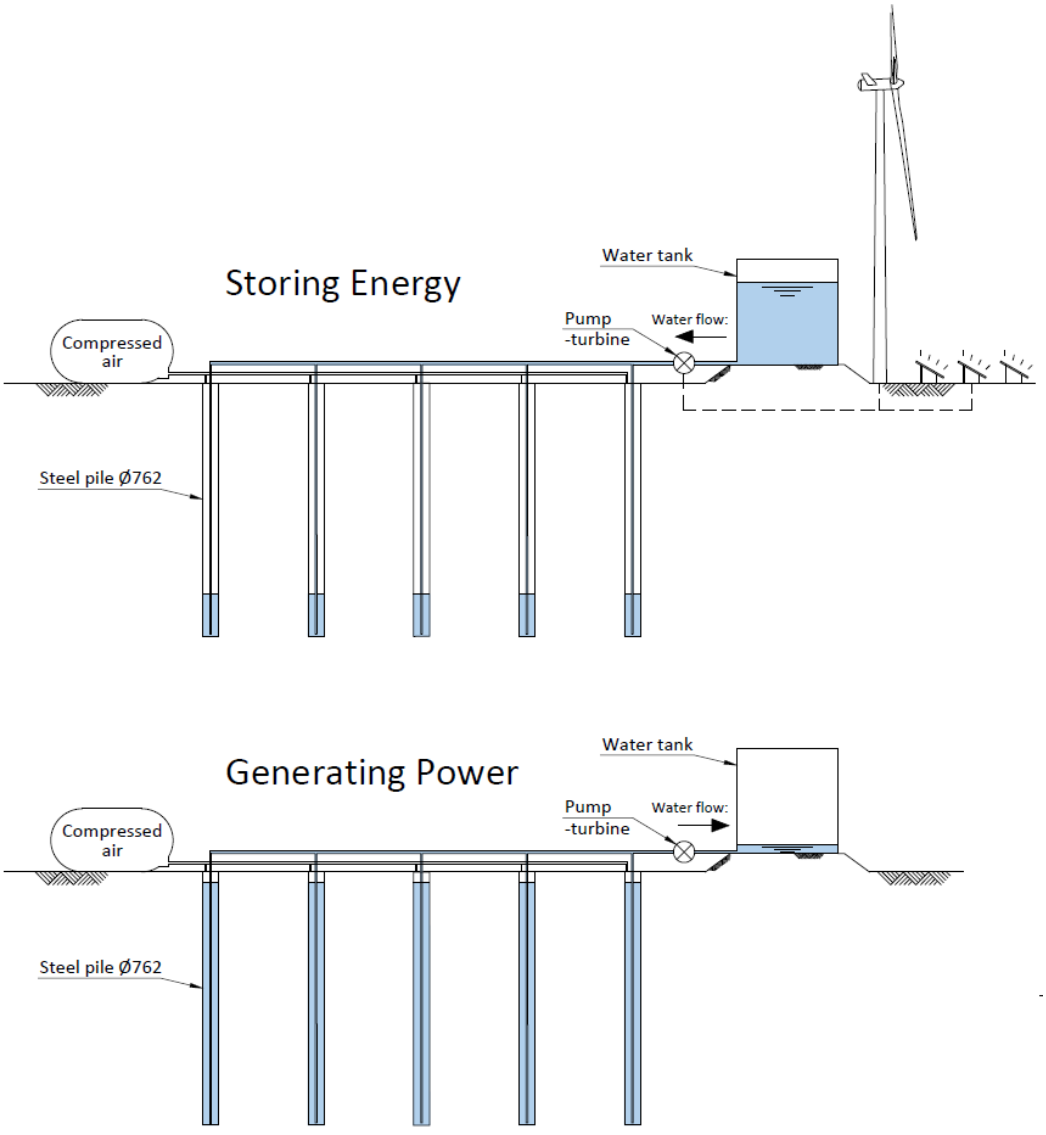

Figure 4-3 Schematic drawing of variant 1

4.2.2 Variant 2, medium piles

For variant 2, four piles with a diameter of 1600 [mm] are foreseen. The piles can be installed by vibration and subsequently hydraulic hammering until the desired position is reached. The CAPHES system further contains a single pump-turbine unit and a compressed air tank, which are connected to the piles by steel tubes. A schematic drawing of this variant is shown in Figure 4-4.

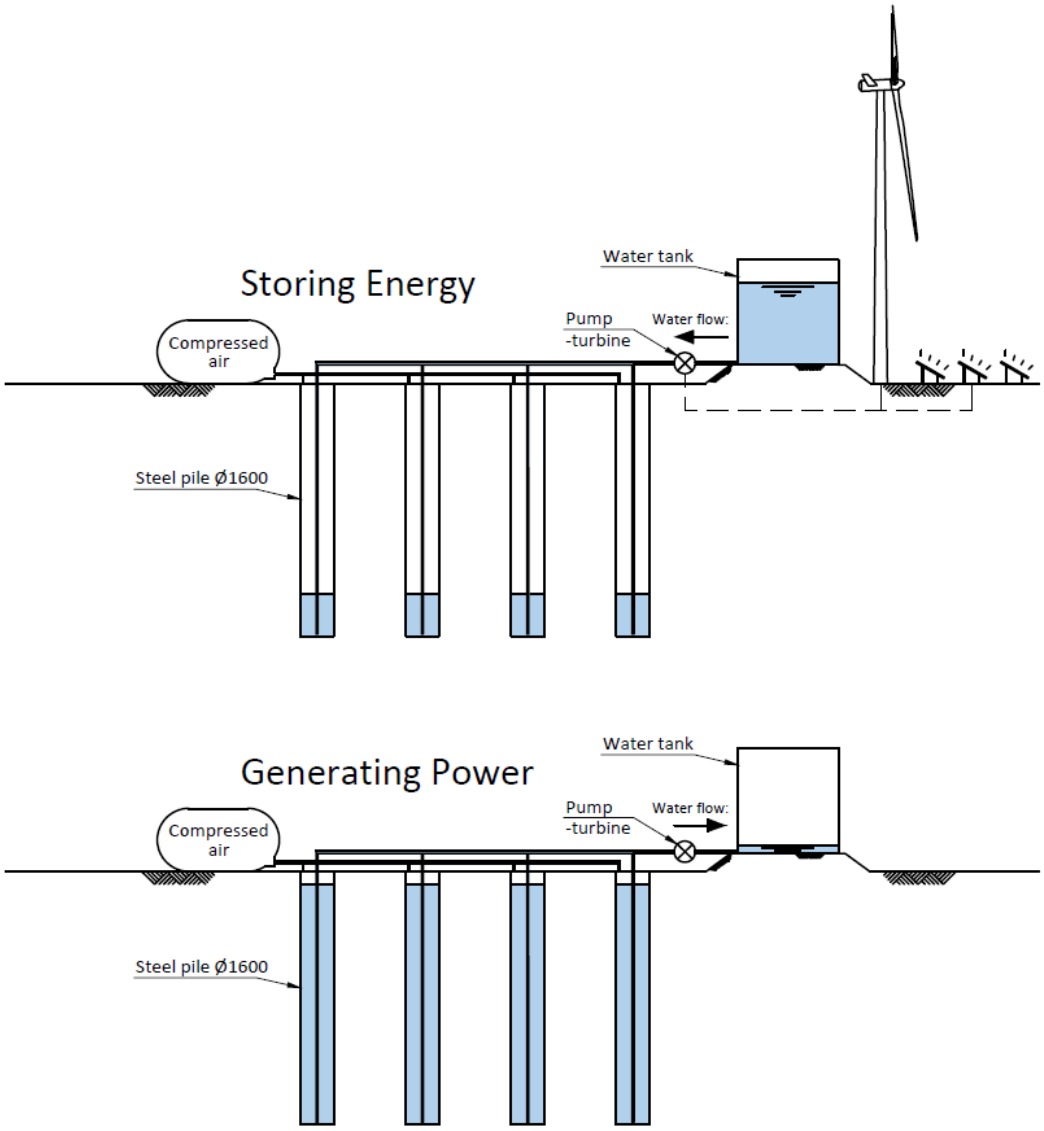

Figure 4-4 Schematic drawing of variant 2

4.2.3 Variant 3, large piles

For variant 3, two piles with a diameter of 3000 [mm] are foreseen. The piles can be installed by vibration and subsequently hydraulic hammering until the desired position is reached. One of the piles will function as a water and compressed air tank and has a steel plate welded in between the two compartments. The other pile will function as a storage shaft. The two piles are connected with each other by an open air tube in the upper end and a water tube with a pump – turbine attached at the bottom end. A schematic drawing of this variant is shown in Figure 4-5.

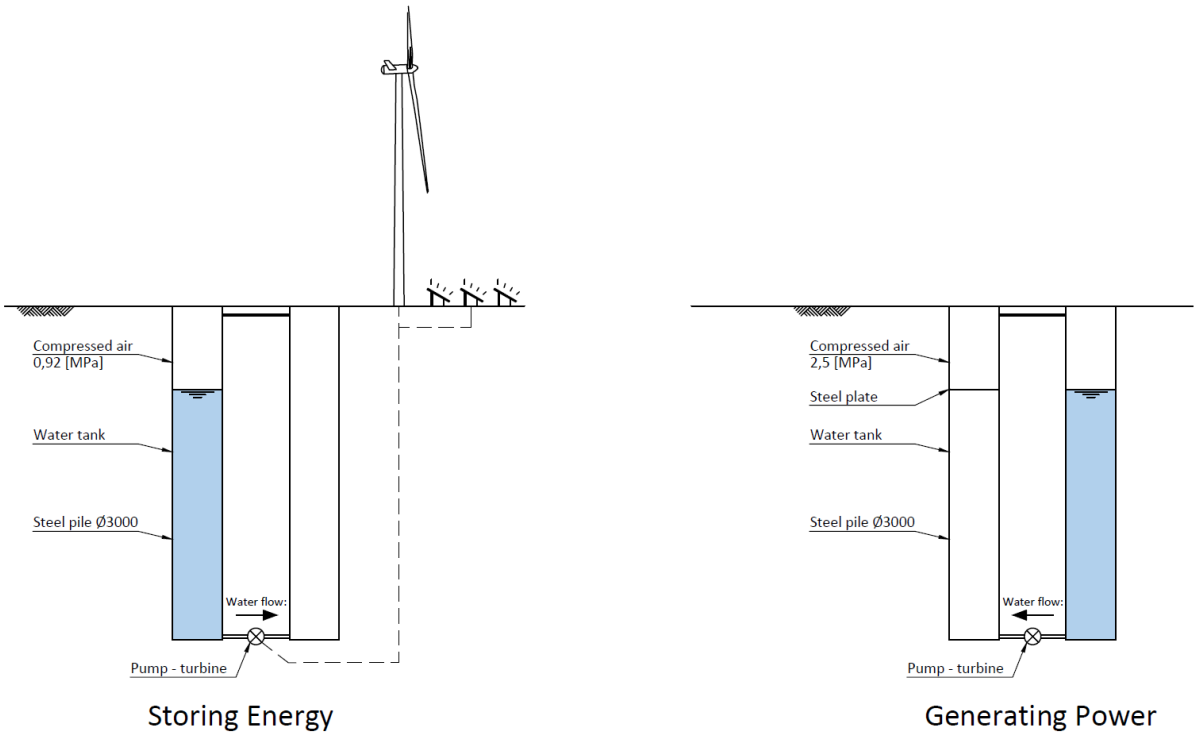

Figure 4-5 Schematic drawing of variant 3

4.3 Possible applications

The variants described could be applied in many different ways. One may think of an application as the foundation of a house for example. This would only be applicable for the smaller piles as described in variant 1. A schematic drawing of such a system is shown in Figure 4-6.

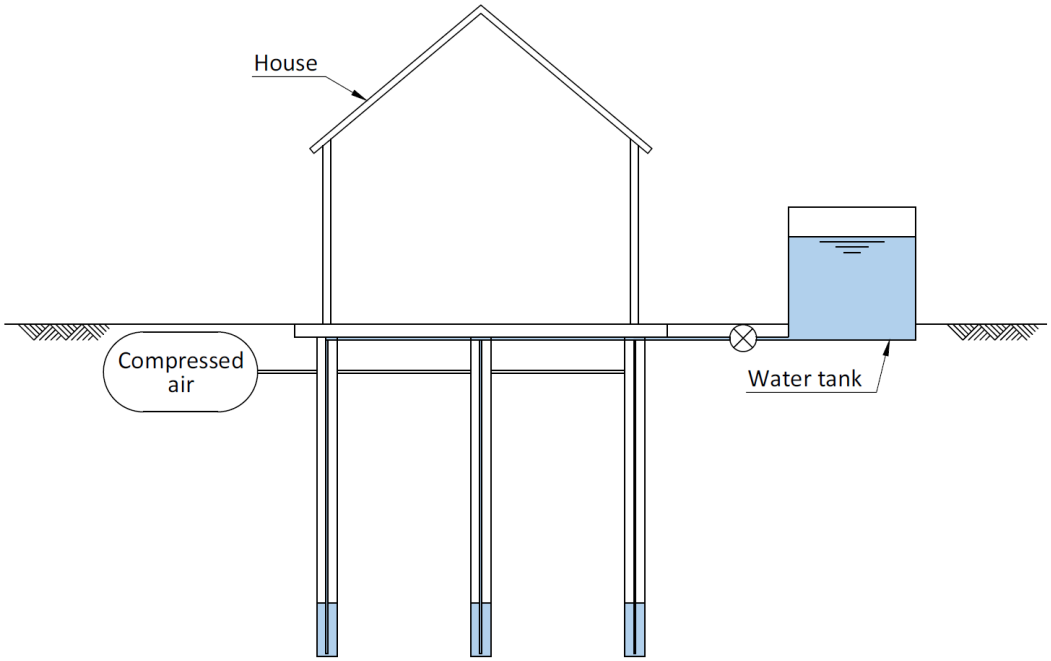

Figure 4-6 Schematic drawing of a CAPHES system integrated the foundation of a house

Another application may be the addition of a storage shaft in the core of an apartment building. This may be an old elevator shaft or a separate core, especially for providing a storage system. Figure 4-7 shows how such a system could look like.

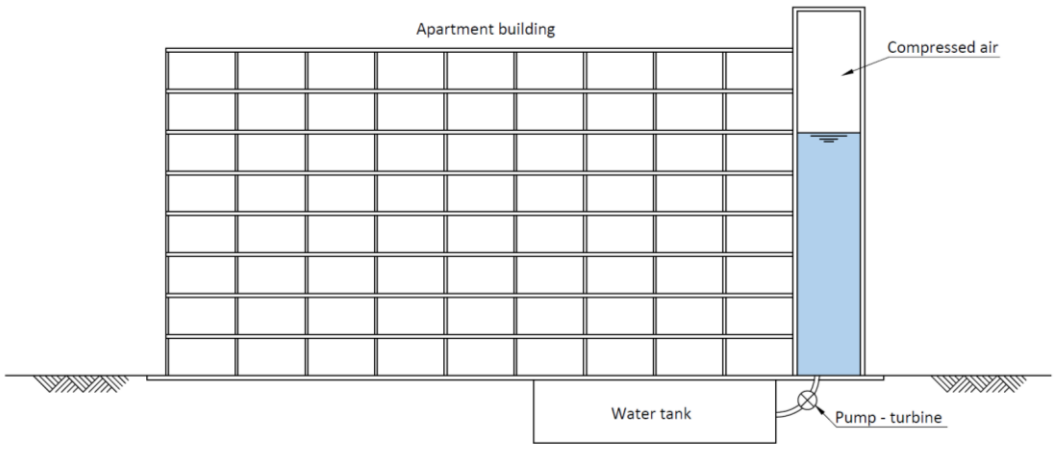

Figure 4-7 Schematic drawing of a CAPHES system integrated in the core of an apartment building

An CAPHES system could also be made as a stand-alone structure. This way, there is no influence from other structures. The system could be made at a reserved spot at the end of the street for instance. An impression of how such a system could look like is shown in Figure 4-8.

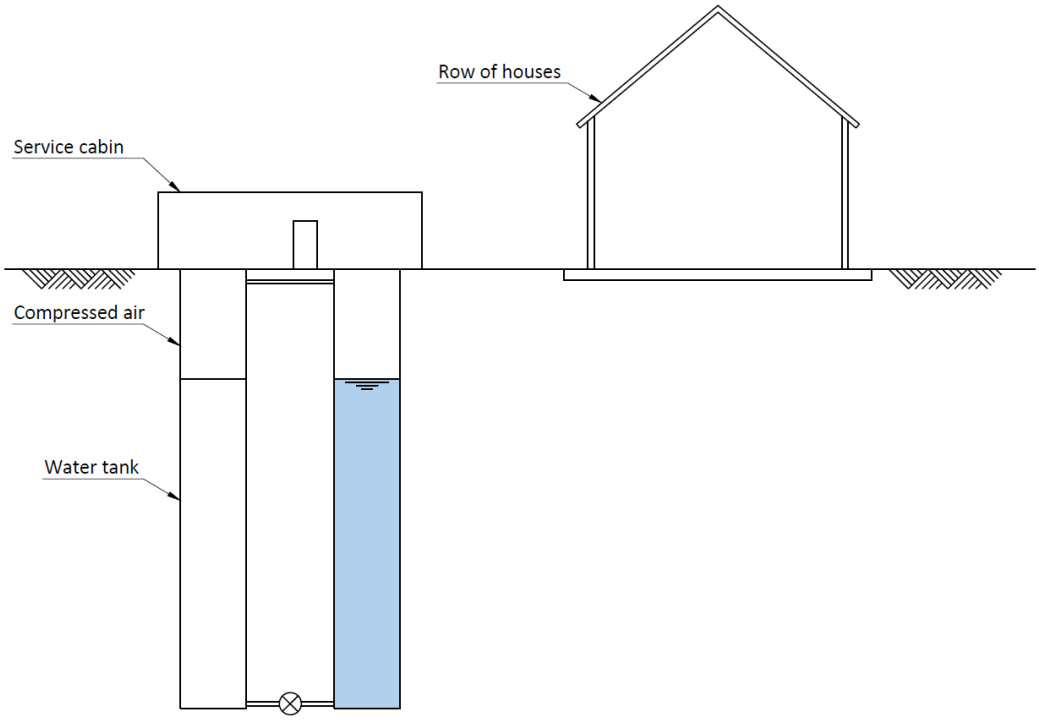

Figure 4-8 Schematic drawing of a CAPHES system as standalone structure

4.4 Multi Criteria Analysis

In order to compare the proposed variants from chapter 4.2, a Multi Criteria Analysis is performed. The variants are compared to each other on a number of criteria to show the weak and strong points of each variant. The criteria are weighed in order to outline their difference in importance, after which the variants are scored and the best one is chosen.

Assumptions

For this MCA, the following assumptions are made:

- It is assumed that all the variants have the same storage capacity and roundtrip efficiency.
- Safety risks are assumed to depend mostly on the application of the system and are therefore not considered as a variable between the three variants.
- All variants are assumed to have the same durability and life time.
- The operational costs are assumed to be the same for all three variants.

The variants are compared with the following criteria:

Constructability

The ability to build the storage system is an important criterion. Especially when relatively small investments are foreseen, a construction error may have serious financial consequences. In Appendix D, we found that smaller piles have a better constructability. The large piles are harder to install and have a bigger chance even to get stuck halfway the instalment.

Construction costs

The costs involved when building the system. If the system needs large investments to be constructed, the economic feasibility is under pressure. The construction costs of the variants is therefore a very important criterion. The variant are rated for this criterion by takin the cost estimation of Figure 4-1 into account.

Large scale applicability.

The ability for a certain variant to be applicable on a large scale. When a system is applied a lot, the cost per system decrease. Furthermore, the system may become more efficient as specific parts like pump-turbines can be optimized for the purpose of energy storage. It is expected that the piles of variant 1 can be applied a lot as foundation of newly-build houses. The piles of variant 3 are expected to be applicable as a standalone tower or (bridge) foundation on a smaller scale.

Robustness

The ability to reduce the chance of failure of the system. Every connection comes with a certain risk of cracking or leaking. In general, it is expected that in a system where a lot of parts are used, the chance of failure is higher than in a system with a low amount of parts. For this reason, variant 3 is considered more robust than the other two.

Weighing factors

In order to outline their difference in importance, the criteria are given a weighing factor. First, the criteria are compared to the rest of the criteria. The most important of the two criteria is given the score 'one'. The other criterion is given the score 'zero'. One point is added to the sum of the scores, in order to avoid one criterion getting a weighing factor of zero. Then, this number is divided by the total amount of points and the weighing factor is known. In the table below, this is done for above criteria.

Table 4-1 Weighing factors for the MCA

		1	2	3	4	total	Total+1	Weighing factor
Constructability	**1**	x	0	1	1	2	3	0,3
Construction costs	**2**	1	x	1	1	3	4	0,4
Large scale applicability	**3**	0	0	x	1	1	2	0,2
Robustness	**4**	0	0	0	x	0	1	0,1
Total							10	1,0

Now that the weighing factors are known, the variants are given a score between one and three for each criteria. With three as the highest and best score possible, and one as the lowest and worst score possible. The scores for each criterion are multiplied with the weighing factor. The sum of this gives the total score of a particular variant.

Table 4-2 Scores of each variant

		Variant 1, small piles		**Variant 2, medium piles**		**Variant 3, large piles**	
	Weighing factor	Score	Weighed score	Score	Weighed score	Score	Weighed score
Constructability	0,3	3	0,9	2	0,6	1	0,3
Construction costs	0,4	3	1,2	2	0,8	1	0,4
Large scale applicability	0,2	3	0,6	1	0,2	2	0,4
Robustness	0,1	1	0,1	2	0,2	3	0,3
Total			2,8		1,8		1,4

From Table 4-2, it is clear that variant 1 has the highest score. Even though this variant does not score best on the robustness criterion, it is the most constructible, economical feasible and large scale applicable variant. Therefore, variant 1 is considered to be the 'most promising' variant.

4.5 Preliminary design choice

As the Multi Criteria Analysis has shown, variant 1, with multiple small piles, is considered the most promising variant. The application where the piles function as the foundation of a house is considered in the design, as this application is expected to be the most realistic and economical feasible one. In order to save space, an external air and/or water tank above ground is not suggested. Instead, a part of the piles will function as a water tank and the other part of the piles will function as a storage shaft, where compressed air as well as water is situated. These piles have a maximum water to air ratio of 1/e as described in chapter 3.5. This corresponds to a part filled with water of 63 % maximum. A schematic drawing of this is shown in Figure 4-9.

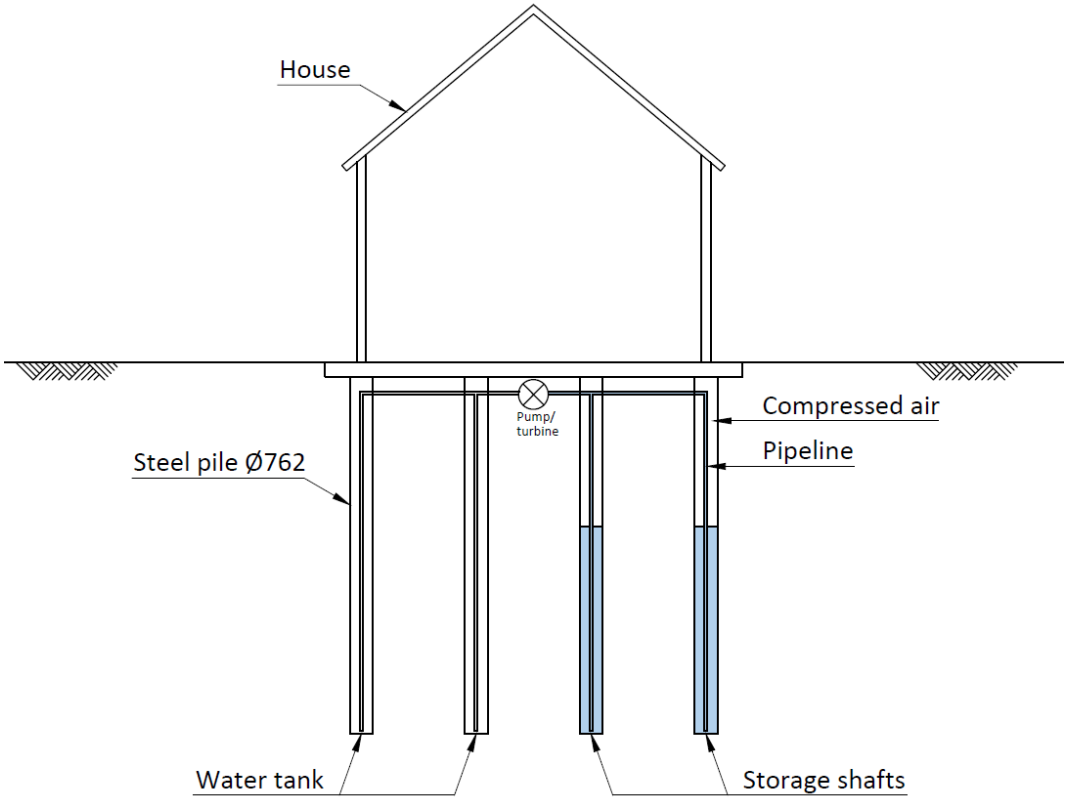

Figure 4-9 Schematic drawing of a CAPHES system integrated in the foundation of a house as elaborated in the preliminary design

Furthermore, the following design choices and assumptions are made:

- The pump-turbine equipment is assumed to be installed above the groundwater level.
- A ground layer with a large bearing capacity is assumed to be situated at -20 [m].
- Hollow, drilled piles with an outside diameter of 762 [mm] reaching 20 meters into the ground are assumed to be used for the storage system.
- The piles are assumed to have sufficient bearing capacity to bear the house on top. Further calculations of the bearing capacity are considered outside the scope of this research.
- The water volumes within the pipelines are neglected for pressure calculations.

5 Preliminary design

In this chapter, the preliminary design of a LHES system is made using the design choices of the previous part. The possible power output of the system is determined first. This will depend on the chosen water flow rate, net head and turbine type and efficiency. When the power output is known, the power input is determined by the type of pump which is used. After this, the safety requirements for the system are mapped and the steel piles and pipelines are designed. The preliminary design is followed by a risk analysis and an economic analysis. The risk analysis maps the different risks that are expected when the LHES system would be build. And the economic analysis gives an estimation about the construction and operational costs of the system. These three parts combined result in a better insight of the technical and economic feasibility of the LHES system.

5.1 Turbine selection

To transfer the potential energy which is stored in the LHES system to electrical power, a turbine is used. The most common water turbines are Pelton-, Kaplan and Francis turbines. Below, a short description is given for each turbine. A comprehensive overview can be found in Appendix E.

Pelton turbines

A Pelton turbine is made using typical curved spoon shaped buckets attached to the rotor blade. The water, which is under pressure, is transported in a penstock pipe and impacts on the buckets which makes the rotor spin. Pelton turbines need small water flow rates but high net heads or pressure to generate power. An impression of a Pelton turbine is shown in Figure 5-1

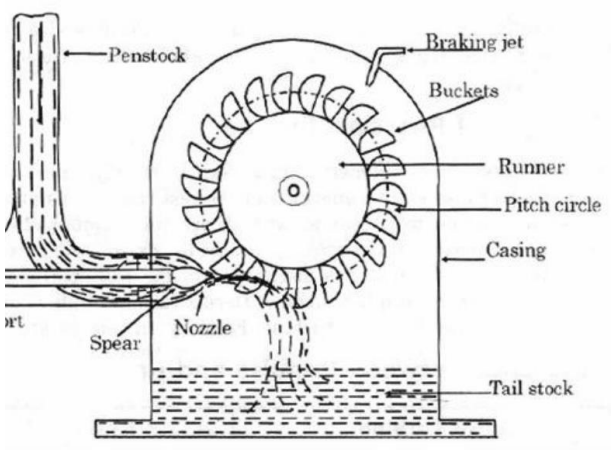

Figure 5-1 Impression of a Pelton turbine

Kaplan turbines

A Kaplan turbine is a axial flow turbine, made using a propeller inside a tube. The water is transported through the inlet guide-vanes, which can be opened and closed in order to regulate the flow rate which passes through the turbine. The flow direction does not change as it crosses the rotor. Kaplan turbines need high water flow rates but small net heads. An impression of a Kaplan turbine is shown in Figure 5-2.

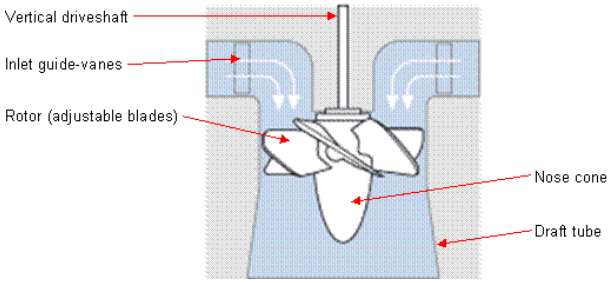

Figure 5-2 Impression of a Kaplan turbine (RenewablesFirst, 2015)

Francis turbines

A Francis turbine could be described as a combination of a Pelton- and a Kaplan turbine. The water is transported through a snail shell shaped spiral casing which moves the water around the runner, where it enters horizontally and exits vertically down through the centre of the turbine. The runner itself converts the energy in the water into rotational motion and torque. Francis turbines are often used for pumped storage pants, as the turbine can be set in reverse to function as a water pump. This is a big advantage with respect to Pelton- or Kaplan turbines, where a separate pump station would be needed in order to pump the water back in the upper basin. Francis turbines need medium ranged flow rates and medium ranged net heads. An impression of a Francis turbine is shown in Figure 5-3.

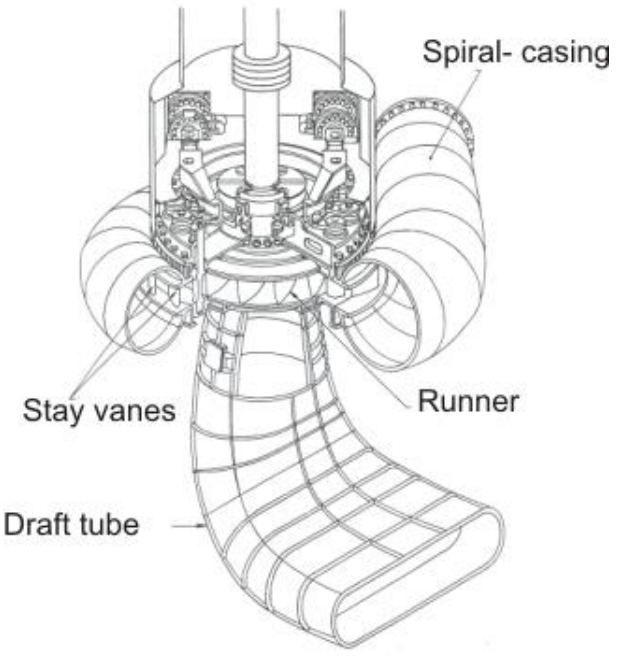

Figure 5-3 Impression of a Francis turbine (Waterturbines, 2016)

In order to compare above turbines with each other, the efficiencies, downsides and advantages of Pelton-, Kaplan- and Francis turbine types are shown in the table below.

Table 5-1 Overview of Pelton-, Kaplan- and Francis turbine characteristics

	Efficiency	Downsides	Advantages
Pelton turbine	90%	Needs separate pump in order to function in a PHS system	High efficiency maintains even for lower flow rates. Typical high rotational speeds make a direct connection to a generator possible. No cavitation problems
Kaplan turbine	92%	Needs very high flow rates, which would increase the needed water reservoir to deliver power for a certain time	Best efficiency with low net heads
Francis turbine	93%	Needs high flow rates, which would increase the needed water reservoir to deliver power for a certain time	Can function as pump as well when put in reverse

Using Table 5-1, we find that the Pelton turbine type has the preference to be used in the LHES system. The main advantages of a Pelton turbine, together with its use of very low flow rates, which can go as low as 5 [l/s] (RenewablesFirst, 2015) are key points in this decision. A side effect of this decision is however, that a separate pump has to be applied in order to pump the water back in the pressurized piles as the Pelton turbine itself cannot function as a pump.

Consulting the turbine production range from the supplier Andritz Hydro, we find that their standard Pelton turbines work for a minimum flow rate of 20 [l/s] as shown in Figure 5-4. However, we are trying to find a turbine which can produce as much electricity with the smallest flow rate possible, as this would decrease the needed water tank capacity. The desired production range for our system (3 – 30 [kW] power output, 5 – 10 [l/s] flow rate) is shown in Figure 5-4 as the purple area, marked as 'Modified Pelton' turbines.

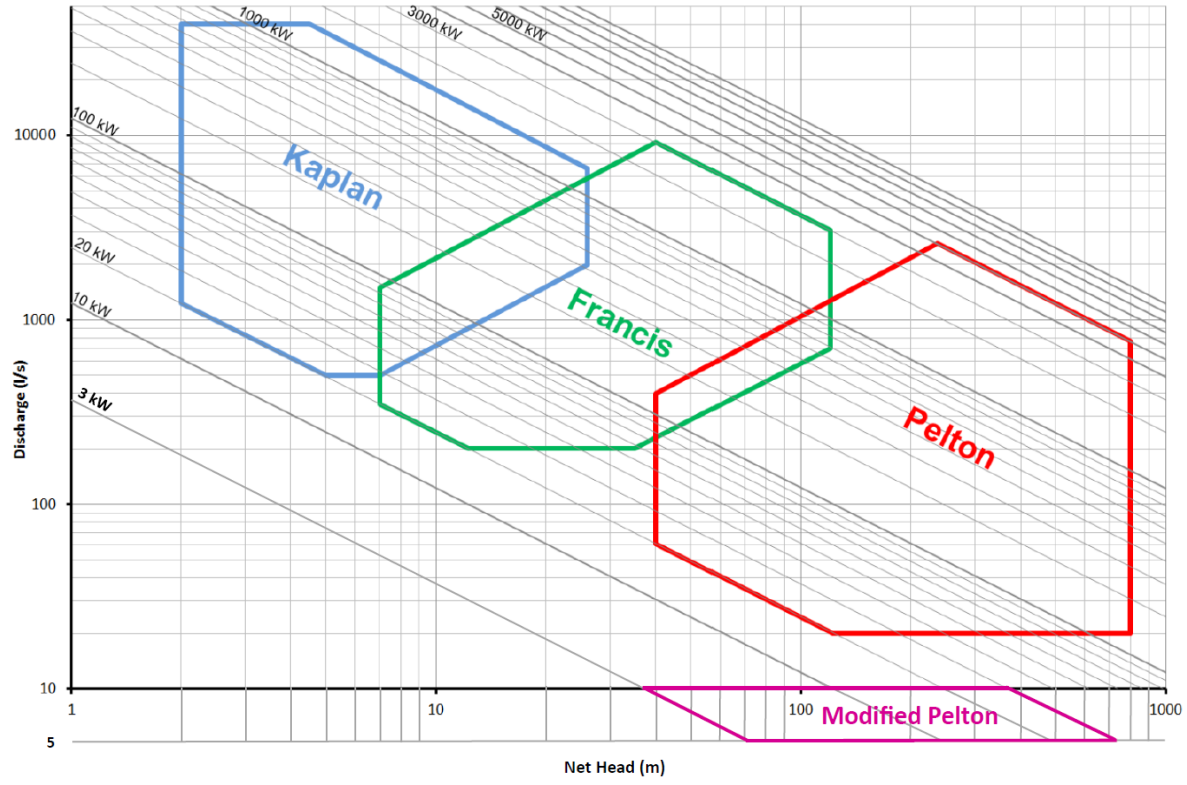

Figure 5-4 Production range for Kaplan-, Francis- and Pelton turbines (AndritzHydro, 2015) and the added 'Modified Pelton' turbine range for the LHES system

As Figure 5-4 shows, the desired 'Modified Pelton' turbine is not a standard production for Andritz Hydro. None of the other Pelton turbine manufactures found show standard models in the purple range. It is assumed however, that the turbines in this range could be produced. Two reference projects of produced Pelton turbines within the purple production range are shown in Appendix E.

In order to reduce the volume and thus the space needed for the water tank, a turbine with a small, constant design flow rate of 5 [l/s] is chosen for the application within the LHES system. The corresponding maximum head within the purple production range is approximately 714 [m] or 70 [bar]. This pressure is set as the maximum pressure inside the piles. As the turbine is generating power and the water flows from the storage shaft piles to the water tank piles, the pressure will decrease to 70/e = 25,8 [bar] as is shown in the figure below.

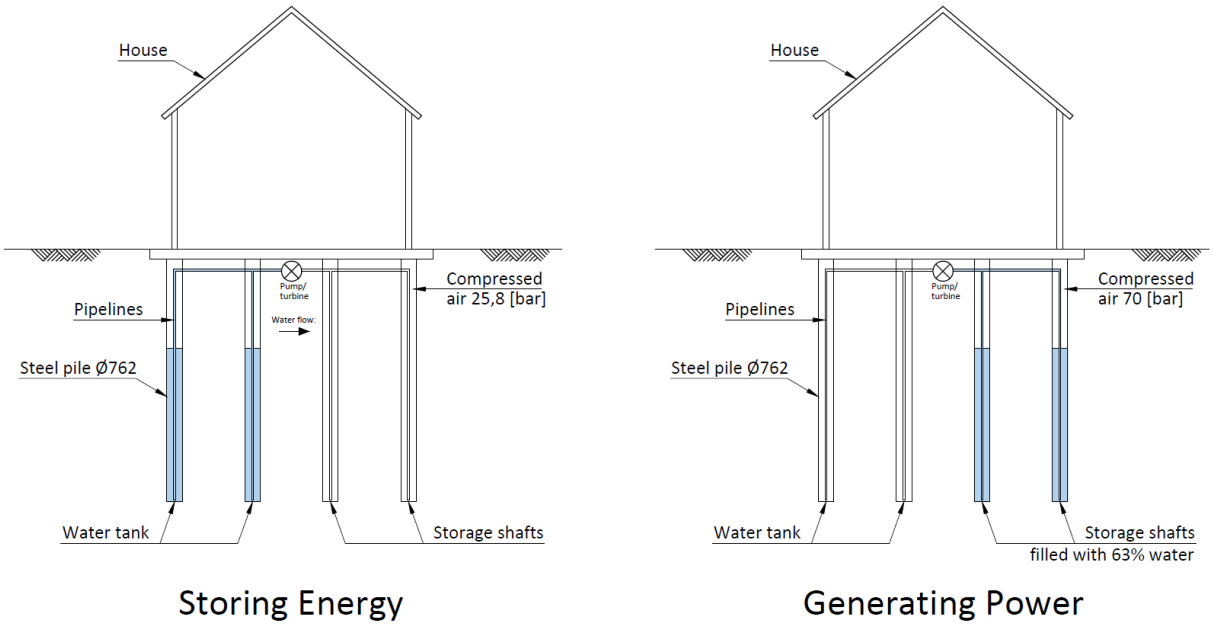

Figure 5-5 Air pressure in piles when starting to store energy (left) and starting to generate power (right)

Using (Duivendijk, 2007) and assuming a power delivery efficiency of 85%, we find that the resulting maximum power which can be delivered can be calculated by:

$$P = \rho * g * Q * H * \eta$$

Where:

P *is the power output which can be delivered* $[W]$
ρ *is the density of water* $[kg/m^3]$
g *is the gravitational acceleration* $[m/s^2]$
Q *is the water discharge* $[m^3/s]$
H *is the water head* $[m]$
η *is the efficiency* $[-]$

Which brings the maximum power output which can be delivered P = 1000*9,81*5*10^{-3}*714*0,85 = 29,8 [kW]. An impression of a same order Pelton turbine is shown in Figure 5-6.

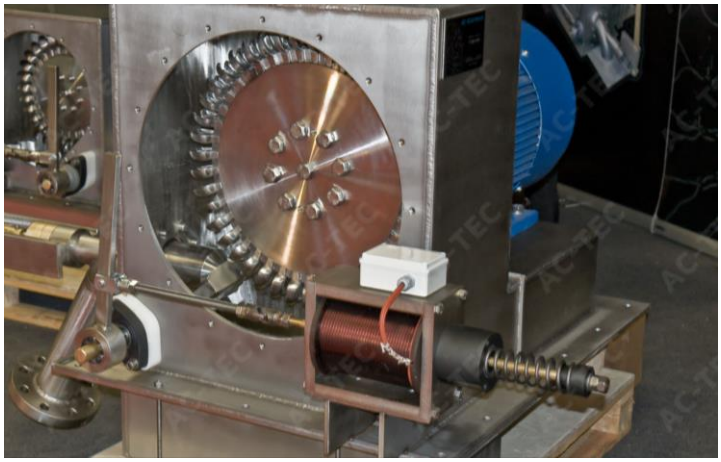

Figure 5-6 An impression of a Pelton turbine which produces 28 [kW] with an head of 389,7 [m] and a flow rate of 10 [l/s] (AC-TEC, 2015)

The minimum power output which can be delivered, at 25,8 [bar] or 262 [m] water head, comes up to a P = 1000*9,81*5*10^{-3}*262*0,85 = 10,9 [kW]. The power output relation with respect to the time it takes for the water to leave the storage shaft is linear. This makes the average, at 47,9 [bar] or 488 [m] water head, to come up to 20,3 [kW] as the figure below shows.

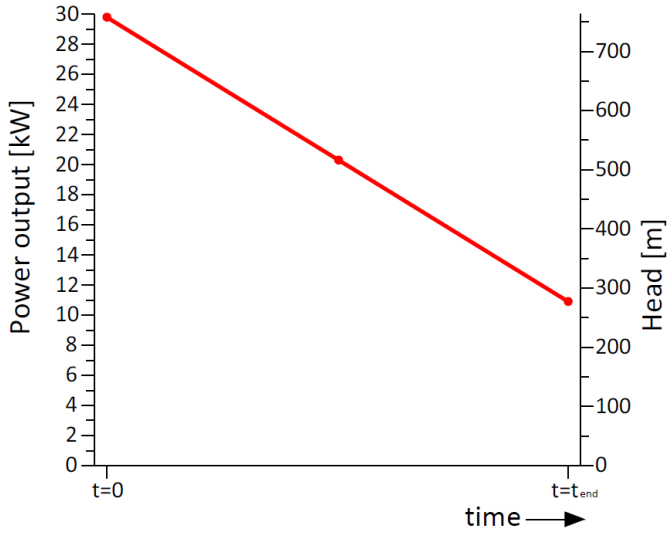

Figure 5-7 Graph of the power output and corresponding head relation of the LHES system with respect to the time

In order to integrate the LHES system in the electricity network of a household, the following design choices and assumptions are made:

- The peak demand for power is assumed to be 2,5 [kW] per household. This assumption is based on an average yearly electricity consumption of 3500 [kWh] per household (Nuon, 2016), which comes down to an average of approximately 10 [kWh] per day. The highest peak power demand could be expected in winter days between 17.30 and 19.30 as Figure 2-3 of Chapter 2 shows. This is assumed to be 2,5 [kW] per household.
- The LHES system is assumed to be a sufficient storage system for eight households. This assumption is based on the average power output of the LHES system, which could provide the peak demand of 2,5 [kW] for at least eight households.

- It is assumed that the households could easily demand power from the grid in case the power delivered by the LHES system is not sufficient. This could happen in case the LHES system runs empty or when all eight households demand too much power at the same time.
- It is assumed that the houses are provided with solar panels which produce sufficient electricity to use during the day and charge the LHES system at the same time.
- It is assumed that the Pelton turbine releases a maximum constant flow of 5 [l/s] by making use of a Pelton spear which controls the size of the water opening and regulates the flow when the pressure fluctuates. When little energy is required, this needle can reduce or even close off the opening completely which results in a larger time span for the turbine to produce electricity. An impression of such a Pelton spear is shown in Figure 5-8.

Figure 5-8 Impression of a Pelton spear, which regulates the flow of water through the nozzle (Waterturbines, 2016)

5.2 Pump design

To store energy into the system, water is pumped back into the storage shaft piles. Basically, there are two types of water pumps, namely centrifugal pumps and positive displacement pumps. Below, a short description is given for each pump type. A comprehensive overview can be found in Appendix F.

Centrifugal pumps

Centrifugal pumps create an increase in water pressure by letting the water flow from the inlet, which is situated in the centre of a rotating impeller, along the blades towards the outside of the impeller. The centrifugal force increases the water velocity and transforms the kinetic energy of the water into water pressure. The water pressure then results in a certain flow. Centrifugal pumps need a certain pressure on the inlet tube as they cannot create suction. A basic diagram of such a centrifugal pump is shown in Figure 5-9.

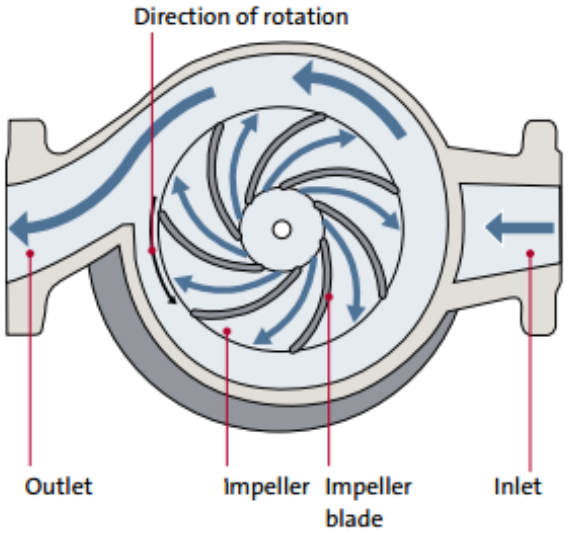

Figure 5-9 A basic diagram of a centrifugal pump (Allpumps, 2016)

Positive displacement pumps

Positive displacement pumps operate by forcing a fixed volume of water from the inlet section into the discharge zone of the pump. There are many kinds of positive displacement pumps, including gear pumps, vane pumps and piston pumps. This latter one is one of the most commonly used. The other two are elaborated in Appendix F. Piston pumps typically use rotary shaft motion converted into axial motion of a piston to produce water flow. As the piston extends, partial vacuum created in the pump chamber draws water through the inlet or suction valve into the chamber. The volume of water drawn into the chamber is then forced out the pump through the discharge valve by the piston. As the piston retracts, the suction of the water closes the discharge and opens the suction valve, letting the same amount of water run into the chamber again. A basic diagram of a piston pump is shown in Figure 5-10.

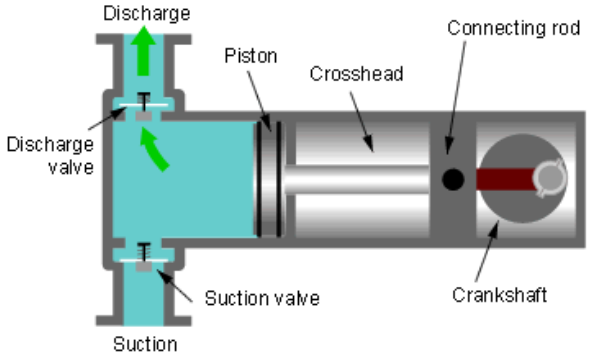

Figure 5-10 Basic diagram of a piston pump (Stackexchange, 2016)

In order to compare above pumps with each other, the typical efficiencies, downsides and advantages of centrifugal- and positive displacement pumps are shown in the table below.

Table 5-2 Overview of centrifugal- and positive displacement pumps characteristics

	Efficiency	Downsides	Advantages
Centrifugal pump	Up to 85%	Does not create suction, which make that a dry pump will not function. Efficiency peaks at best efficiency point. At higher or lower pressure, the efficiency decreases. Flow rate depends a lot on pressure	Relatively easy and therefore cheap construction. Little moving parts. Easy maintenance
Positive displacement pump	Up to 92%	More complicated and therefore more expensive construction. Many moving parts. No easy maintenance	Does create suction. Efficiency depends hardly on pressure. Flow rate depends hardly on pressure

Using Table 5-2, we find that the positive displacement pump has the preference to be used for the LHES system. The main advantages of this pump, together with the high efficiency are key in this decision. The variant of a bend-axis piston pump has the preference, as this particular pump has a rather high efficiency and can operate under high pressures. A bend-axis piston pump works with a number of pistons, which are connected to a rotating disk. Because the plane of rotation of the pistons is at an angle, the distance between each one of the multiple pistons and the valving surface change continually during rotation. Each piston moves away from the valving surface during one half of the rotation, and during the other half it moves towards it. An impression of such a bend-axis piston pump is shown in Figure 5-11.

Figure 5-11 Impression of a bend-axis piston pump (Hydrotech, 2007)

A catalogue of the American bend-axis piston pump manufacturer Parker shows a number of pumps which would work for the LHES system. Three of Parker's F11-010 pumps are chosen to operate. These pumps can easily reach the desired pressure of 70 [bar] and have an individual pumping capacity of 1,67 [l/s], which makes the combined capacity to come up to 5 [l/s]. An impression of such a bend-axis piston pump is shown in Figure 5-12.

Figure 5-12 Impression of a F11-010 pump (Parker, 2016)

Using (Duivendijk, 2007) and assuming a motor efficiency of 95% and a pump efficiency of 92%, we find that the power needed to operate these pumps can be calculated by

$$P = \frac{\rho * g * Q * H}{\eta_m * \eta_p}$$

Where:

P *is the power imput which is needed to operate the pump* $[W]$
ρ *is the density of water* $[kg/m^3]$
g *is the gravitational acceleration* $[m/s^2]$
Q *is the water discharge* $[m^3/s]$
H *is the water head* $[m]$
η *is the efficiency* $[-]$

Which brings that the maximum power input needed to operate all three pumps is P = (1000*9,81*5*10^{-3}*714)/(0,95*0,92) = 40 [kW].

The minimum required power input needed to operate all three pumps is P= (1000*9,81*5*10-3*262)/(0,95*0,92) = 14,7 [kW]. The power input required to operate all three pumps has a linear relation with respect to the time when the storage shaft fills up with water, which increases the pressure inside. This means that the maximum power output of 40 [kW] is only needed to pump the last litres of water back into the storage shaft by all three pumps. However, it is assumed that the pumps are powered by solar panels. When only little power can be delivered by the solar panels, the system is made as such that only one or two of the pumps will operate. This will decrease the pumping capacity by as much as two thirds, but it will also decrease the required power by the same amount. As a rule of thumb, solar panels can deliver a power output of 150 [W/m^2] (Nuon, 2016). This would mean that the maximum required power output of 40 [kW] could be delivered by 267 [m^2] of solar panels on a sunny day, which corresponds to 33 [m^2] of solar panels per household. On a cloudy day, it could happen that the panels do not produce enough energy to fully fill up the storage shafts. This would make the system less useful. A study about the suns behaviour and its optimum storage facility would be useful but is considered outside the scope of this research.

5.3 Safety requirements

In order to identify the safety requirements which have to be met, the Directive 2014/68/EU about pressure equipment (European Parliament , 2014) or PED is consulted. This directive is applicable for the design, manufacture and conformity assessment of pressure equipment and assemblies with a maximum allowable pressure greater than 0,5 [bar]. The requirements described are global in scope and are further elaborated in European Standards NEN-EN 13445-1 to 7. With this standard, a 'Presumption of conformity' can be obtained after which the CE marking can be acquired.

There are four different safety categories stated in the PED, each having different safety modules and requirements which have to be met. Assessment and conformity procedures are different for each category, ranging from self-certification for the lowest safety category (category I), up to full ISO9001 quality management and/or notified body type examination for category IV equipment. The different safety categories are shown in Table 5-3.

Table 5-3 Safety categories of pressure equipment and their modules, as stated in (European Parliament , 2014)

I	=	Module A
II	=	Modules A2, D1, E1
III	=	Modules B (design type) + D, B (design type) + F, B (production type) + E, B (production type) + C2, H
IV	=	Modules B (production type) + D, B (production type) + F, G, H1

Where the modules stand for the following:

Module A: Internal production control
Module B: EC type-examination
Module C: Conformity to type
Module D: Production quality assurance
Module E: Product quality assurance
Module F: Product verification
Module G: Unit verification
Module H: Full quality assurance

The four different categories are classifications on the basis of:

- The maximum allowable pressure 'PS' in the system
- The volume 'V' of the equipment
- The group of fluids for which the equipment is intended

When these values are known, the safety category of the system can be found by filling the maximum allowable pressure and volume into the graphs which correspond to the fluid (gases and liquids) group. For our system, the maximum allowable pressure is set at 70 [bar], and the volume –which depends on the number of piles use, is larger than 10.000 [L]. In the directive, a distinction between two groups of fluids is made. Our design describes a pressure vessel which houses water as well as air. As both of

these fluids are non-toxic, non-flammable and non-oxidising, they are classified in fluid group 2. Taking above into account, we can find the corresponding safety categories as shown in the graphs below.

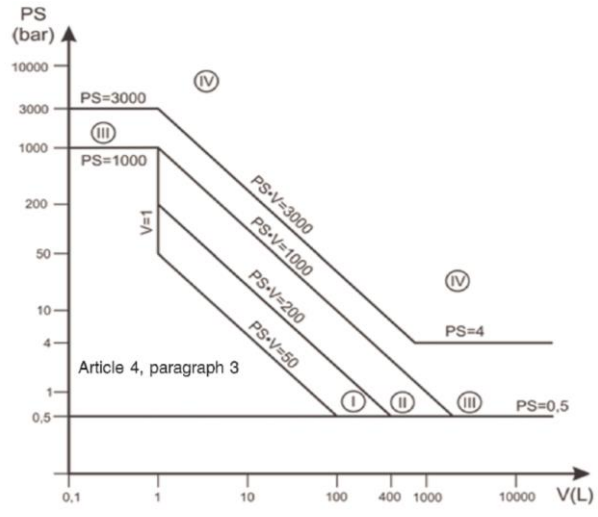

Figure 5-13 Graph with safety categories for pressure vessels with gases of group 2 (European Parliament , 2014)

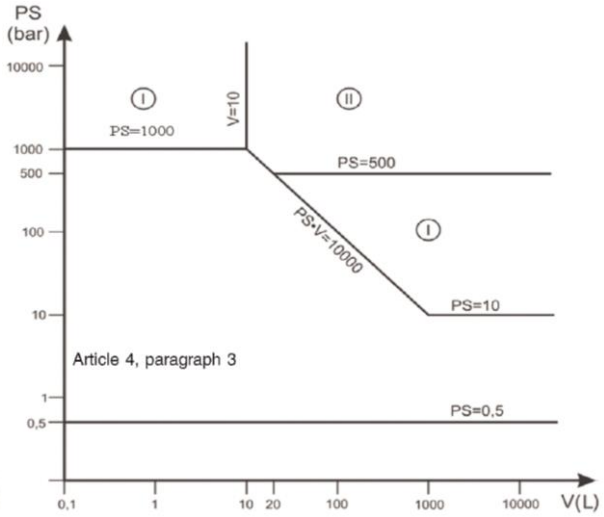

Figure 5-14 Graph with safety categories for pressure vessels with liquids of group 2 (European Parliament , 2014)

From above graphs, we find that the pressurized air in our system is situated in category IV and the water under pressure is situated in category I. When the pressure vessel contains more than one fluid, the classification has to be on the basis of the fluid which requires the highest safety category. It is therefore that our system should fulfil the safety requirements of category IV and thus the Modules B (production type) + D, B (production type) + F, G and H1.

These modules state (in broad outlines) the following safety requirements:

Protection requirements

- The equipment must be designed for adequate strength taking into account internal and external pressure, temperature changes due to operation or climate, static pressure and mass of contents in operating and test conditions, traffic, wind, earthquake loading, corrosion and erosion, fatigue, etc.
- The equipment must be provided with means to ensure safe handling and operation and of examination, draining and venting.
- The equipment must be provided with protection against exceeding the allowable limits of pressure.
- Where necessary, pressure equipment must be designed and fitted with suitable accessories to meet damage-limitation requirements in the event of an external fire
- Non-destructive tests of permanent joints must be carried out by suitable qualified personnel. The personnel must be approved by the relevant authorities. Suitable procedures must also be established to provide traceability of materials and components from supply to finished product.

- The manufacturer shall operate an approved quality system for production, final product inspection and testing of the pressure equipment and shall be subject to surveillance by a notified body.
- A notified body shall carry out the appropriate examinations and tests in order to check the conformity of the pressure equipment with the approved type described in the EU-type examination certificate and with the appropriate requirements of this Directive.
- The examinations and tests to check the conformity of the pressure equipment with the appropriate requirements shall be carried out by examination and testing of every product under its design pressure.

Administration requirements

In addition to ensuring that the equipment is capable of meeting the essential performance requirements of the directive, manufacturers must also provide adequate instructions with equipment they sell, they must complete a specified declaration of conformity and they must maintain a technical file of information about how the equipment was designed and manufactured. These files and certificates of conformity has to be kept available for inspection by the relevant authorities for 10 years after the pressure equipment has been placed on the market. Furthermore, the pressure equipment itself has to be provided with at least:

- The identification of the manufacturer
- The unique identification of model and serial number
- The year of manufacture
- The maximum/minimum allowable pressure limits
- The CE-logo

Further specific requirements depend on the individual product which is considered, and are therefore not described in the directive.

5.4 Steel pile design

The following assumptions are made for the design of the steel piles:

- Temperature changes are not taken into account. A constant temperature of 20 degrees is assumed
- The self-weight of the piles is neglected
- The piles are considered to have enough bearing capacity to bear the structure on top
- Upscaling the thickness of the shell or adding (local) stiffeners as a result of the weight on top is assumed not to be necessary
- A design lifetime of 50 years is chosen
- Wind, snow, ice and earthquake loading are not taken into account
- Shock loads caused by water hammering or surging of the piles are not taken into account
- Fatigue is not taken into account, as the number of expected pressure cycles is relatively low (< 20.000 cycles)

In order to design the piles for our system, the 'NEN-EN 13445 Unfired pressure vessels' European Standard is consulted.

Internal pressure

The piles must be designed for adequate strength taking the maximum allowable internal pressure into account. The required thickness of a cylindrical shell can be calculated using:

$$e = \frac{p * D_e}{2f * z + p}$$

Where:

p	*is the calculation pressure*	*= 7 [MPa]*
D_e	*is the outside diameter*	*= 762 [mm]*
f	*is the nominal design stress*	*[MPa]*
z	*is joint coefficient*	*= 1 [-]*

The nominal design stress of our steel 'f' can be found with f = (R_m)/2,4. With R_m being the tensile strength of steel. In order to reduce the required wall thickness but remain within standard material quality, steel grade S355 is the chosen quality for the steel piles. For S355 steel, we find a R_m of 355 [MPa] and an 'f' of 147,92 [MPa], which gives a required thickness 'e' of 18 [mm].

Corrosion allowance

In order to allow a certain amount of corrosion, an additional thickness sufficient for the design life of the piles shall be provided. This way, a cathodic protection is not needed. The definitions of the various thicknesses are shown in the figure below.

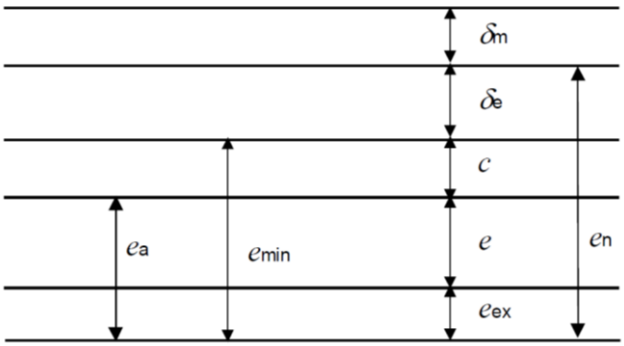

Figure 5-15 Definitions of the various wall thicknesses (NEN-EN, 2014)

Where:

e *is the required thickness*

e_n *is the nominal thickness*

e_{min} *is the minimum possible fabrication thickness* ($e_{min} = e_n - \delta_e$)

c *is the corrosion allowance*

e_a *is the analysis thickness* ($e_a = e_{min} - c$)

δ_e *is the absolute value of the possible negative tolerance on the nominal thickness*

δ_m *is the allowance for possible thinning during manufacturing process*

e_{ex} *is the extra thickness to make up to the nominal thickness*

The minimum possible fabrication thickness for these diameter piles is 8 [mm] (ArcelorMittal, 2016). The corrosion allowance is assumed to be 2 [mm]. This assumption is based on the fact that the inside of the pile is a closed off area, where fresh air only comes in during maintenance, and the fact that the outside of the pile has to deal with possible fluctuation of the groundwater. For the negative tolerances no additional thickness is taken into account, as these tolerances are considered to be very small. Furthermore, the piles are assumed not to be thinned during the manufacturing process, which brings the nominal thickness of the piles to be 20 [mm].

External pressure

The external soil- and water pressure is considered to be not normative for the wall thickness of the piles. In the situation where the piles are 'empty' and do not have an internal pressure, the external pressure, existing of maximum 18 meters water column and 20 meters soil pressure will still be order of magnitude 10 to 20 times smaller than the maximum internal pressure.

Domed end thickness

The circular, upper domed end of the piles has to withstand the same maximum pressure of 70 [bar]. Furthermore, the domed end will be provided with an opening as the figure below shows. This opening is needed so a pipeline fits through and the system is able to move water back and forward.

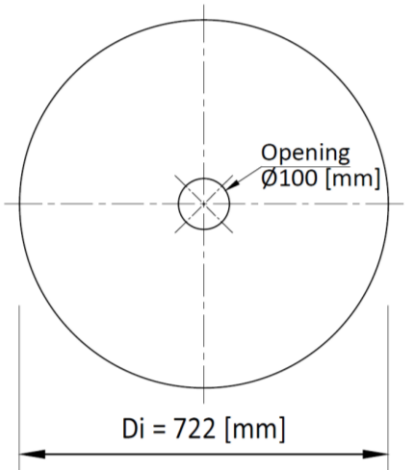

Figure 5-16 Top flat end of the piles, provided with an opening for a pipeline

For a domed end welded to the shell, the thickness can be calculated using:

$$e = \frac{5p * D_i}{12 * f}$$

Where:

e	*is the required thickness of the domed end.*	
D_i	*is the inside diameter*	*= 722 [mm]*
p	*is the calculation pressure*	*= 7 [MPa]*
f	*is the nominal design stress*	*= 147,92 [MPa]*

Which gives a thickness of the domed end of e = (5*7*722)/(12*147,92) = 15 [mm].

Furthermore, additional local stiffeners are expected around the central opening.

Lower end drill tip

In order to install the piles, a drilling method is used. Therefore, at the lower end of the pile, a drill tip is welded. It is assumed that the welding quality of this weld is sufficient to withstand the maximum internal pressure of the system. The drill tip, solidly connected to the pile, guides the pile into the soil as the drill machine applies axial pressure and torque on the pile.

Figure 5-17 A drill tip is welded to a steel foundation pile (Solines, 2016)

5.5 Pipelines

The pipelines of the LHES system transport the water from the storage shaft through the pump-turbine chamber into the water tanks and vice versa. The outside diameter of the pipelines is chosen to be 100 [mm], the wall thickness 5 [mm]. The expected friction losses can be expressed in the form of a head loss in meters by making use of the Darcy – Weisbach equation:

$$h_L = f * \frac{L}{D_i} * \frac{v^2}{2g}$$

Where:

h_L	*is the calculated head loss*	*[m]*
f	*is the friction factor*	*[-]*
L	*is the length of the pipeline*	*= 50 [m] (approximately)*
D_i	*is the inside diameter of the pipeline*	*= 0,09 [m]*
v	*is the velocity of the water*	*[m^2/s]*
g	*is the gravitational acceleration*	*= 9,81 [m/s^2]*

The velocity of the water can be calculated using $v = q/(\pi * D_i^2/4) = 0{,}005/(\pi * 0{,}09^2/4) = 0{,}79$ [m/s]. The friction factor '*f*' can be calculated using the Aldsul equation:

$$f = 0{,}11 * \left(\frac{\varepsilon}{D_i} + \frac{68}{Re}\right)^{1/4}$$

Where 'ε' is the absolute roughness coefficient of the material, which is 0,045 [mm] for a commercial steel pipe (Engineering Toolbox, 2016). The Reynolds number 'Re' can be calculated taking into account that our system contains water with a ρ_{water} = 1000 [kg/m^3] and a kinematic coefficient of viscosity *v* = 10^{-6} [m^2/s]. The Reynolds number $Re = v*D_i/v = 0{,}79*0{,}09/10^{-6} = 70735$ (turbulent flow). This gives a friction factor '*f*' of 0,0215.

The head loss then becomes: $h_L = (f*L*v^2)/(D_i*2g) = (0{,}0215*50*0{,}79^2)/(0{,}09*2*9{,}81) = 0{,}38$ [m]. This number is considered as negligibly small and is therefore not taken into account when calculating the roundtrip efficiency of the system.

5.6 Installation plan

The pipelines are installed as such, that every elbow or other connection point is relatively easy reachable. As such connection points are always weak spots, it is preferred that inspection on leakages or other malfunctions can happen relatively easy. A horizontal pipeline enters the steel pile through an opening on the side of the pile. An elbow piece connects the horizontal pipeline with a vertical pipeline which pierces the domed end of the steel pile and runs all the way through to about 5 cm of the bottom end of the pile. The steel pile itself is equipped with a drill tip at the lower end and is supporting a concrete beam which is loaded with the weight of the houses on top. A principle sketch of this is shown in Figure 5-18.

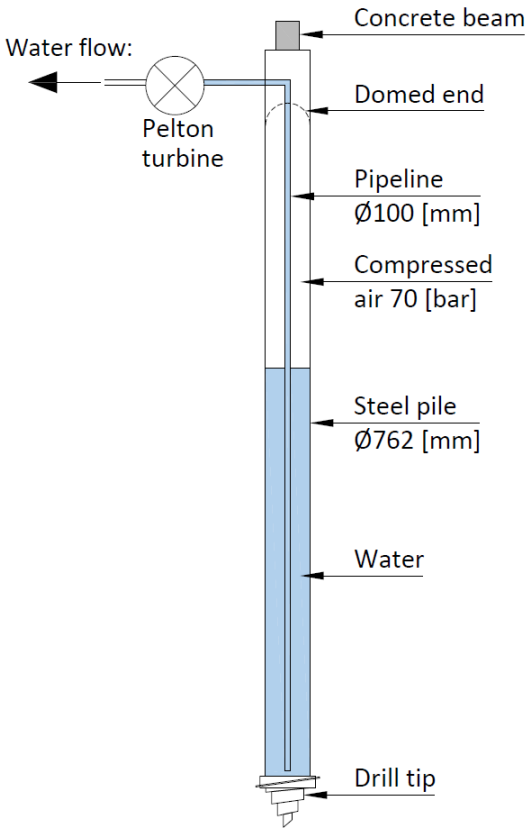

Figure 5-18 Principle sketch of the steel pile and the pipelines of the LHES system

The LHES system is considered to store a sufficient amount of energy for eight households, using the following assumptions:

Table 5-4 Assumptions for a single household

Characteristics	Value	[unit]	Source
Yearly electricity demand of a household	3500	[kWh]	(Nuon, 2016)
Yearly electricity production of solar panels	130	[kWh/m^2]	(Nuon, 2016)
Amount of solar panels needed per household	27	[m^2]	
Typical storage needed per household	8-12	[kWh/day]	

If we make a pile plan for a street with eight houses, we find that the foundation of such a street could consist of nine rows of three piles. This would mean that the total amount of steel piles comes up to 27 as can be seen in Figure 5-20. Part of these piles are storage shafts, the other part will function as a water tank. As the storage shafts contain a maximum of 63% of water, the amount of water tank piles needs to be at least 0,63 times the amount of storage shaft piles. For this reason, the LHES system will consist of sixteen storage shaft piles and eleven water tank piles. The piles, with an inside diameter of 722 [mm] and a length of 20 [m], have a volume of 8,2 [m^3]. This means that the sixteen storage shaft piles house a combined water volume of 82,7 [m^3].

With a maximum flow rate of 0,005 [m^3/s], this system could provide electricity for a minimum of 4,5 hours before it would run out of water. The LHES system capacity is 93 [kWh]. To give an idea of how this would look like in practice, the supply and demand of electricity for the eight houses provided with the LHES system are graphed in Figure 5-19 for a typical day. In this figure, the supply curve of the solar panels and the demand curve of the households are suggestive, as they depend on many variables. For the supply curve, the solar power production on a perfect sunny day in spring is suggested. The dashed demand curve is an estimation of what power the eight households could use, taking into account the different machines used in a household and a typical peak when electric stoves are being used. The maximum delivery curve of the LHES system is projected on the right end in red. This curve shows the maximum delivery of the system. In case less power is required, the LHES system could deliver its 93 [kWh] capacity over a longer period of time.

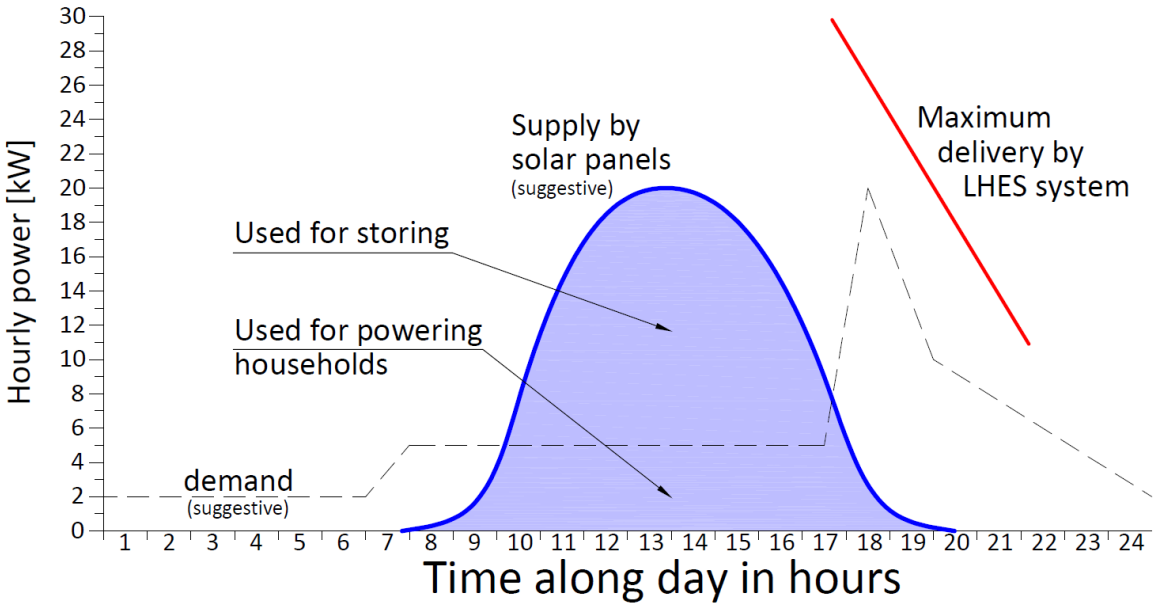

Supply:	Power delivered by LHES system or by grid	Power delivered by solar panels	Power delivered by LHES system	
Activity:	People are sleeping. Alarm clock, fridge & freezer	Breakfast. Lights, kitchen machines	People are working during the day. Laundry machine, vacuum cleaner, computer	Cooking, lights, kitchen machines	Lights, TV, computer, dishwasher, coffee machine

Figure 5-19 Usage of the LHES system on a typical day

Furthermore, the turbine and pumps are placed in a small technical room on the corner of the street. This way, the equipment is easily accessible for maintenance. Two water taps are installed on each side of the turbine. These taps are opened when the turbine is generating power and closed when the pumps are storing the water back in the storage shafts. Furthermore, a pressure relief valve is installed to make sure the maximum pressure of 70 [bar] is not exceeded. A schematic drawing of this installation plan is shown below and in Appendix G.

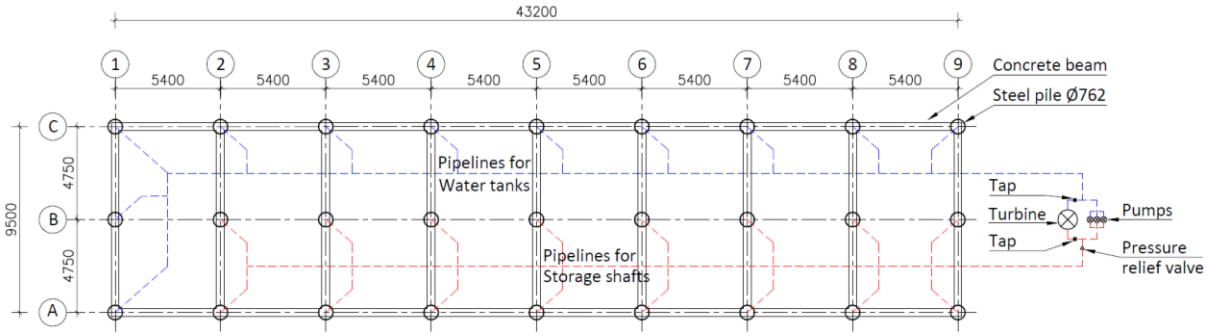

Figure 5-20 Schematic drawing of the installation plan (top view)

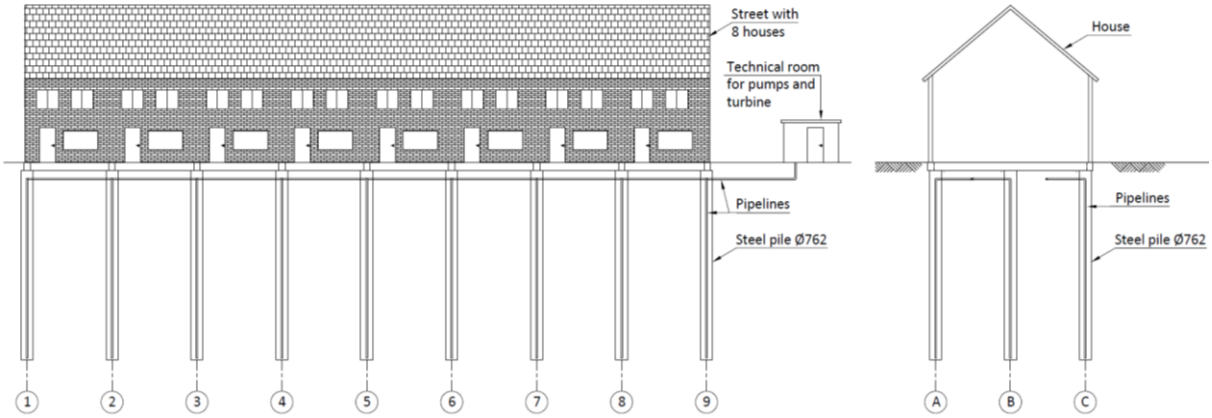

Figure 5-21 Situation sketch of the LHES system (front and side view)

Figure 5-22 Impression of a street of houses equipped with a LHES system

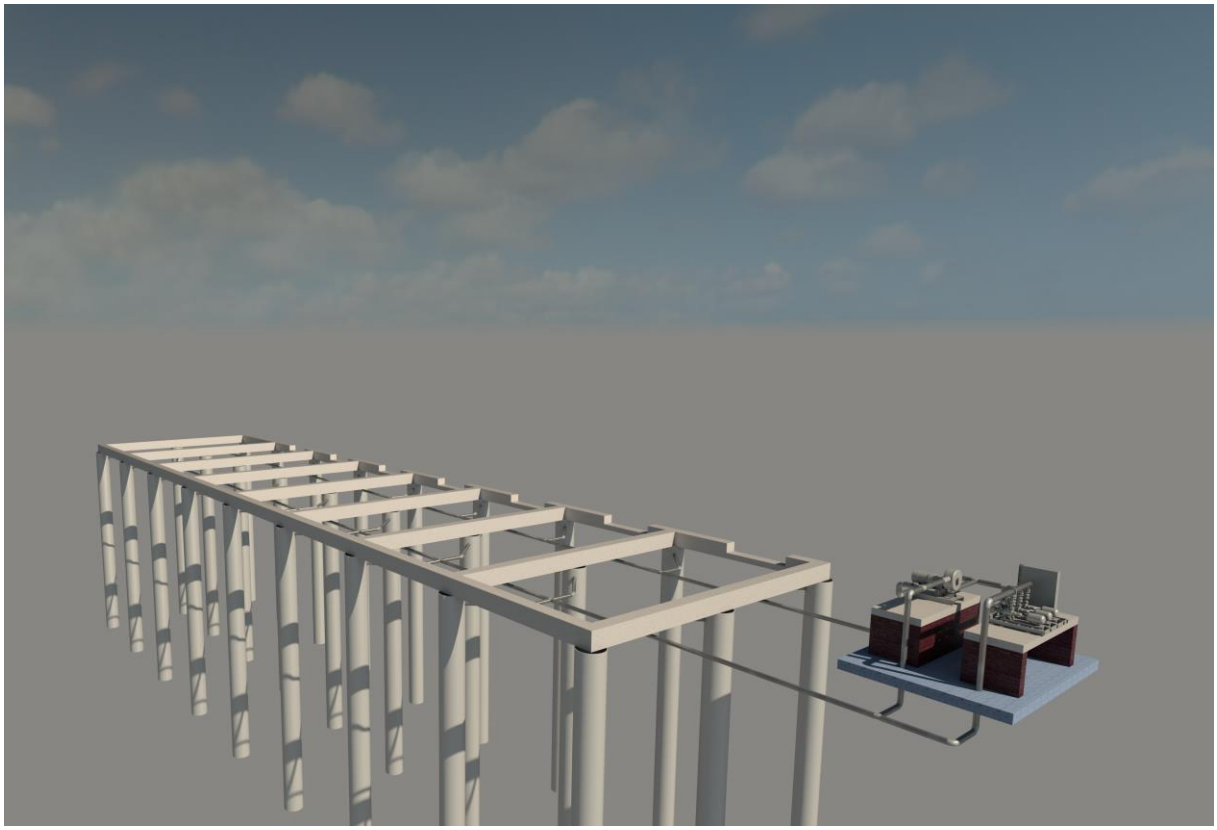

Figure 5-23 Impression of the LHES system without the houses on top. The steel piles, foundation beams, pipelines and the technical room are shown

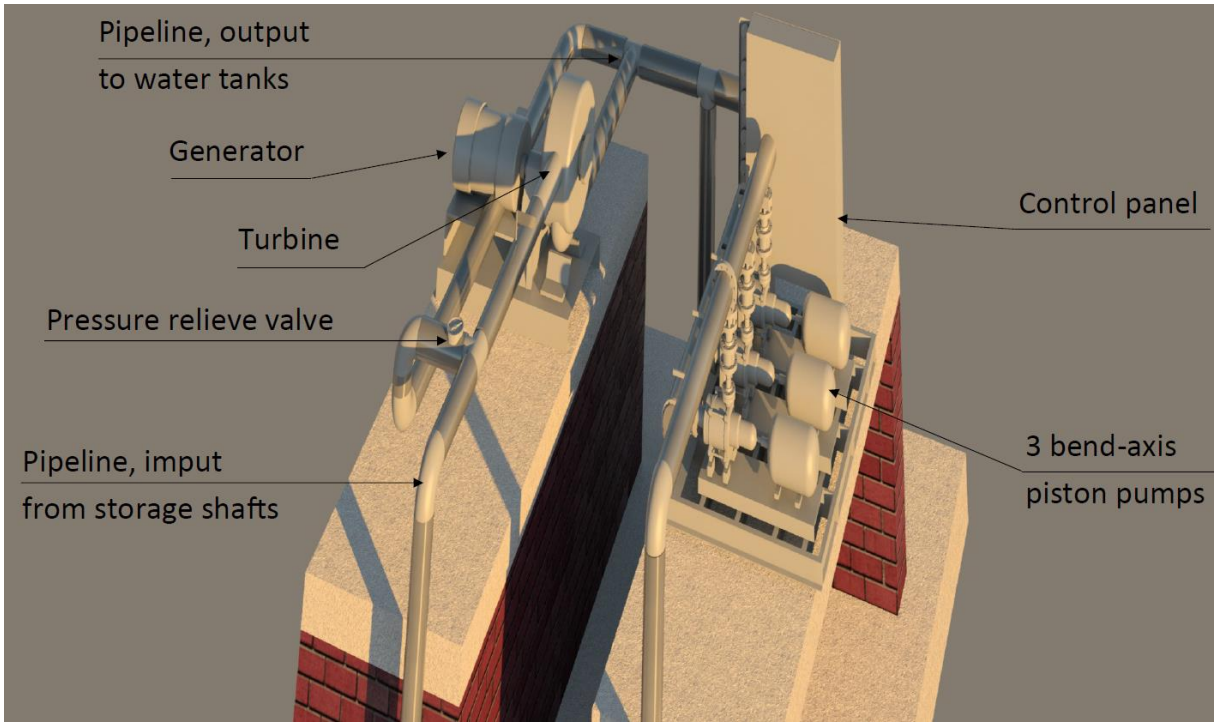

Figure 5-24 Impression of the inside of the technical room

5.7 Roundtrip efficiency

Where the previous part of this chapter showed that the friction losses in the pipelines are negligible, a head loss calculation due to the fact that the water must stream is shown in this part. The total amount of losses is then summed up, which results in the roundtrip efficiency of the system.

5.7.1 Head loss

When water flows from an open reservoir through a turbine, a certain amount of the potential energy is lost due to the fact that the last water parts lack the water pressure to power the turbine. Basically, the energy head ΔH can be subdivided into a resistance part ΔHr and a part which powers the turbine ΔHt as the figure below shows.

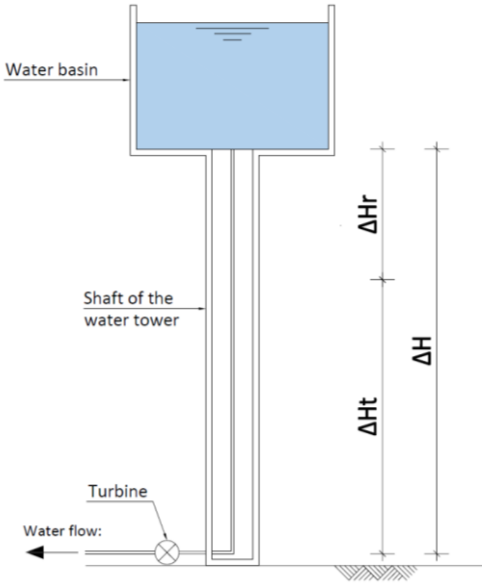

Figure 5-25 Subdivision of ΔH into ΔH_r and ΔH_t

Both ΔHt and ΔHr can be written as a part of ΔH using a loss factor α, where:
ΔHt = α * ΔH
ΔHr = (1 - α) * ΔH

In order to determine this loss factor α, we need the Bernoulli equation for incompressible flows, which states that the sum of pressure, elevation and flow speed at any arbitrary point along a streamline should constant. Normalizing this equation in terms of energy head, we find:

$$h + \frac{p}{\rho * g} + \frac{v^2}{2g} = constant$$

Where:

h	*is the elevation of a point above the reference level*	*[m]*
p	*is the pressure at the chosen point*	*[Pa]*
ρ	*is the water density*	*[kg/m³]*
g	*is the gravitational acceleration*	*[m/s²]*
v	*is the water flow speed at a point of the streamline*	*[m/s]*

In our LHES system, the water reservoir is loaded by compressed air, as Figure 5-26 shows. Two points are looked at. Point 1 is situated on top of the maximum water level. At this point, the flow speed is assumed to be zero. Point 2 is situated on the reference level, right when the water leaves the Pelton nozzle. The pressure which is acting on the water is equal to the atmospheric pressure here. The corresponding Bernoulli equation is:

$$h_1 + \frac{p_1}{\rho * g} = \frac{p_2}{\rho * g} + \frac{v_2^2}{2g}$$

Which results in:

$$\frac{v_2^2}{2g} = h_1 + \frac{p_1}{\rho * g} - \frac{p_2}{\rho * g}$$

Where:

$p_1 = 7 * 10^6$ [Pa]
$\rho = 1000$ [kg/m^3]
$g = 9{,}81$ [m/s^2]
$h_1 = -4{,}5$ [m]
$p_2 = 1$ [atm] = $1{,}01325 * 10^5$ [Pa]

Which results in a total energy head of:

$$\Delta H = h_1 + \frac{p_1}{\rho * g} - \frac{p_2}{\rho * g} = 699\ [m]$$

And a water velocity of:

$$v = \sqrt{2g * \Delta H}$$

We know that the flow rate 'Q' can be calculated by multiplying the cross sectional area 'A' of the pipeline times the velocity of the water 'v':

$$Q = A * v$$

And that the flow rate at the turbine (point 2) should be the same flow rate as anywhere in the pipeline, which gives:

$$Q_t = Q_r = A * \sqrt{2g * \Delta H_r}$$

With ΔHr = (1 - α) * ΔH, we find:

$$Q_t = A * \sqrt{1 - \alpha} * \sqrt{2g * \Delta H}$$

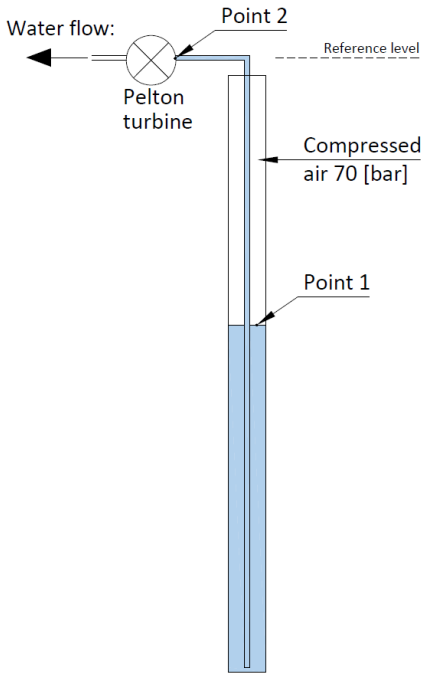

Figure 5-26 Principle of the situation in the LHES system

For our given flow rate of 0,005 [m^3/s], pipeline with D_e = 100 mm, e = 5 [mm] and A = 2256 * 10^{-6} [m^2], we find a loss factor 'α' of 0,9996. This value is so near to 1,0 that we can assume the turbine energy head 'ΔHr' to be equal to our potential energy head 'ΔH'. The corresponding velocity of the flow right when the water leaves the Pelton nozzle is 117 [m/s].

5.7.2 System efficiency

In order to determine the total efficiency of the system, the estimated efficiencies for all the different parts are multiplied with each other. When the system is just build, an air compressor fills up the piles until an air pressure of 25,8 [bar] is reached. This air compressor has an estimated efficiency of 70% (mainly due to heat losses), but is only used before the first storage cycle and after each maintenance and is therefore not taken into account when determining the roundtrip efficiency of one storage cycle.

When the storage piles are filled up with compressed air, the water is pumped in. The motor which drives the pump as an estimated efficiency of 98%. The pump itself has an efficiency of 92%. Transport losses in the pipelines are neglected. The system can now be used to generate power by using a Pelton turbine with an efficiency of 90% and a generator with an estimated efficiency of 98%. The electricity is then delivered to the grid using a transformer with an efficiency of 95%.

Multiplying these numbers gives us a roundtrip efficiency of 76%.

6 Preliminary risk Analysis

To give an idea about the potential risks which may come with the LHES system, a preliminary risk analysis is made. A comprehensive risk analysis for this system should be made, but is considered outside the scope of this research. First, a comparison with other systems which are used in households is made. Then, the possible risks of the LHES system are mapped, shown in fault trees and quantified using failure probabilities per year.

6.1 Comparison with other systems

To get a feeling of what risks might be involved with our LHES system, a comparison is made with other pressurized systems used in a household.

Refrigerators

Refrigerators use a compressor to compress and circulate a fluid refrigerant. Typically refrigerators use a mixture of butane and propane as a refrigerant and compress it to around 8 [bar] (Real Simple, 2016). Compressing the fluid makes its temperature rise. The relatively cool temperature of the air in the kitchen cools the fluid down, making it a liquid. The liquid is then slightly expanded by a expansion device. This makes the fluids temperature drop even further. The fluid then flows into the coils inside the fridge, cooling it down. Eventually, the fluid evaporates to a gas and flows back to the compressor where the cycle starts all over. A schematic sketch is shown in Figure 6-1.

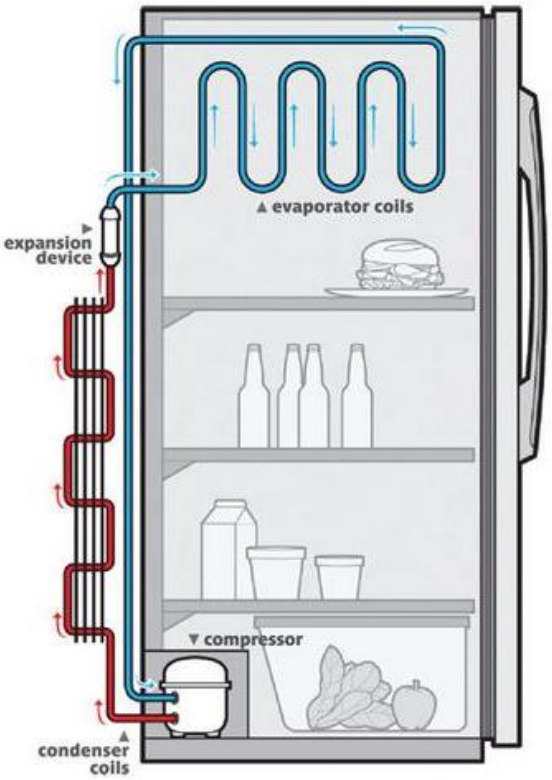

Figure 6-1 Schematic drawing of a refrigerator (Real Simple, 2016)

Heat pumps

Low temperature waste heat flow can be used and upgraded to high temperature heat, with the use of a heat pump. This works by making use of an increased boiling point of a fluid when the pressure of this fluid has increased. Typical heat pumps work with Ammonia as a fluid. At low pressure and temperature, the Ammonia is evaporated in the evaporator. The energy needed for this is provided by the waste heat flow, for instance the outside air. Then, the compressor increases the pressure of the Ammonia, typically up to about 40 [bar] (Industrialheatpumps, 2016). This will increase the temperature of the Ammonia, making it useful for heating purposes. After heating the desired space (for instance the inside of a house), the Ammonia is transported to the expansion device, which lowers

the pressure. The gas condenses back to liquid and flows back to the starting point of yet another cycle as is shown in the figure below.

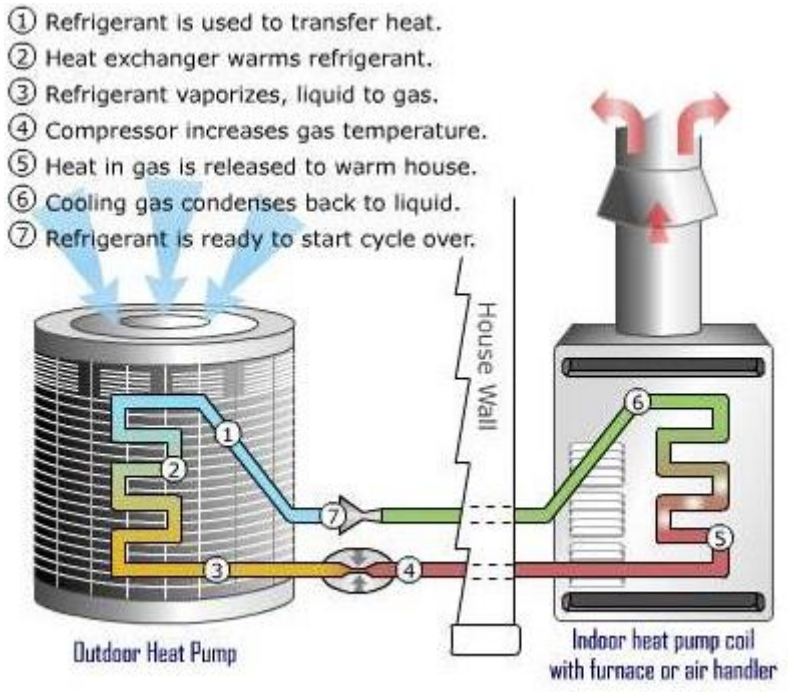

Figure 6-2 Chart which shows how a heat pump works (Sterling Heating and AC, 2016)

6.2 Possible risks

The safety risks of the LHES system are mapped and calculated in this chapter. These risks can be subdivided into a reliability risk, which is the risk that the system will not operate, and a fatality risk, which is the risk of an accident happening which may cause a fatal accident. The LHES system considered exists of 27 steel piles of which sixteen function as a storage shaft. These sixteen storage shafts have a total volume of 131 [m^3] and are put under a maximum pressure of 70 [bar]. Pressurized air and water is stored here at environmental temperatures. Both these fluids are non-toxic and non-flammable. Furthermore, a safety valve is installed and programmed to open at pressures above 70 [bar]. Before the first use, a compressor is used to pump air up to 25,8 [bar] into the storage shafts. Furthermore, the water tanks are filled with water. The LHES system can now start storing energy by pumping the water from the water tanks into the storage shafts. When this water is released, it runs through the turbine which generates power.

6.2.1 Reliability risk

The reliability risks of the LHES system are determined by accident scenarios of the underground shafts, its pipelines, pump- turbine equipment and of the compressor used during filling. For the reliability risks a fault tree is shown in the figure below. For the shaft and pipelines, a distinction is made between a small leakage and an actual breach of the elements. This fault tree shows the different scenarios which can cause operation failure of the LHES system.

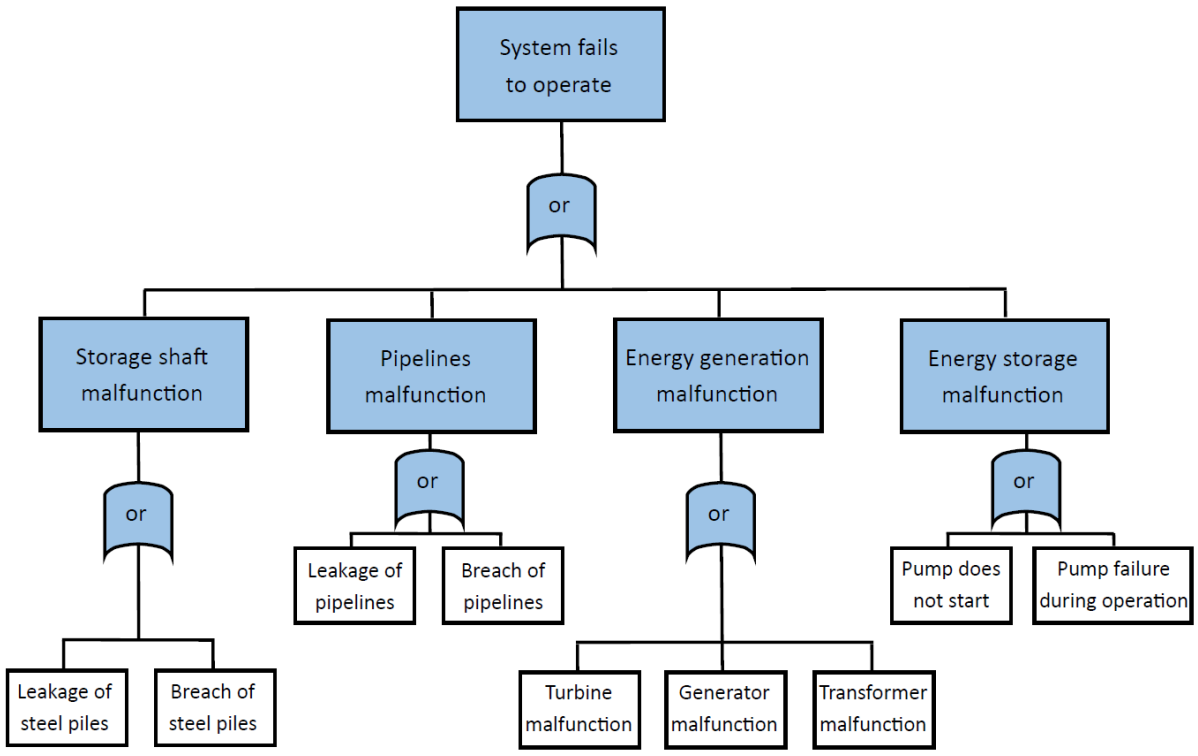

Figure 6-3 Fault tree of the reliability risks

By quantifying the probability of a certain scenario to occur, the total probability of a system failure can be calculated. For different scenarios, probabilities of occurrence are found in different literature studies. For scenarios without a known occurrence probability, an assumption is made. The scenarios for the reliability risks and their probability of occurrence per year are shown in the table below.

Table 6-1 Scenarios causing system failure with their chances of occurrence

Scenario	Probability [/yr]	Source	Explanation
Leakage of steel piles	$1,6 * 10^{-4}$	(RIVM, 2009)	Based on sixteen piles times 20 [m] and a $5*10^{-7}$ leakage probability per meter pile per year
Breach of steel piles	$3,2 * 10^{-5}$	(RIVM, 2009)	Based on sixteen piles times 20 [m] and a $1*10^{-7}$ breaching probability per meter per year
Leakage of pipelines	$4 * 10^{-4}$	(RIVM, 2009)	Based on approximately 200 [m] pipeline and a $2*10^{-6}$ leakage probability per meter per year
Breach of the pipelines	$6 * 10^{-5}$	(RIVM, 2009)	Based on approximately 200 [m] pipeline and a $3*10^{-7}$ breaching probability per meter per year
Turbine malfunctions	$1 * 10^{-4}$	Assumption	
Generator malfunctions	$3 * 10^{-4}$	Assumption	
Transformer malfunctions	$1,2 * 10^{-3}$	(TAW, 2003)	Based on 1200 running hours a year and $1*10^{-6}$ failure probability per hour ($P = 1-(1-1,0*10^{-6})^{1200}$)
Pump does not start	$1,0 * 10^{-4}$	(RIVM, 2009)	For positive displacement pumps
Pump failure during operation	$4,4 * 10^{-3}$	(RIVM, 2009)	For positive displacement pumps

Using these different scenarios, we can calculate the failure probability of the system. We find a storage shaft malfunction probability of $1,9*10^{-4}$, a Pipeline malfunction probability of $4,6*10^{-4}$, an energy generation malfunction probability of $1,6*10^{-3}$ and an energy storage malfunction probability of $4,4*10^{-3}$. This brings the probability that the system will fail to operate to come up to $6,6*10^{-3}$. The consequence of such a failure is that the LHES system does not produce power and the users will have to use power from the grid instead. The largest risks and their control measures are listed in the following table:

Table 6-2 Largest reliability risks of the LHES system

Scenario	Failure probability per year	Control measure
Pump failure during operation	$4,4 * 10^{-3}$	Regular inspections. Possibly installing a reserve pump or decide to accept one of the three pumps to fail and repair/exchange it
Transformer malfunctions	$1,2 * 10^{-3}$	Repair/exchange it when needed

As can be seen from Table 6-2, the largest reliability risks of the LHES system are rather easy to control. Therefore, no serious operation problems are expected. Furthermore, the average downtime of the system in case of a failure is expected to be small (< 1 day), as most of the failure scenarios are easy to fix. The expected unavailability of the system can then be estimated by multiplying the failure probability times the downtime. This brings the expected yearly availability to come up to $1 - 6,6*10^{-3} * (1/365) = 99,9982\%$. Compared to the Dutch electricity grid, which was available for 99,9937% of the time in 2015 (H. Wolse, 2016), one may conclude that these low failure rates are not uncommon.

6.2.2 Fatality risk

The fatality risks of the LHES system focus on the possibility of a fatal accident to occur. Since the system works with fluids under pressure, a number of scenarios with fatal consequences could happen. A number of these scenarios are:

- Explosion due to damage of a storage shaft. A sudden breach of a storage shaft may cause the pressurized air to escape at once and cause an explosion. The breach can happen due to corrosion or fatigue of the material. Impacts from outside could also be of influence.
- Explosion due to damage of a pipeline. If a pipeline breaches, the pressurized air inside will try to escape at once and may cause an explosion. Breaches can happen due to corrosion or fatigue of the material. Impacts from outside, such as uneven subsidence of the piles, could also be of influence.

- In theory a so called 'BLEVE' scenario (Boiling Liquid Expanding Vapour Explosion) could also occur. This could happen when an outside heating source, for instance a fire, heats up the LHES system. However, it can only occur if the water temperature inside the storage shafts increases a lot. At atmospheric pressure, the boiling point of water is 100 °C. But water under pressure has a much higher boiling point. For water under 70 [bar] of pressure, as is the case in the LHES system, the boiling point lies at 290 °C (Engineering Toolbox, 2016). When the water temperature comes above this value, the water vaporizes. As the liquid changes to a gas it expands, making the pressure inside the LHES system to rise. The pressure relief valve would normally open to release this additional pressure, making the thread of a BLEVE disappear. But in case the pressure relief valve is not close or large enough or fails due to another matter, the pressure inside the storage shaft may increase until it ruptures. If the rupture is catastrophic, the pressure which prevented the water from boiling at 100 °C will be immediately lost. Suddenly the large mass of liquid water, which has a very high temperature and a very low pressure, will boil instantaneously, which in turn causes an extremely rapid expansion. Depending on the temperatures and pressures involved, that expansion may be so rapid that it can be classified as an explosion, fully capable of causing severe damage to the outside world (Peterson, 2002). The scenario of a BLEVE to occur in the LHES is considered not possible, as the water is stored underground for most part, and therefore kept cool even during a fire.

A fault tree of the fatality risks is shown in the figure below. This fault tree shows the different scenarios which can cause a fatal accident to occur.

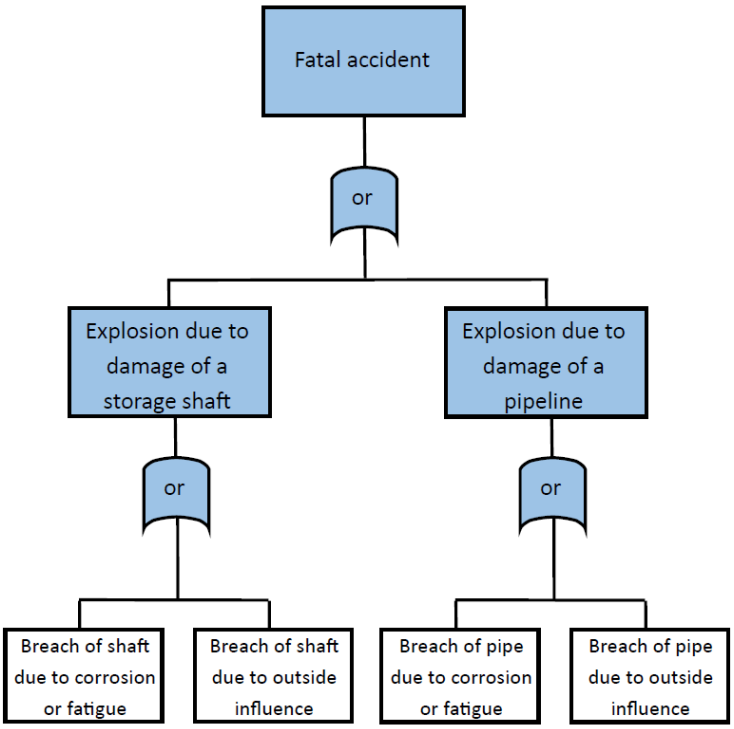

Figure 6-4 Fault tree of the fatality risks

For above scenarios, the chances of occurrence per year are shown in the table below:

Table 6-3 Scenarios causing system failure with their chances of occurrence

Scenario	Probability [/yr]	Source	Explanation
Breach of shaft due to corrosion or fatigue	$3,2 * 10^{-5}$	(RIVM, 2009)	Based on sixteen piles times 20 [m] and a $1*10^{-7}$ breaching probability per meter per year
Breach of shaft due to outside influence	$1*10^{-8}$	Assumption	
Breach of pipeline due to corrosion or fatigue	$6 * 10^{-5}$	(RIVM, 2009)	Based on approximately 200 [m] pipeline and a $3*10^{-7}$ breaching probability per meter per year
Breach of pipeline due to outside influence	$1*10^{-7}$	Assumption	Taking subsidence of the piles and possible heavy traffic loading op top the pipelines into account

Calculation the failure probabilities, we find an 'explosion due to damage of a storage shaft' probability of $3,2*10^{-5}$, and an 'explosion due to damage of a pipeline' probability of $6*10^{-5}$. If such a scenario will occur, casualties can be expected. To make an estimation about the number of potential casualties, it is assumed that on average 2,4 people live in each house (VROM, 2007). These people are assumed to present 50% of the time during the day (from 08.00 until 18.30 o clock) and 100% of the time during the night (from 18.30 until 08.00 o clock) (VROM, 2007). This makes that the number of potential casualties for all eight households lies between 10 and 20.

Although the number of potential casualties is considered high, the probability of a failure to occur is considered to be very low. The largest risks and their control measures are listed in the following table:

Table 6-4 Largest fatality risks of the LHES system

Scenario	Failure probability per year	Control measure
Breach of shaft due to corrosion or fatigue	$3,2 * 10^{-5}$	Regular inspections. Provide extra thickness for corrosion allowance. Installing of safety taps on each storage shaft.
Breach of pipeline due to corrosion or fatigue	$6 * 10^{-5}$	Regular inspections. Replacement of damaged parts.

As can be seen from Table 6-4, the largest fatality risks of the LHES system are well controllable. The pipelines and tops of the steel piles are positioned as such, so regular inspection is possible. All elbow- and other connection pipeline pieces are situated below the ground floor of the houses, but above the soil level. They are therefore easily reached, inspected and replaced when needed. However, the failure probabilities used above are standard values obtained from literature, and applied for a very specific application. One may question reliability of these numbers and thereby the reliability of the system. Therefore, a comprehensive risk analysis of the LHES system is desirable, before a definitive conclusion about the safety can be made. Such a comprehensive risk analysis is, however, considered outside the scope of this research.

7 Economic analysis

In order to make a proper economic analysis, the total construction and operation costs of the LHES system are determined. Then, the benefits and possible cost-saving quantities are calculated for a worst case- and best case scenario. The economic feasibility of the system is determined using these numbers.

7.1 Costs of the LHES system

Steel piles

The steel foundation piles that are used in the LHES system are expected to be largest part of the total expenses. Using prices of steel found in (Breedveld Staal, 2015), a price of € 0,90 per kilogram is assumed for the 27 steel piles with steel grade S355, an outside diameter of 762 [mm], a wall thickness of 20 [mm] and a length of 20 [m]. This assumption is based on the fact that the piles can be delivered in a rather large quantity, which lowers the price per pile. When the piles are delivered, a drill head needs to be attached. This is assumed to cost € 500,- per drill head. The piles are then installed. The mobilisation and demobilisation of the install equipment is expected to cost € 3000,-. The installing of the piles is expected to last for four days, with two workers and one machine. The cost per day are expected to be € 1500,-. When the piles are installed, the domed ends are welded upon them. Each domed end is expected to cost € 500,- for delivery and welding.

Pipelines

The pipelines, with an outside diameter of 100 [mm], a wall thickness of 5 [mm] and a total length of approximately 200 [m] will cost around € 30,- per meter (Breedveld Staal, 2015). The 100 elbow- and T-shaped pieces which are connecting the pipelines are assumed to cost € 30,- each, and the pressure valve, water taps and other small equipment is expected to cost € 3.000,-. Installing the pipelines is assumed to last for five working days with six workers, lifting machinery, welding robots and equipment and is expected to cost € 3.000,- per working day. When the pipelines are installed, the storage shafts can be tested (assumed costs: € 10.000,-) as the safety requirements describe. When this is done, the system can try to obtain the CE mark, which is assumed to bring an additional € 30.000,- of costs.

Installations

The production costs of the Pelton turbine are estimated using the following formula retrieved from (Lancaster University, 2008): PC = 3200 * (amount of [kW])^{0,54}. Which gives a production costs of € 20.000,- for our Pelton turbine with a power output of 29,8 [kW]. The assisting generator is estimated to cost around a € 1.000,- and the transformer is estimated to cost € 3.000,-. Furthermore, the F11-010 bend-axis piston pumps can be purchased in the web shop of Parker for € 1.210,- each (Parker, 2016). Installation and wiring of above installations is assumed to cost € 5.000,- in total and building the technical room which houses it all is assumed to cost € 15.000,-.

The total construction costs of the LHES system are shown in Table 7-1.

Table 7-1 Construction costs of the LHES system

Item	Units	Price per unit	Costs
Delivering 27 steel piles Ø 762-20 [mm] * 20 [m], S355	7320 [kg]	€ 0,90	€ 177.890,-
Delivering and attaching drill heads	27 [pieces]	€ 500,-	€ 13.500,-
Mobilization/demobilization drilling equipment	[-]	€ 3.000,-	€ 3.000,-
Instalment of 27 piles	9 [days]	€ 2.500,-	€ 22.500,-
Delivering and attaching domed end	27 [pieces]	€ 500,-	€ 13.500,-
Delivering pipelines Ø 100-5 [mm]	200 [m]	€ 30,-	€ 6.000,-
Delivering elbow- and T-shaped pieces	100 [pieces]	€ 30,-	€ 3.000,-
Delivering taps, pressure valve and other small equipment	[-]	€ 3.000,-	€ 3.000,-
Instalment of pipelines	5 [days]	€ 3.000,-	€ 15.000,-
Testing of the 16 storage shafts	[-]	€ 10.000,-	€ 10.000,-
Obtaining CE mark	[-]	€ 20.000,-	€ 20.000,-
Delivering Pelton turbine	[-]	€ 20.000,-	€ 20.000,-
Delivering Generator	[-]	€ 1.000,-	€ 1.000,-
Delivering Transformer	[-]	€ 3000,-	€ 3000,-
Delivering 3 F11-010 bend-axis piston pumps	3 [pieces]	€ 1.210,-	€ 3.630,-
Installation and wiring	[-]	€ 5.000,-	€ 5.000,-
Making technical space consisting of concrete floor and roof and masonry walls	[-]	€ 15.000,-	€ 15.000,-
Total construction costs:			**€ 335.020,-**

Maintenance costs

To estimate the maintenance costs, the lifetime of the different items is taken into account. The LHES system is designed for a lifetime of 50 years. The steel piles are expected to be normative in this matter, as it will be rather hard and expensive to replace one or multiple of these elements. The steel piles, including the drill heads and domed ends are therefore designed to last for 50 years as well.

The pipelines are assumed to last 25 years before they need to be replaced. The same assumption is made for the elbow- and T-shaped pieces, the taps, the pressure valve and other small equipment. The labour and equipment costs to do this replacement after 25 years is assumed to be € 20.000,- (ten working days, with 4-5 workers plus equipment). A small budget of € 250,- a year is reserved for the case when small repairs or simple replacements needs to be done. The Pelton turbine and its generator are designed on a 25 year life expectancy. The transformer has a life expectancy of 20 years (Electrical Technology, 2016). The bend axis piston pumps are assumed not to need any repair over their 10 years' life expectancy (Parker, 2016).

Visual inspection and testing of the welds, pipelines and all the moving materials (pumps, turbine, etc.) is done once every four years as the PED (European Parliament , 2014) describes and is assumed to cost approximately € 1000,- (one day, with 2-3 inspectors). An overview of the total maintenance cost is shown in Table 7-2.

Table 7-2 Yearly maintenance costs of the LHES system

Item	Item lifetime	Cost of item	Costs per year
Pipelines Ø 100-5 [mm]	25 [years]	€ 6.000,-	€ 240,-
Elbow- and T-shaped pieces	25 [years]	€ 3.000,-	€ 120,-
Taps, pressure valve and other small equipment	25 [years]	€ 3.000,-	€ 120,-
Labour and equipment costs to replace pipelines	25 [years]	€ 20.000,-	€ 800,-
Pelton turbine	25 [years]	€ 20.000,-	€ 800,-
Generator	25 [years]	€ 1.000,-	€ 40,-
Transformer	20 [years]	€ 3000,-	€ 150,-
Three F11-010 bend-axis piston pumps	10 [years]	€ 3.630,-	€ 180,-
Inspection of welds, pipelines and moving materials	4 [years]	€ 1.000,-	€ 250,-
Other small repairs			€ 250,-
Total maintenance costs per year:			**€ 2.950,-**

7.2 Benefits of the LHES system

The LHES system is able to provide a number of benefits. Besides the fact that the system functions as a foundation of the houses, it stores energy which can save the home owners on their electricity bill and helps when making a carbon-neutral house.

Function as foundation

As the LHES system consists of 27 large steel piles, an additional foundation is not needed. Smaller prefab concrete piles are typically used for house foundations when the LHES system is not applied. Delivery and instalment of such piles, with a dimension of approximately 300 times 300 [mm] and a length of 20 [m], is assumed to costs € 1500,- per pile. Approximately 36 of these piles would be applied as the foundation of the street with eight houses. The total costs for this alternative foundation then becomes 36*1500 = € 54.000,-. This amount of money can be subtracted from the construction cost of the LHES system in order to calculate the extra investment which is needed to build the system.

Revenues from storing electricity

To calculate the financial benefits for the amount of electricity which is stored throughout a year, a worst case and a best case scenario is projected. For both scenario's the following assumptions are made:

- When the households require electricity from the grid, a rate of € 0,22 per [kWh] (Nuon, 2016) will have to be paid. This assumption is based on the fact that the 'balancing of electricity' legislation, where home owners with solar panels can extract their produced electricity from the amount of electricity which was required from the grid, will end in 2020 (Schoenmakers, 2015).
- When the households deliver electricity which is generated by their solar panels to the grid, no compensation from the electricity companies is received. This assumption is based on the expectation that the amount of private owners of solar panels will increase rapidly. And as the panels do not provide a reliable constant energy production, the electricity companies will still need their own power plants to supply a constant power and may be flooded with 'unwanted' solar power on a sunny day.
- The solar panels on the roof of the eight households are assumed to produce sufficient electricity to meet the expected power demand of 28.000 [kWh] per year, which is equal to 3500 [kWh] per household. It is assumed that 20% of this demanded power can be delivered straight from the solar panels production. This assumption is based on the yearly average usage of own produced solar power published in (Hetkanwel, 2015). The other 80% of the demanded power is either delivered by the LHES system or by the grid.

In the Netherlands, solar panels with a power output of 150 [wp/m^2] are delivering an average energy production of 130 [kWh/m^2] per year (Nuon, 2016) as they are assumed to deliver for 850 full sun hours (without any clouds) per year. This means that in case a 100% efficient storage system would be used, each household needs approximately 27 [m^2] of solar panels in order to produce the expected power demand of 3500 [kWh]. To estimate how many times per year the LHES is fully charged, the amount of full sun hours per month for 2015 is shown in Table 7-3.

Table 7-3 Average amount of full sun hours per day for each month of the year (NovaVolt, 2016)

Month	Average amount of full sun hours per day	Month	Average amount of full sun hours per day
January	0,63	July	5,27
February	1,59	August	4,68
March	2,57	September	3,01
April	4,74	October	1,85
May	5,13	November	0,77
June	5,79	December	0,56

During the full-, but also the normal sun hours, power generated by the solar panels could be used to store energy in the LHES system. Filling the system can be done in 4,5 hours. But since the amount of power supply needed for the 3 pumps increases linear with the increasing pressure, it is expected that 1 or 2 pumps are turned off during the filling process as a result of insufficient solar power capacity. It is therefore estimated that it takes approximately six hours on average to fill up the system completely. Keeping this in mind, the yearly amount of energy delivered by the LHES system is assumed to be 40% of the total 28.000 [kWh] electricity demand in the worst case, up to as much as 80% in the best case scenario.

With these assumptions made, we can calculate the financial benefits of the LHES system (Table 7-4). The energy costs are calculated for the worst case and best case scenario, and for a scenario with solar panels where no LHES system is applied. As the LHES system has a roundtrip efficiency of 76%, additional solar power is required when energy is stored. The yearly costs of this additional solar power needed are estimated. To calculate the potential savings per year, the costs of the worst- and best case scenarios are subtracted from the costs of the situation with no LHES system applied.

Table 7-4 Calculation of potential savings of the LHES system per year

	Worst case scenario			**Best case scenario**			**No LHES system applied**		
	%*	Amount	Yearly costs	%*	Amount	Yearly costs	%*	Amount	Yearly costs
Solar power used right away	20%	5600 [kWh]	€ 0,-	20%	5600 [kWh]	€ 0,-	20%	5600 [kWh]	€ 0,-
Power delivered by LHES system	40%	11200 [kWh]	€ 0,-	80%	22400 [kWh]	€ 0,-	0%	0 [kWh]	€ 0,-
Electricity required from the grid	40%	11200 [kWh]	€ 2464,-	0%	0 [kWh]	€ 0,-	80%	22400 [kWh]	€ 4928,-
Additional solar power required	**+12, 5%**	**3500 [kWh]**	**€ 250,-**	**+25%**	**7000 [kWh]**	**€ 500,-**	**0%**	**0 [kWh]**	**€ 0,-**
Total costs per year:	€ 2714,-			€ 500,-			€ 4928,-		
Savings per year:	€ 2214,-			€ 4428,-			€ 0,- (reference case)		

* percentage of the power demand

As Table 7-4 shows, applying the LHES system could potentially save between € 2214,- and € 4428,- per year on the electricity bill. Which comes down to a saving between € 277,- and € 554,- per year per household.

Off grid house

Besides the environmental benefits of a house which does not need power from the grid, a number of financial befits could come with it. An off grid house does not need power lines or other electricity infrastructure to be connected, which saves costs. The large scale effects are still to be investigated properly, but it can be imagined that in case a large amount of houses becomes off grid, less power is required from power stations and therefore less investments are needed to build new ones.

7.3 Storage costs per [MWh]

In order to calculate the storage costs per [MWh], the total lifetime costs are calculated first. The amount of electricity storage is then determined after which the storage costs per [MWh] can be found. The calculation is shown in Table 7-5.

Table 7-5 Storage costs per [MWh] calculation

Item	Units	Amount per unit	Amount
Construction costs			€ 335.020,-
Maintenance costs over lifetime	50 [years]	€ 2.950,-	€ 147.500,-
Benefit from function as foundation			- € 54.000,-
Total costs over lifetime			€ 428.520,-
Annual electricity storage	120-240 [full cycles]*	93 [kWh]	11,16-22,32 [MWh]
Lifetime electricity storage	50 [years]	11,16-22,32 [MWh]	558-1116 [MWh]
Storage costs per [MWh]:		**Between € 384,- and € 768,-**	

* follows from worst- and best case scenario

A comparison of costs per [MWh] is made with other electricity storage methods, using values and figures from (de Ingenieur, 2016). The different storage methods all have a different capacity range. This range follows from the typical power output of a certain method, as well as its discharge time as is shown in Figure 7-1, which is based on (de Ingenieur, 2016) for all methods but the Local Hydroelectric Energy Storage. For this method, the typical capacity is spanned by a power output between 10 and 500 [kWh] and a discharge time between half an hour and one day.

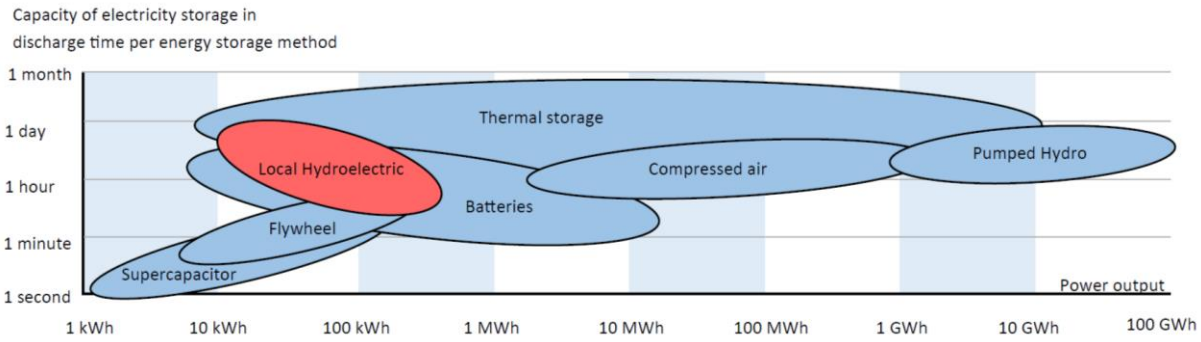

Figure 7-1 Capacity range of each electricity storage method

As can be seen in Figure 7-1, only the thermal storage system and batteries overlap the same range as the LHES system. In Figure 7-2, a comparison of the different storage methods is made for the costs per [MWh] now and the expected costs per [MWh] in 2030. The values for the Local Hydroelectric Energy Storage are calculated in Table 7-5 for the current situation and expected to become a lot cheaper after more research and development is done by 2030.

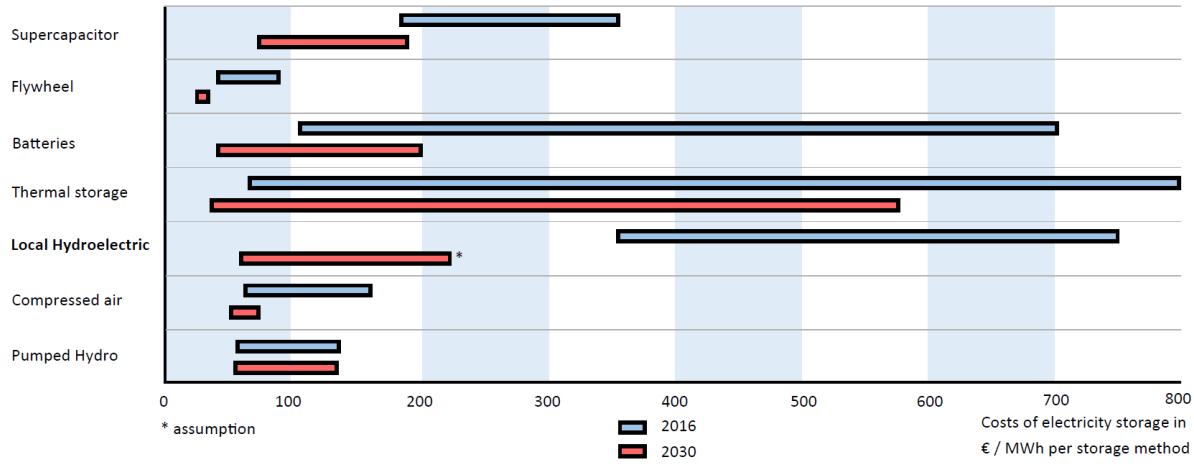

Figure 7-2 Cost of electricity storage in €/ MWh per storage method

As can be seen in Figure 7-2, the Local Hydroelectric Energy Storage system, with its € 384,- to € 768,- storage costs per [MWh], is performing in the same range as its competitors which are the thermal storage methods and batteries when it comes to electricity storage costs over its lifetime. The LHES system does however, require an investment which is considered to be rather large for private home owners to make. Due to the high construction- and maintenance costs shown above, the payback period of the LHES system which follows from the revenues for storing energy is longer than its lifetime. Further developing and/or applying the LHES system on large scale could decrease the costs, making the system a very accessible investment for private home owners.

Another option could be to let the investment (partly) be done by a third party. Such party could be:

- An energy company, which can rent- or lease out multiple LHES systems to private users. The main benefits for the energy company are:
  - The LHES system can help stabilizing the grid
  - Costs can be saved on expensive power plants, as renewable energy can be made much more reliable
  - Less production capacity is needed as peaks are lower
  - Money can be made when storing facility is used to store (cheap) foreign electricity at night and sell it for normal rates during the day
  - Costs can be saved on electricity infrastructure in case houses become off grid
  - Income can be gained from rent or lease contract
- The government, which can (partly) subsidize the construction of LHES systems. The main benefits for the government are:
  - The use of fossil fuels can be drastically reduced, as renewable energy can be made much more reliable
  - European renewable energy targets can be met
  - The general health of the people can improve, as pollution of the air reduces

8 Conclusions, discussion and recommendations

In this final chapter a short conclusion about this master thesis is given in chapter 6.1, A discussion is shown in chapter 6.2 and recommendations are mentioned in 6.3.

8.1 Conclusions

This feasibility study has shown that it is technologically and economically feasible to apply a Local Hydroelectric Energy Storage system in the built environment. Furthermore, the following can be concluded:

- *Integrating compressed air and hydropower in the foundation of a house is technologically and economically the most feasible way to apply a local energy storage system.* The Local Hydroelectric Energy Storage system uses compressed air and pumped hydro energy storage to store the largest amount of energy in the smallest amount of space. Other techniques, like gravity- or mechanical spring power are by far less efficient when applied on a local scale, as can be seen in the figure below.

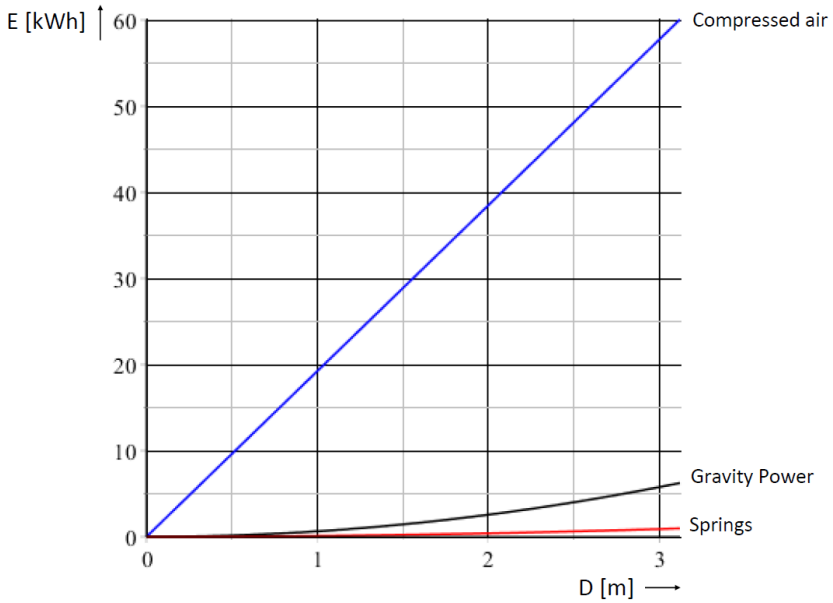

Figure 8-1 The relationship curves between the amount of energy storage 'E' and the diameter of the shaft 'D' for a compressed air-, gravity- and spring power system

- *Hollow, steel foundation piles are very suitable to be used as storage shafts of a Local Hydroelectric Energy Storage system.* The preliminary design of the Local Hydroelectric Energy Storage system has proven that hollow, drilled steel piles are very suitable to be used to store energy on a local scale. When the piles are situated underneath a house, there is hardly any electricity transport loss when the system is storing or delivering electricity. Furthermore, the use of foundation piles makes that no additional land is needed, which is very beneficial within the built environment.

- *The main challenge when applying a Local Hydroelectric Energy Storage system in the built environment is to guarantee the safety of people living around it.* When standard failure probabilities are used, the Local Hydroelectric Energy Storage system describes a low risk solution to store energy. However, the consequences of a failure are high as fatal accidents could occur. Attention need to be paid to make the system robust and the risks well controllable with the use of simple control measures and inspections.

- *The use of a Local Hydroelectric Energy Storage system is economically feasible.* The storage costs per [MWh] are calculated to be between € 384,- and € 768,- over the lifetime of the system, which is comparable to some thermal storage systems and batteries. Furthermore, the storage costs per [MWh] are expected to drop as the system can be developed further and the construction and operational costs can decrease when the system is applied on a larger scale.

8.2 Discussion

The application of local hydroelectric energy storage can definitely change the future of the electricity market. Renewable energy sources, like wind- and solar power, are expected to generate a greater part of our electricity production each upcoming year. They are, however, simply in need of a solution to mitigate supply fluctuations and deliver electricity even during dark and low-wind periods. It can therefore be concluded that storing electricity is very necessary and eventually inevitable.

This feasibility study has shown good prospects about Local Hydroelectric Energy Storage systems in the built environment. The use of mechanical springs to store energy is strongly discouraged in this research, as cheaper alternatives with a higher storage to volume ratio where found. However, there may be other reasons why mechanical spring storage would have a preference over other systems, which is why this option is not completely excluded as a feasible energy storage method. The same goes for gravity power energy storage. In this research, gravity power is investigated for a storage shaft with a diameter up to 3 meters. The results were not spectacular. For larger diameters it can however be lucrative to use gravity power instead of other methods.

The preliminary design in this research makes use of proven technology from Pumped Hydro Storage plants combined with compressed air, which results in a high energy density storage system. It would be very worthwhile for energy companies or the government to invest in further research and development of Local Hydroelectric Energy Storage systems. In particular to make the system as safe as possible. The design in this research shows a first step of many possible iterations. It will be possible to optimize the design of a LHES system even further, for instance by taking a better look at the power demand behaviour of the users. Furthermore, many possible applications for a LHES system can be considered. The MCA of this research showed a clear prospect where the application as a foundation of a house came out as (financially) the most feasible. However, certain risks will come with this application. These potential risks should be examined excessively. The chances of an explosion event for instance are very small, but the possible fatal consequences could be considered unacceptable. In that case the application as a standalone construction could still be considered, as the possible risks could be mitigated by applying the LHES system at a closed off area. Such design choices will depend on many factors and is therefore considered outside the scope of this research.

8.3 Recommendations

In this feasibility study, a number of steps are made towards a preliminary design of a Local Hydroelectric Energy Storage system. For some parts, estimates or assumptions are made in order to get a feeling about the possible potential of the system. It is recommended however, that some of these parts are investigated further, in order to improve the possibility of a LHES system to be built in the future. The recommendations are listed below:

- *The potential risks which come with applying the LHES system need to be examined excessively.* In this research, a preliminary risk analysis is made. In order to make the construction of a LHES system realistic, a comprehensive risk analysis needs to be conducted.
- *A suitable location is needed:* A suitable location for the LHES needs yet to be found. As long, hollow foundation piles are used for the LHES system, a location with a soft soil top layer and a deeper load-bearing soil layer is preferred.
- *The Pelton Turbine needs an elaborated design:* As the key part to gain power from the stored energy, the Pelton Turbine needs an elaborated design which shows the limits of the flow rate versus the power output. If a very high efficient turbine with a flow rate as small as possible under a high pressure could be developed, a smaller LHES system with the same power output may result.
- *The optimal electricity storage with respect to the demand behaviour needs to be found*: As LHES systems can store a variable amount of energy, it will be very useful to research the electricity demand behaviour of the users, in order to come to an optimal storage capacity of the LHES system.
- *The effects on the electricity market need to be investigated:* A study about the effects of a large scale implementation of local energy storage would be very valuable.
- *Other applications for a LHES system need to be investigated further:* Various applications for a LHES system are briefly shown in this research (Chapter 4.3 and Appendix H). A further elaboration on potential applications could prove another economically feasible project.
- *Further development of the LHES system is needed:* A number of key points of the LHES system need further development. One can think about improving the continuity of the power supply of the system and a solution to prevent erosion inside the system.

References

A.A. Slocum, G. F. (2013). Ocean renewable energy storage (ORES) system: analysis of an undersea energy storage concept. *Proceedings of the IEEE 101(4)*, 906-924.

AC-TEC. (2015). *AC-TEC Hydropower turbines*. Retrieved from http://www.ac-tec.it/index_en.html

Allpumps. (2016). *Allpumps centrifugal pumps*. Retrieved from https://www.allpumps.com.au/applications/centrifugal-pumps

AndritzHydro. (2015). *Mini Compact Hydro, dedicated solutions for small hydropower plants.* Vienna: Andritz Hydro.

ArcelorMittal. (2016, May 23). *ArcellorMittal long steel products.* Retrieved from http://sheetpiling.arcelormittal.com/

Bergum, E. v. (2014). *Pumped Hydro Storage: Pressure Cavern (Master Thesis).* Delft: TU Delft.

Boer, W. W. (2007). *The Energy Island - An Inverse Pump Accumulation Station.* Arnhem: DNV KEMA Consultin, Lievense BV.

Breedveld Staal. (2015). *Prices of steel tubes.* Retrieved from http://www.staalprijzen.nl/images/archief/2015/20150130/20150130_bruto_prijslijst_staalprijzen.pdf

BulgariaSerbia. (2014). *Comparative study of small hydropower stations.* Bulgaria - Serbia IPA Cross border Programme.

CBS. (2016, April 28). *Statistics Netherlands, CBS*. Den Haag.

de Ingenieur. (2016). Kostenoverzicht Energieopslag. *de Ingenieur, maart 2016*, 8.

de ingenieur. (maart 2016). Kostenoverzicht energieopslag. *de Ingenieur*, 8.

Dominion. (2016, March 22). *Bath County pumped storage station*. Retrieved from https://www.dom.com/corporate/what-we-do/electricity/generation/hydro-power-stations/bath-county-pumped-storage-station

Duivendijk, J. v. (2007). *Water Power Engineering, Principles and Characteristics.* Delft: VSSD, Delft University of Technology, Faculty of Civil Engineering and Geosciences, Section of Hydraulic Engineering.

Ecademy, G. (2016). *Grundfos Ecademy, about pump curves.* Retrieved from http://us.grundfos.com/training-events/ecademy/all-topics.html

ECN, E.-N. N. (2014). *Energietrends 2014.* Retrieved from http://www.energie-nederland.nl/wp-content/uploads/2013/04/EnergieTrends2014.pdf

Electrical Technology. (2016). *Electrical Technology*. Retrieved from http://www.electricaltechnology.org/2013/01/what-is-normal-or-average-life.html

Engineering Toolbox. (2016). *Engineering Toolbox*. Retrieved from Engineering Toolbox: http://www.engineeringtoolbox.com/surface-roughness-ventilation-ducts-d_209.html

ENTSO-E. (2015). *European Network of Transmission System Operators for Electricity.* Retrieved from https://www.entsoe.eu/data/Pages/default.aspx

Enymate. (2016). *Verbruik per type apparaat*. Retrieved from http://www.enymate.nl/besparen/verbruik

European Commission. (2014). *A policy framework for climate and energy in the period from 2020 to 2030.* Brussels: EN.

European Parliament . (2014). *DIRECTIVE 2014/68/EU OF THE EUROPEAN PARLIAMENT AND OF THE COUNCIL on the harmonisation of the laws of the Member States relating to the making available on the market of pressure equipment.* European Union .

Fundex. (2016, May 23). *Fundex Tubex palen.* Retrieved from http://www.fundexgroup.com/index.php/nl/beheer-tekstpaginas/25-tubex-paal.html

Gebr.deKoning. (2016, May 23). *Fundering en remmingwerk Rijnhavenbrug Rotterdam.* Retrieved from http://www.gebrdekoning.nl/projecten/remmingwerk-rijnhavenbrug-rotterdam.php

Golbach, G. (2014). *Risicoanalyse propaantank Veerdam 1 in Aalst.* Enschede: Adviesgroep AVIV BV.

GravityPower. (2008). *Gravity Power, Grid scale energy storage*. Retrieved from http://www.gravitypower.net/

H. Wang, L. X. (2013). A Novel Pumped Hydro Combined with Compressed Air Energy Storage System. *Energies 6*, 1554–1567.

H. Wolse, L. D. (2016). *Betrouwbaarheid van elektricitetisnetten in Nederland, resultaten 2015.* Den Haag: Netbeheer Nederland.

Heindl, E. (2013). *Hydraulic Rock Storage An innovative energy storage solution for 24 h energy supply*. Retrieved from http://www.heindl-energy.com/

Hetkanwel. (2015). *Petitie: géén belasting op zelf opgewekte zonnestroom*. Retrieved from http://www.hetkanwel.net/2015/12/18/petitie-geen-belasting-op-zelf-opgewekte-zonnestroom/

Hydrotech. (2007). *Hydrotech piston pumps*. Retrieved from http://www.hydrotech-bg.com/en.php?p=view&r%5Bpage%5D=12

IEN. (2016, April 26). *Engineering Springs for Large Valve Actuators*. Retrieved from Industrial Engineering News: http://www.ien.eu/article/engineering-springs-for-large-valve-actuators/

Imambaks, R. (2013). *Gravity Power Storage, a preliminary feasibility study.* Delft: TU Delft.

Industrialheatpumps. (2016). *industrial heat pumps, how it works*. Retrieved from http://www.industrialheatpumps.nl/en/how_it_works/

J. Bi, T. J. (2013, July). Research on Storage Capacity of Compressed Air Pumped Hydro Energy Storage Equipment. *Energy and Power Engineering, Vol. 5 No. 4B*, pp. 26-30. Retrieved from http://www.scirp.org/journal/epe

J. Lemmens, J. v. (2014). *Het potentieel van zonnestroom in de gebouwde omgeving van Nederland.* Arnhem: DNV GL - Energy.

Karremann, J. (n.d.).

Kibrit, B. (2013). *Pumped Hydropower storage in the Netherlands (Master Thesis).* Delft: TU Delft.

Kusteilanden. (2016, March 16). *kusteilanden, eilanden voor de kust*. Retrieved from http://kusteilanden.be/

Lancaster University. (2008). *Hydro Resource Evaluation Tool*. Retrieved from http://www.engineering.lancs.ac.uk/lureg/nwhrm/engineering/turbine_costs.php

Madehow. (2016, April 26). *Kamatech spring machines*. Retrieved from http://www.madehow.com/Volume-6/Springs.html

NEN-EN. (2014). *NEN-EN 13445 Unfired pressure vessels, Nederlandse norm (en).*

NovaVolt. (2016). *NovaVolt Solar Energy* . Retrieved from Zonuren calculator: http://www.zonurencalculator.nl/sun_hours_calculation

Nuon. (2016, May 2). *Opbrengst zonnepanelen*. Retrieved from https://www.nuon.nl/zonnepanelen/opbrengst-rendement.jsp

Oberhausen, G. (2016, March 22). *Gasometer Oberhausen*. Retrieved from http://www.gasometer.de/en/

O-PAC. (2009). *O-PAC, Ondergrondse Pompaccumulatie Centrale*. Retrieved from http://www.o-pac.nl/opac.html

Parker. (2016). *Parker, Hydraulic pump division.* Retrieved from https://www.parker.com/literature/PMDE/Catalogs/Fixed_Motors/F11_F12/HY30-8249-UK.pdf

Peterson, D. F. (2002). *fireengineering.com*. Retrieved from http://www.fireengineering.com/articles/print/volume-155/issue-4/features/bleve-facts-risk-factors-and-fallacies.html

Real Simple. (2016). *Real Simple*. Retrieved from Real Simple: http://www.realsimple.com/food-recipes/tools-products/appliances/how-does-refrigerator-work

RenewablesFirst. (2015). *RenewablesFirst*. Retrieved from RenewablesFirst: http://www.renewablesfirst.co.uk/hydropower/hydropower-learning-centre/pelton-and-turgo-turbines/

RIVM. (2009). *Handleiding Risicoberekeningen Bevi.* Retrieved from http://www.rivm.nl/dsresource?objectid=rivmp:22449&type=org&disposition=inline&ns_nc=1

Rotterdam. (n.d.). Port of Rotterdam.

Schoenmakers, H. (2015). *EC PRO, kenniscentrum zonnepanelen*. Retrieved from https://www.bespaarbazaar.nl/kenniscentrum/veelgestelde-vragen/omvormer/salderen-2017/

Solines. (2016). *Solines*. Retrieved from solines: http://www.solines.nl/nl/boorpalen

Stackexchange. (2016). *Stackexchange engineering, characteristics values of a piston pumps*. Retrieved from http://engineering.stackexchange.com/questions/200/what-are-characteristic-values-for-a-piston-pump

Sterling Heating and AC. (2016). *Sterling Heating and AC*. Retrieved from Sterling Heating and AC: http://www.sterlingheating.com/blog/2013/10/heat-pumps-work/

Strathclyde, U. o. (2002). *Energy Systems & Environment, Transmission of Renewable Energy*. Retrieved from http://www.esru.strath.ac.uk/EandE/Web_sites/01-02/RE_transmission/index.htm

T. Petersen, B. E. (2013). *Adiabatic Liquid Piston Compressed Air Energy Storage.* Danish Technological Institute.

Tarigheh, A. (2014). *Gravity Power Module (Master Thesis).* Delft: TU Delft.

TAW. (2003). *Leidraad Kunstwerken.* Retrieved from Helpdesk Water: http://www.helpdeskwater.nl/algemene-onderdelen/structuur-pagina'/zoeken-site/@7337/trob062/

van der Toorn, A. (n.d.). *Pump Storage Plants in the Netherlands.* TU Delft, Delft.

Voorbij. (2016, May 23). *Voorbij funderingstechniek, grote diameter open buispaal*. Retrieved from http://www.voorbijfunderingstechniek.nl/producten/staalconstructies/grote-diameter-open-buispaal.html

VROM. (2007). *Handreiking verantwoordingsplicht.* Retrieved from groepsrisico.nl: http://www.groepsrisico.nl/doc/Handreiking%20verantwoordingsplicht%20groepsrisico.pdf

Vroom. (2016, May 23). *Vroom, stalenbuis heipalen*. Retrieved from http://www.vroom.nl/nl/products/2-stalenbuis-heipalen

Waalpaal. (2016, May 23). *Waalpaal, stalen buispalen inwendig geheid.* Retrieved from http://www.dewaalpaal.nl/NL/97/stalen-buispaal-inwendig-geheid.html

Water21. (2014). *Detailed information about Kaplan turbines*. Retrieved from http://www.water21.org.uk/hydropower/ossberger-hydroturbines/kaplan-turbine/kaplan-detailed-information/

Waterturbines. (2016). *Different types of water turbines*. Retrieved from http://waterturbines.wikidot.com/main:types-of-water-turbines

werktuigbouw.nl. (2016, 06 10). *Werktuigbouwkundige calculator*. Retrieved from http://www.werktuigbouw.nl/sub17.htm

List of Figures

List of Tables

Appendixes

Appendix A – Energy storage technologies

Appendix B – Spring power dependence on wire thickness

Appendix C – Thin walled pressure vessels

Appendix D – Delivery and instalment costs of steel piles

Appendix E – Turbines

Appendix F – Pumps

Appendix G – Drawings

Appendix H – Other applications

Appendix A – Energy storage technologies

In this appendix the current state of hydropower, gravity power, spring power and compressed air energy storage technologies is represented.

A1 Hydropower

A1.1 Pumped hydroelectric storage

A pumped hydroelectric storage system (PHS) is a system which is typically equipped with pumps and generators connecting an upper and a lower water reservoir. The pumps use relatively cheap electricity from the power grid during off-peak hours to transport water from the lower reservoir to the upper one to store energy. During periods of high energy demand (peak hours), water is released from the upper reservoir to generate power which is returned to the grid and sold for a higher price. PHS is a very widely used electricity storage technology.

Table A-1 Main properties of pumped hydroelectric storage.
Based on Bath County Pumped Storage Station (Dominion, 1985)

Power output	300 - 3000 MW
Efficiency	75-85 %
Discharge at capacity	6+ hours
Head	400 m
Water volume	$34{,}5*10^6$ m^3

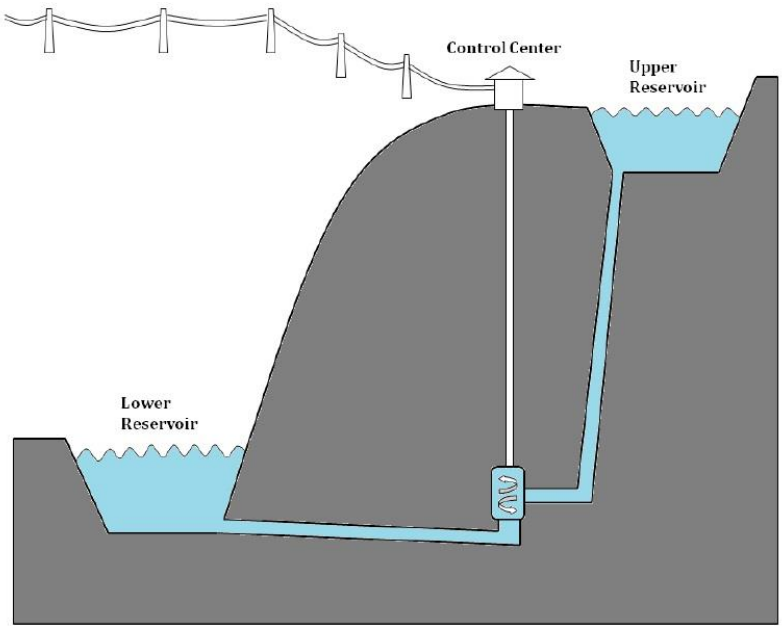

Figure A-1 Pumped Hydroelectric Storage diagram

A1.2 Compressed air PHS

Another promising innovative design is to use compressed air in a pumped hydro storage (figure 2). In such a system the upper reservoir is replaced with a pressurized water container. The air within the pressure vessel becomes pressurized when water is pumped into the vessel. This way, the energy can be stored in compressed air instead of elevated water. The system is less dependent on geographic requirements and could be made at almost any location with flexible and scalable capacity.

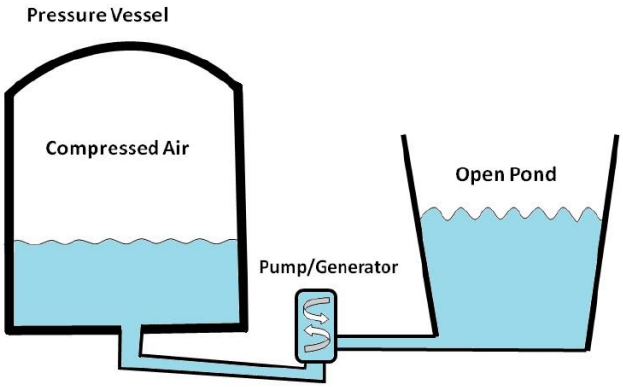

Figure A-2 Diagram of a compressed air in a pumped hydro storage

ALP-CAES system

An ALP-CAES system (Petersen, 2013) which is short for 'Adiabatic Liquid Piston Compressed Air Energy Storage system', describes a compressed air energy storage system (CAES) with a modification to avoid any heat loss. When air is being compressed by an air compressor, as used commonly in CAES systems, additional heat can come free. If this additional heat energy is not 'captured', the system may become less efficient. The ALP-CAES system uses a motor/pump to pump water into an air cavern which is pre-compressed to, for example, 200 bar. The water is taken from a pond at ground level and at atmospheric pressure. The temperature increase by pressurizing the water is insignificant, making this system more efficient. In addition, it is expected that the efficiency of a pump/turbine using a liquid as a medium is favorable compared to compressors/turbines using air as a medium. Such a system could also be applied in empty salt caverns as described in (Berchum, 2014) for instance.

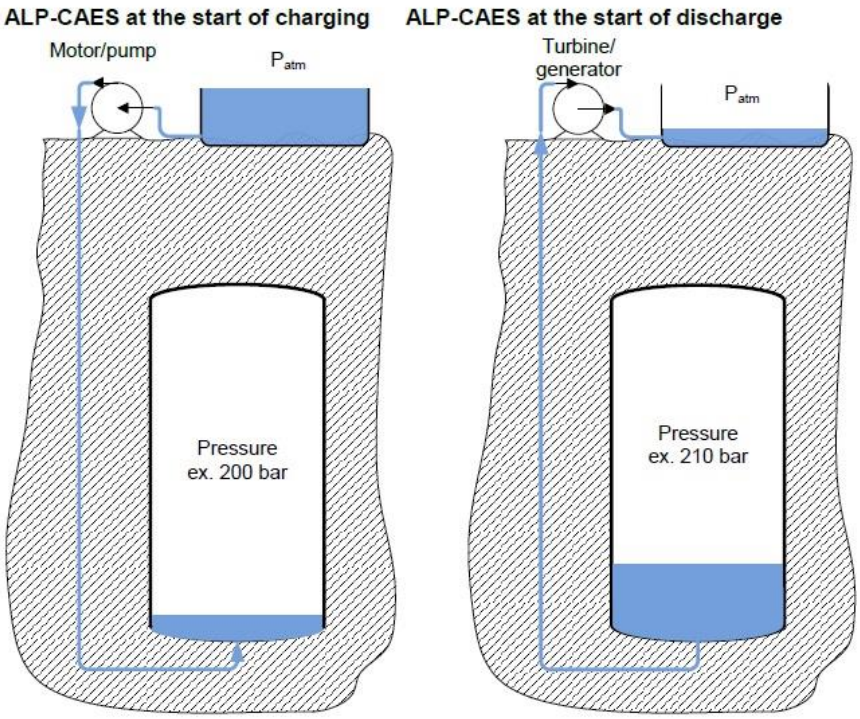

Figure A-3 Diagram of a basic ALP-CAES system (Petersen, 2013)

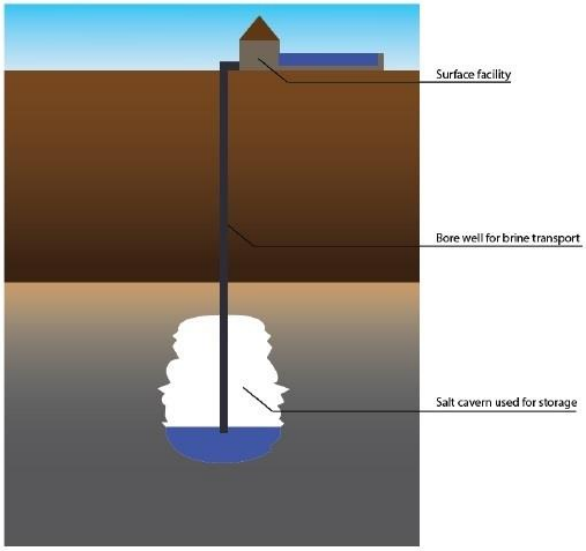

Figure A-4 Compressed air in an underground salt cavern Pumped Hydro Storage (Berchum, 2014)

Table A-2 Main properties of an underground salt cavern Pumped Hydro Storage. Based on (Berchum, 2014)

Capacity	156 MWh
Power output	65 MW
Efficiency	74 %
Discharge at capacity	3 hours
Pressure	153 - 165 bar
Volume	$3*10^6$ m^3

A1.3 Undersea PHS

Another innovative concept is to use the water pressure on the bottom of the sea to store electricity. This could be very interesting for off-shore wind turbines for instance. The system uses a submerged pressure tank, firmly placed on the sea floor. It then uses electricity to pump water out of the tank, creating a negative pressure inside the vessel that can be used as a storage area. To generate electricity, seawater flows into the tank again through the generator. The capacity and cost per kwh of such a system would depend on a lot of factors, including the materials used and the depth of the sea bed. An innovative idea could be to reuse an old submarine as a pressure vessel for instance.

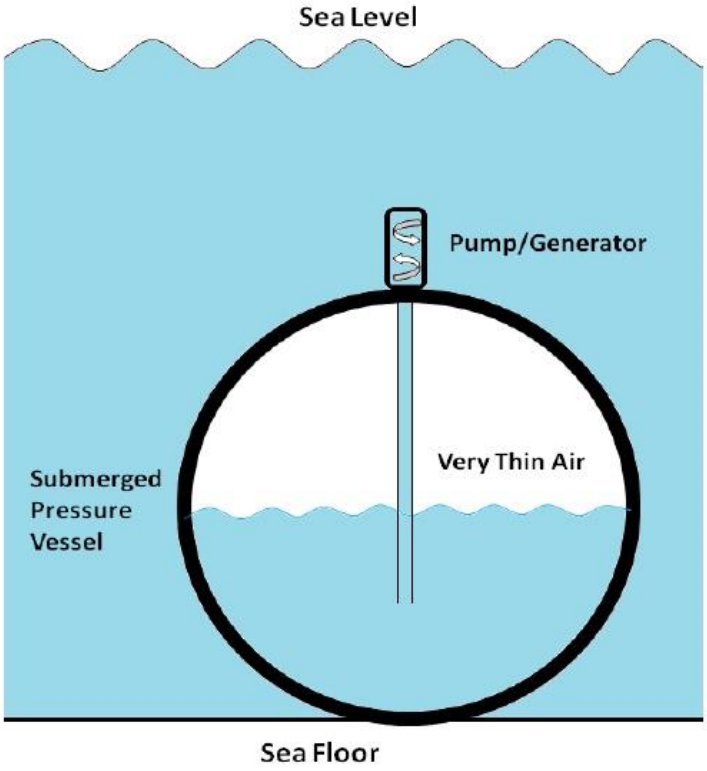

Figure A-5 Diagram of undersea PHS

Figure A-6 Zr. Ms. Bruinvis submarine (J.M. Karremann / Marineschepen.nl)

Figure A-3 Main properties of undersea pumped hydro storage. Based on (Slocum, 2013)

Capacity	Up to 6,1 MWh
Efficiency	Up to 71 %
Discharge at capacity	10 hours

A1.4 Pump accumulation station

Instead of focussing on a high pressure- or big height difference, one could also focus on a high water discharge Q. This could be particularly interesting for relatively flat countries or areas for instance. A big, closed off water area could be used as a pumped hydropower storage by pumping the water in and raising the water level when energy is leftover. Such a system may be called a pump accumulation station or a atoll. In times of high energy demand, the water can be lowered, running through turbines to produce power again. A research to apply such a system in the Netherlands was first done by Mr. Lievense in 1981. A research to apply a pump accumulation station in an already existing closed of area in the Netherlands was done by (Kibrit, 2013). It describes a plan to use and raise the existing dikes of the Slufter in the Port of Rotterdam which will increase the total amount of storage capacity of the system. Turbines are placed between the Slufter and the North Sea which are projected to have a maximum head difference of 40 meters, creating a medium size energy storage system.

Table A-4 Main properties of a pump accumulation station at the slufter as described in (Kibrit, 2013)

Capacity	2,16 GWh
Power output	350 MW
Efficiency	78 %
Discharge at capacity	6+ hours
Head	40 m
Water volume	$24{,}6*10^6$ m^3

Figure A-7 Aerial view of the Slufter (Portofrotterdam, 2013)

A1.5 Inverse off shore pump accumulation station

Instead of elevating the water level to store energy, one could also lower the water level in order to store energy. In 2007, such a system was developed by (Boer, 2007) and was called 'Energy Island'. It describes a ring of dikes build in the middle of the North Sea. The maximum head difference of approximately 40 meter is relatively small, but this is compensated by the enormous water area of 40 km^2 and a very large water discharge Q. The water is pumped out of the island when energy is leftover. In times of high electricity demand the water can be let back in, running through turbines to produce power again. The North Sea in particular would be a perfect place for such a system, since the soil consists of some very thick clay layers that could prevent water seepage. In Belgium, an idea comparable to the 'Energy Island' is about to be executed about 5 km of the West coast (Kusteilanden, 2013).

Table A-5 Main properties of an inverse off shore pump accumulation station as described in (Boer, 2007)

Capacity	30 GWH
Power output	2500 MW
Efficiency	80 %
Discharge at capacity	12+ hours

Figure A-8 Artist impression of an inverse off shore pump accumulation station (Boer, 2007)

A2. Gravity power energy storage

In urban or other flat areas where a traditional PHS system is not suitable, gravity power storage could be a solution. Two most promising variants of this rather new concept are discussed below.

A2.1. Gravitricity

The technology of Gravitricity is based on the principle of raising a heavy weight to store energy (Gravitricity, 2012). First, a shaft in the ground is made or reused, in case of an abandoned mine shaft for instance. A cylindrical weight is connected to a number of cables and guide wires and placed inside this shaft. Excessive energy can be used to raise the weight. Energy is then yet regenerated by simply dropping the weight.

While the weight system can be used on its own, the capacity of the overall system can be very much increased when the hole in the ground is used as a pressure vessel for compressed air. This involves adding a pressure-tight "lid" to the top of the shaft and lining the shaft to prevent leakage. The ground provides the bursting resistance other than at the very top of the shaft. The cables and generators are normally contained in the pressurized space so that only electrical cables need to penetrate the pressure vessel walls. Compressed air can be released either by using the compressor in reverse as an air motor or turbine, so as to generate electricity, or a separate air-motor/turbine can be applied. In addition, it is also possible to recover some of the heat of compression by a heat exchanger between the compressor and the storage space to improve cycle efficiency.

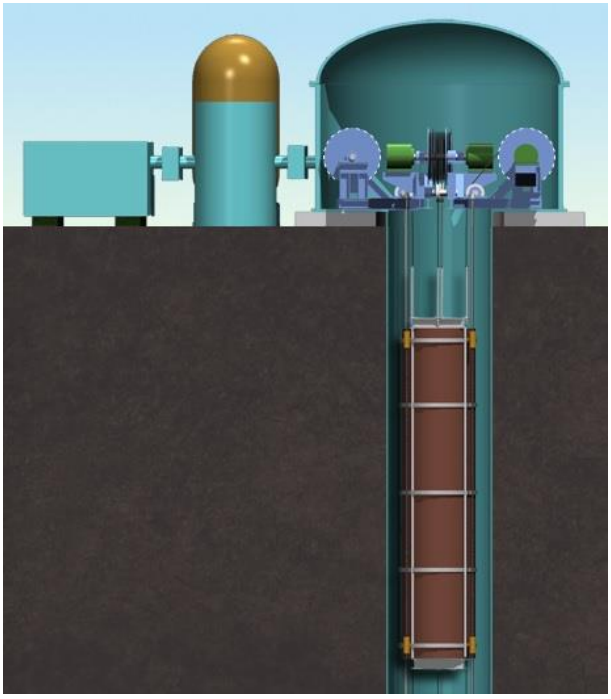

Figure A-9 Principle of the gravitricity technology (Gravitricity, 2012)

Table A-6. Main properties of a gravitricity energy storage system, based on (Gravitricity, 2012)

Power output	1 - 100 MW
Efficiency	90+ %
Discharge at capacity	4+ hours
Response time	< 0,5 sec.

A2.2 Gravity power module

The Gravity Power Module (Gravity Power, 2008) (Imambaks, R. 2013) is made of a very large piston that is placed in a 500-1000 meter deep, water-filled shaft. It is made of reinforced rock or concrete and equipped with sliding seals to prevent leakage. As the piston drops, it forces water down the store shaft, up into a return pipe, through a turbine which spins a generator to produce electricity, to the upper chamber. To store energy, the generator can be driven in reverse, spinning the pump to force water down the return pipe and into the lower chamber of the storage shaft again. This will lift the piston up. A great advantage of this system, is that is does not need a any elevation difference. The excavation for the shaft can be made using proven technology from the open pit mining industry. Furthermore, the installation requires a small footprint which allows it even to be constructed in dense urban areas.

Table A-7 Main properties of the gravity power module, based on (Gravity Power, 2008)

Power output	1600 MW
Efficiency	80+ %
Discharge at capacity	4 hours
Diameter	30 m
Depth	500 m

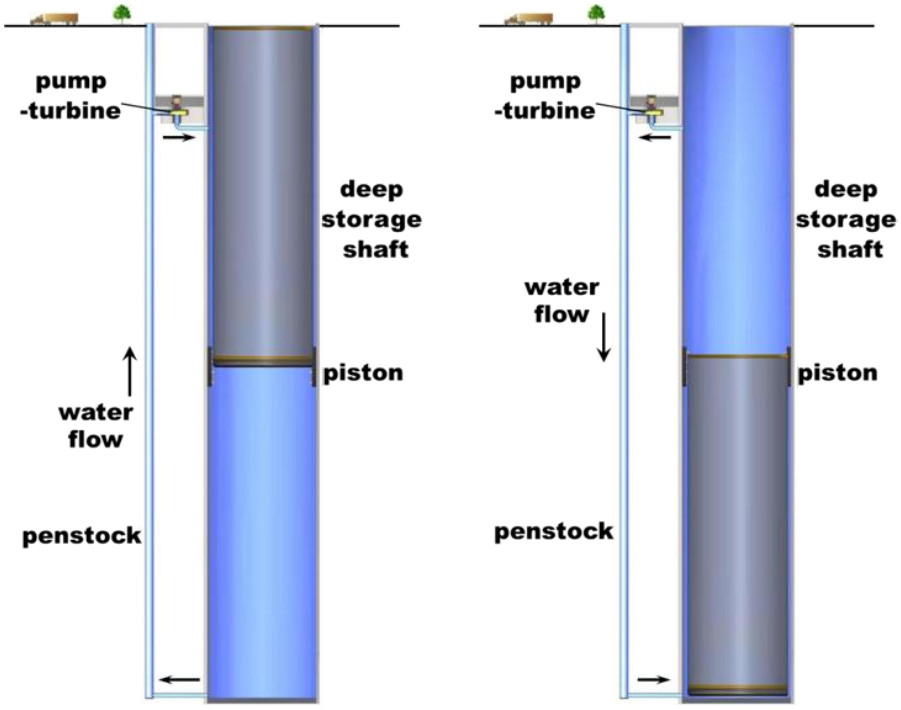

Figure A-10. The gravity power module (Gravity Power, 2008)

A2.3 Hydraulic Rock Storage

Hydraulic Rock Storage is a concept for storing power in the scale of multi- GWh (Heindl, 2013). The idea, made by Professor Eduard Heindl is based on a piston of rock of a diameter of 150 meter or more that is situated in the ground, separated from the natural surrounding rock and sealed water tight by a rolling membrane which causes hardly any friction losses. In times of excess power, water is pumped under the piston. When additional power is needed, water is pressed down by the piston and used to drive turbines. Generator are then used to produce electricity, which can be delivered to the power grid. A great advantage of this system is that it does not need any elevation difference. Suitable geological conditions are required, but these can be found in many regions around the world. When the diameter of the piston would be doubled, the storage capacity increases with a rate that is roughly to the fourth power of the diameter (D^4) while construction cost are estimated only to increase at a rate that is roughly to the second power of the diameter (D^2). This makes this concept very suitable for a large amount of energy storage.

Table A-8 Main properties of Hydraulic Rock energy storage, based on (Heindl, 2013)

Capacity	1+ GWh
Efficiency	80+ %
Discharge at capacity	24 hours

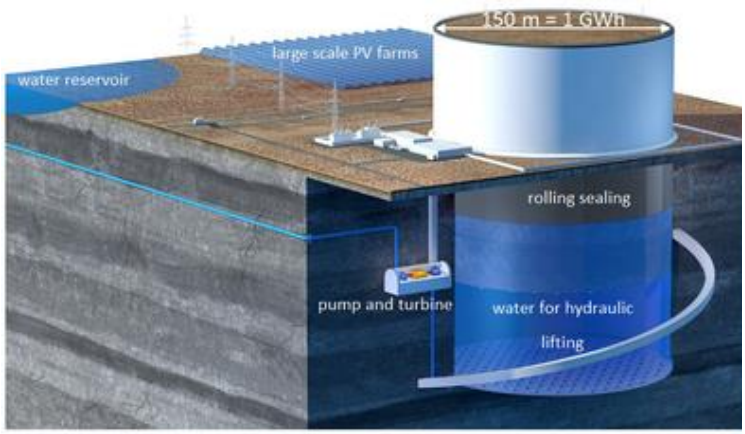

Figure A-11 The principle of Hydraulic Rock Storage (Heindl, 2013)

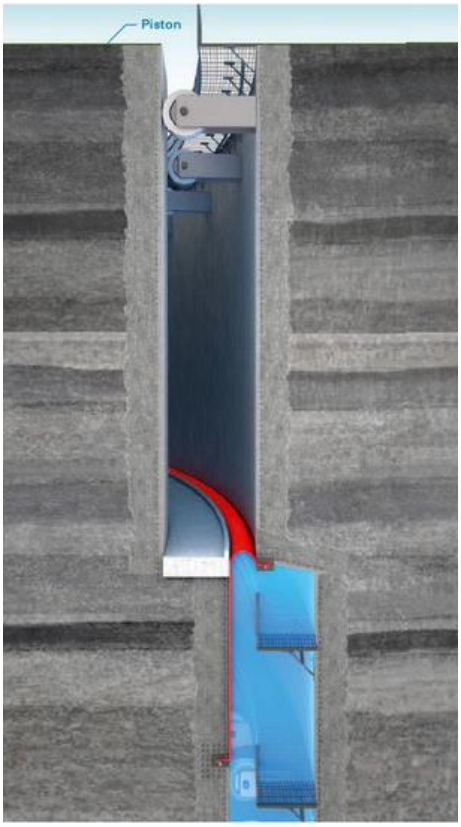

Figure A-12 A rolling membrane seals the system (Heindl, 2013)

A2.4 The Gasometer in Oberhausen

One great example of an applied gravity power energy storage system, is the Gasometer in Oberhausen. This gas holding tower was used to store excess gas in order to release it again when demand exceeded production. It was built in 1929 and was used until the late 1980's. A framework of 24 steel girders was built on a concrete base, and a skin of 5 mm thick sheet metal was attached to the framework. Inside, a 1200 ton gas-tight pressure disc was mounted which could freely move up and down, floating on top of the gas underneath and keeping it at a constant pressure.

Table A-9 Main properties of the Gasometer in Oberhausen, as described in (Gasometer, 2016)

Capacity	347.000 m^3 gas
Height	117,5 m
Diameter	67,6 m

Figure A-13 The Gasometer in 1929, showing the logo of the Gutehoffnungshütte (Gasometer, 2016)

A3. Spring power energy storage

In contradiction to hydro power storage, there are not many known spring power electricity storage systems. Below, an idea stated in an United States patent application from 2012 is briefly explained.

A3.1 Energy storage system using springs

This energy storage system uses compression springs and a high pressure fluid bladder to store potential energy (figure 8). A liquid is pumped into the fluid bladder when more energy is produced than demanded. The springs are pressed downwards when more and more liquid fills up the bladder, storing potential energy. Once the demand for energy rises, a valve is opened, making the fluid that is still under high pressure flow through a generator and produce energy.

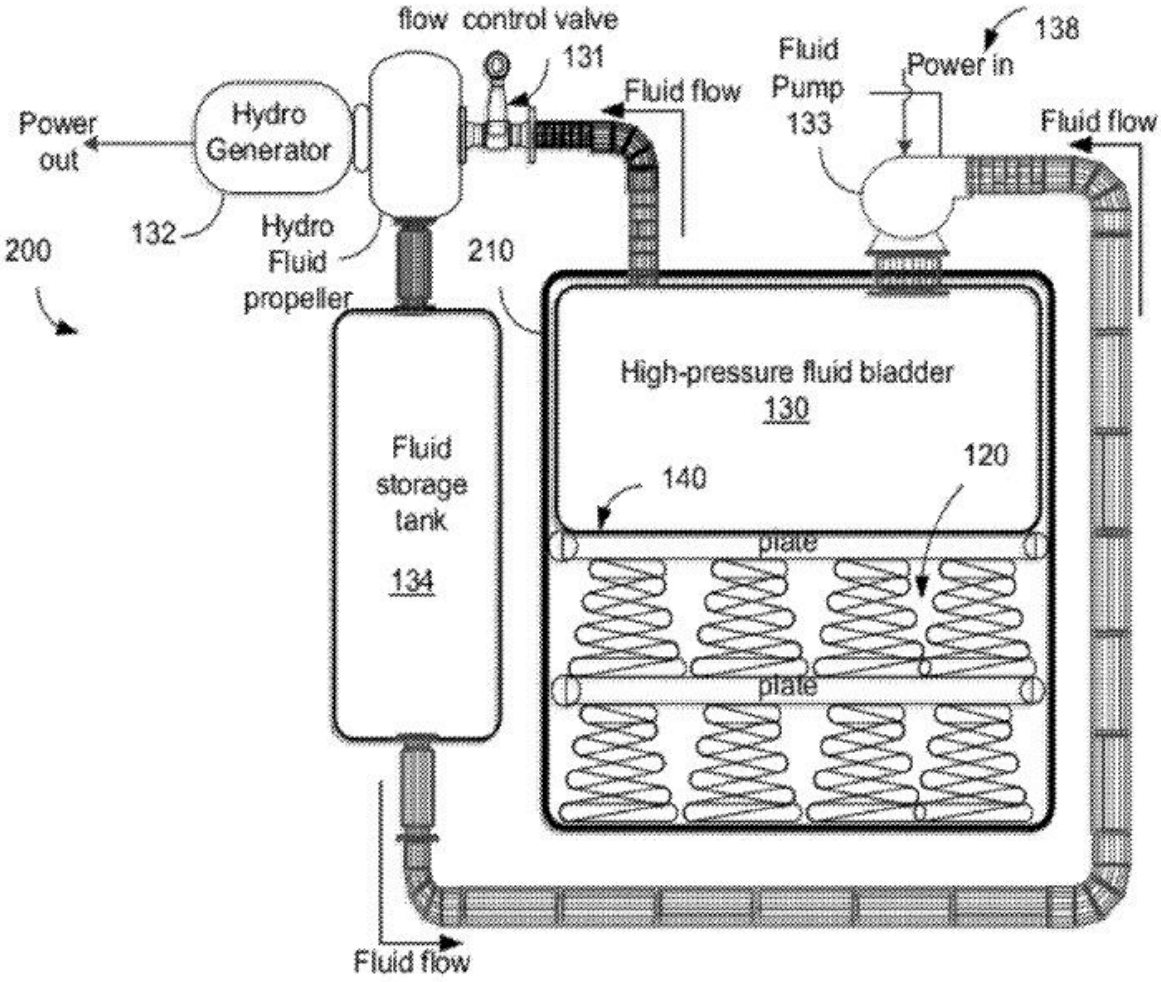

Figure A-14 Energy storage system using springs (Ogaz, 2012)

A3.2 Everyday items

Besides large scale energy storage systems, spring power is more used in everyday items. Examples of this may be an ordinary pen or a wind-up toy car. The spring of the pen, situated at the bottom, is activated when the pen is 'clicked downwards'. This makes the pen to come out of its casing, so the user can use it to write. The spring functions as a device that stores the energy, so it can be used to pull the pen back inside its casing when the user finished writing. In case of the wind-up toy car, the spring is storing energy as the user winds up the torsion spring. Once the user lets go of the car, the spring will release the energy, making the car to move forward.

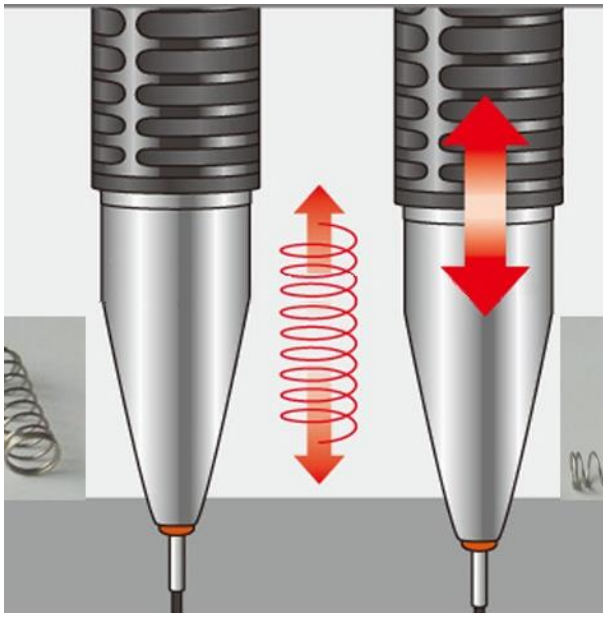

Figure A-15 An example of a spring inside a pen

Figure A-16 An example of a wind-up toy car

Appendix B – Spring power dependence on wire thickness

B1 Realistic dimensions of a spring

In order to make a proper design for a spring, one should realize how springs are being made. For this research two types of springs would be applicable, namely extension and compression springs.

Extension springs typically have their coils connected to each other. As a force is applied to stretch the spring, the coils separate. They are made by a steel wire which is cold drawn into the shape of the spring. For cold winding, a wire up to 18 [mm] thickness can be coiled at room temperature (madehow, 2016). This may be done on a spring-winding machine. A guiding mechanism is used to align the wire into the desired distance between successive coils as it wraps around as is shown in Figure B-1:

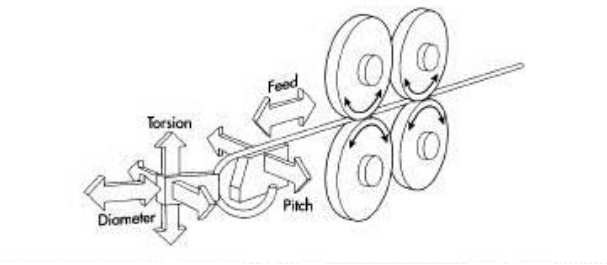

Figure B-1 Schematic view of a cold drawing spring machine (madehow, 2016)

Figure B-2 Impression of an extension spring

In contrast, a compression spring typically has space in between its coils. When a force is applied to shorten the spring, the coils are pushed together. They are typically made by a thicker steel wire or bar which is hot winded into the desired shape. The material is heated to make it flexible. Standard industrial coiling machines can handle steel bars up to 75 [mm] thickness, and custom springs have reportedly been made from bars as much as 150 [mm] thickness (madehow, 2016). The steel is coiled around a spindle while red hot after which it is cooled and hardened.

Figure B-3 A Steel bar being coiled around a spindle while red hot (IEN, 2016)

The length of the bar needed to make the spring is normative for the total height the spring. A spring with a diameter of 500 [mm] needs already 1500 [mm] bar length for each coil, while the longest bars available are between 12 to 14 meters long (IEN, 2016). If we need to go above this range, assembling multiple springs together might be an option.

Figure B-4 An impression of a compression spring with a large wire thickness (IEN, 2016)

B2 Relation of Energy 'E' to wire thickness 'd'

Since the total amount of potential energy 'E' depends on 'k' and 'u_{max}', we investigate the relationships of these values with respect to the dimensions 'd' and 'D' as well as the number of active coils 'N' of the spring. Using the dimensional requirement $D_m = D - d$ and for the maximum allowable force on the spring $F_{max} = (\pi * d^3 * \tau_w)/(8 * D)$ (werktuigbouw.nl, 2016), we find the following formula's for 'k' and 'u_{max}' which can be applied for both extension- as compression springs:

$$k = \frac{G * d^4}{8 * D_m^3 * N} = \frac{G}{8 * N} * \frac{1}{\left(3\frac{D}{d^2} - 3\frac{D^2}{d^3} + \frac{D^3}{d^4} - \frac{1}{d}\right)}$$

$$u_{max} = \frac{8 * N * D_m^3 * F_{max}}{d^4 * G} = \frac{\pi * N * D_m^3 * \tau_w}{d * D * G} = \frac{\pi * N * \tau_w}{G}\left(3d - 3D + \frac{D^2}{d} - \frac{d^2}{D}\right)$$

B2.1 Extension springs

If we let the outer diameter of the spring 'D' depend on the wire thickness 'd', the minimum requirement of the outer diameter is D = 7*d for the wire to work as a spring. In practice, most of the springs that are made have an outer diameter roughly in the range of 10*d < D < 20*d. The number of active coils of the spring 'N' depends on the neutral length of the spring 'L_n' and the wire thickness 'd'. The minimum requirement of $N = L_n/d$, in which case the coils are touching each other. For most extension springs this is the case.

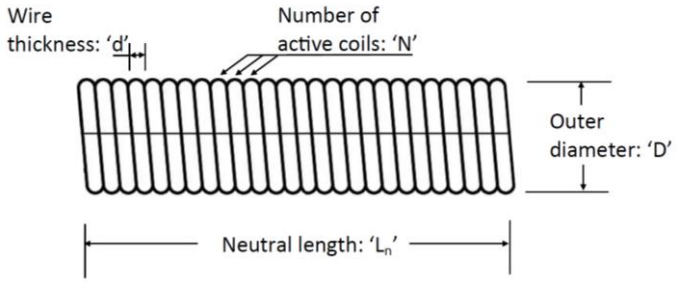

Figure B-5 The measurements of an extension springs

Using the potential energy equation found in chapter 3.3 ($E = ½ * k * u_{max}^2$), we find a relation between the wire thickness 'd' and the potential energy storage 'E' for different outer diameters as shown in Figure B-5. The neutral length is set at 3000 [mm] and the wire thicknesses vary from 3 to 18 [mm] in these graphs. Furthermore, typical spring material Music Wire ASTM A228 with a shear modulus of G = 80.000 [N/mm^2] and an allowable torsional stress of τ_w = 650 [N/mm^2] is assumed in these calculations.

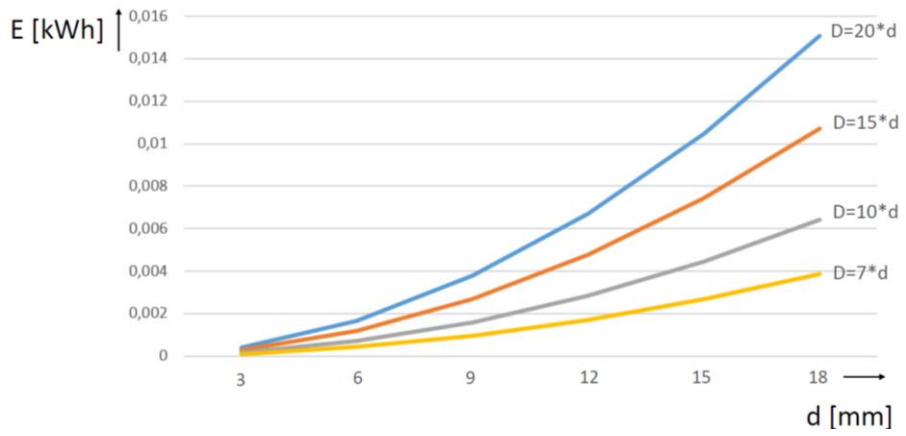

Figure B-6 Relation between the wire thickness 'd' and the potential energy storage 'E' for a single extension spring

Since not a single, but multiple springs will be applied to make the energy storage system, one should take the number of springs which can be applied in a certain amount of space into account. When a smaller diameter spring is used, more springs would fit into the same amount of spacing. Multiplying the amount of potential energy storage of a single spring (Figure B-6) with the amount of springs which could physically be installed in a certain amount of space, we find a relation between the wire thickness 'd' and the total potential energy storage 'E' for different outer diameters as shown in Figure B-7. In these graphs, it is assumed that the springs are installed in a storage shaft with a diameter of 3 [m].

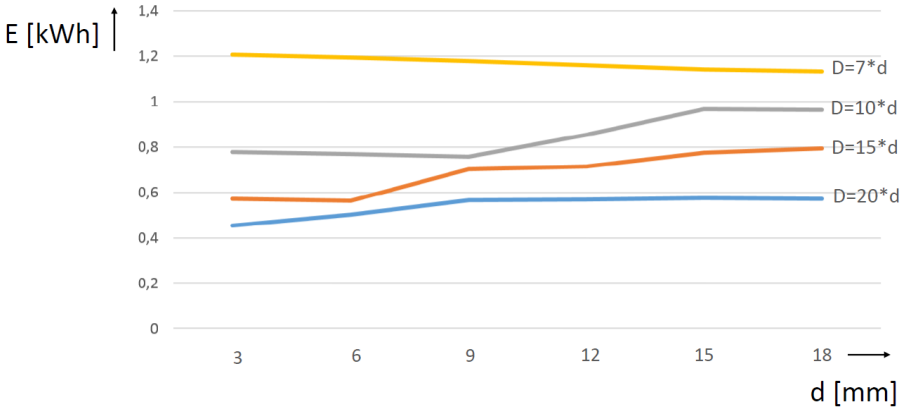

Figure B-7 Relation between the wire thickness 'd' and the potential energy storage 'E' for the amount of springs fitting in a storage shaft with a diameter of 3 [m]

From Figure B-7, we find that using a large amount of springs with a small diameter would result in the largest potential storage capacity. We should however, also consider the maximum extension length which is possible with these springs, as this might determine the stroke and thus the amount of movable water of the energy storage system. A small stroke as a result of the use of small diameter springs is therefore not desirable. A schematic view of a spring system inside a storage shaft is shown in Figure B-8. In this figure, the stroke is assumed to be four to five times the neutral length of the spring.

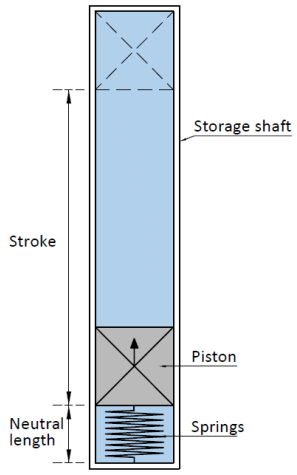

Figure B-8 Schematic view of the neutral length and stroke of an extension spring inside a storage shaft

Using above formula for u_{max}, we find the following relationship curve between the D/d factor and the stroke of the spring with respect to its neutral length. For the desired stroke implied in Figure B-8, the corresponding D/d ratio is about 14,5 [-] as can be seen in Figure B-9. A smaller D/d ratio would increase the potential energy storage of a system of springs. However, the corresponding stroke of the spring would become lower than desired as shown in the figure below.

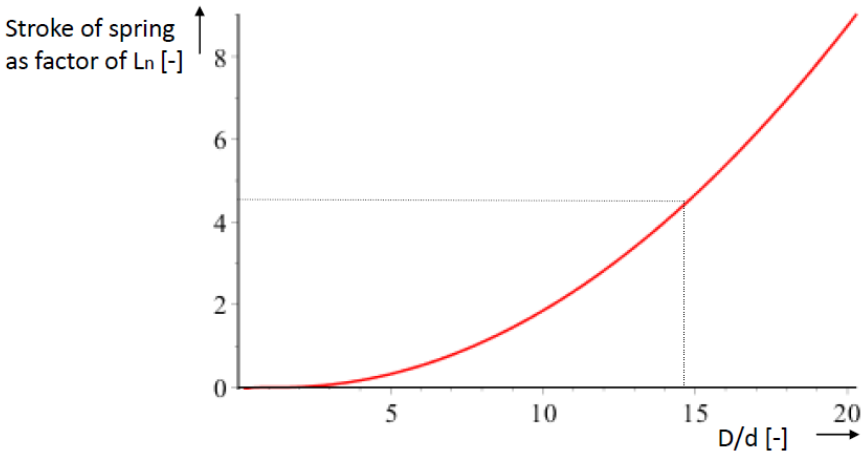

Figure B-9 Relationship curve between the D/d factor and the stroke of the extension spring with respect to its neutral length

Example calculation extension springs

Assume a storage shaft with a diameter of 3 [m], a height of 20 [m] and a watertight piston with a negligible weight (Figure B-11). 71 extension springs with a wire thickness of d = 18 [mm] and an outside diameter of D = 15 * 18 = 270 [mm] are connected to the piston, in the following pattern:

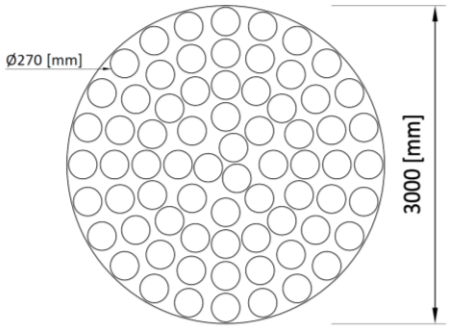

Figure B-10 Top view with the pattern of the 71 extension springs inside a 3 [m] storage shaft

The neutral length Ln is 3000 [mm], which makes the number of active coils N = 3000/18 = 167 [-]. Furthermore, the springs have the following material values:

Material	:	Music Wire ASTM A228
Shear modulus	:	G = 80.000 [N/mm^2]
Allowable torsional stress	:	τ_w = 650 [N/mm^2]

The 'k' factor now becomes (80.000*18^2)/(21952*3000) = 0,39 [N/mm] = 0,39 * 10^3 [N/m] and 'u_{max}' = (2744*π*3000*650)/(15*80.000) = 14008 [mm] = 14,00 [m]. Using the optimal energy equation, we find a total amount of potential energy storage for the 71 springs of E = 71*½*0,39*10^3*14,00^2 = 2,71 [MJ] Assuming the power will be delivered for four hours, we find P = (2,67*10^6)/(4*60*60) = 0,19 [kW] and the capacity of one storage cycle is 0,75 [kWh].

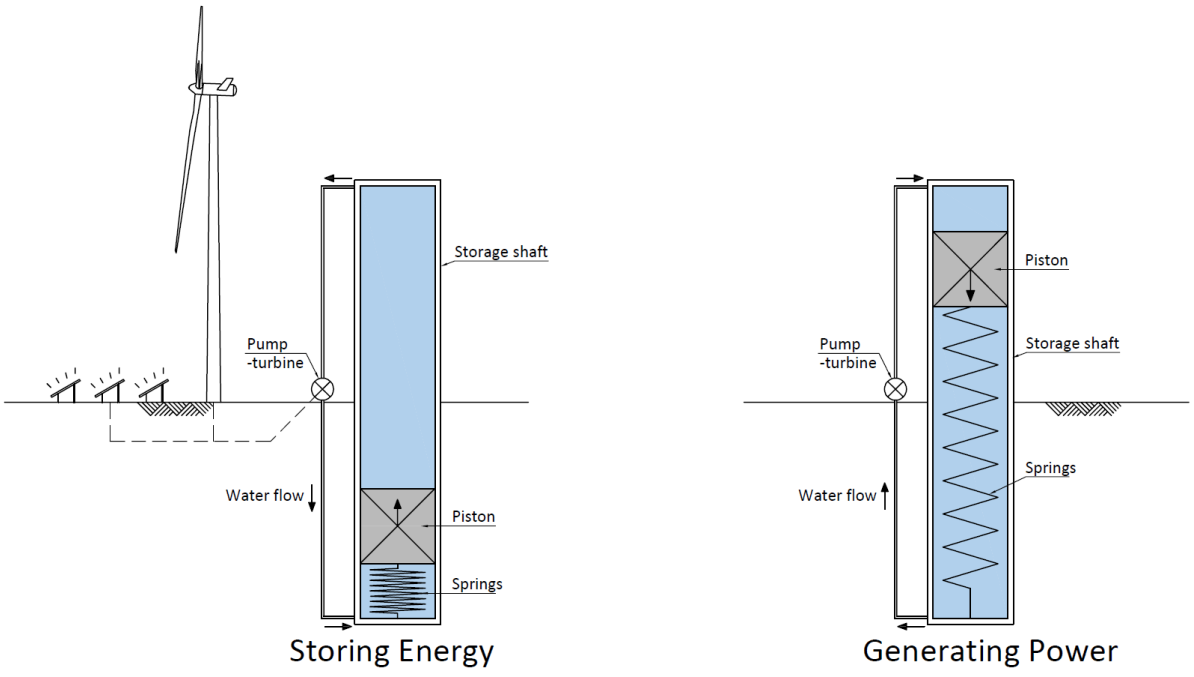

Figure B-11 Schematic view of an extension spring power system in a storage shaft

B2.2 Compression springs

For compression springs, besides the maximum compression length u_{max}, the spacing in-between the coils might determine the amount of compression which is possible. In practice, most of the compression springs are made with an in-between spacing roughly in the range from one- up to 20 times the wire thickness. The corresponding coil heart to heart distance is called the pitch and is equal to the neutral length of the spring 'L_n' divided by the number of coils 'N'. Whether the theoretical maximum compression length u_{max} or the spacing in-between the coils is normative for the stroke of the spring, will depend on the D/d ratio as well as the L_n/(N*d) ratio.

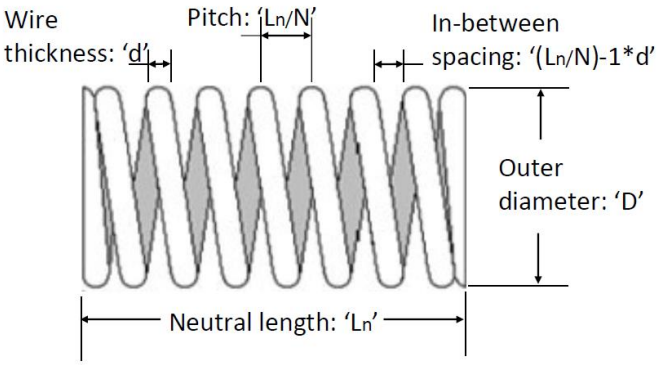

Figure B-12 The measurements of a compression spring

If we again let the outer diameter of the spring 'D' depend on the wire thickness 'd', we find a relation between the wire thickness 'd' and the potential energy storage 'E' for different outer diameters as shown in Figure B-10. The neutral length is set at 14.000 [mm], the L_n/(N*d) ratio to 5 [-] and the wire thicknesses vary from 25 to 150 [mm] in these graphs.

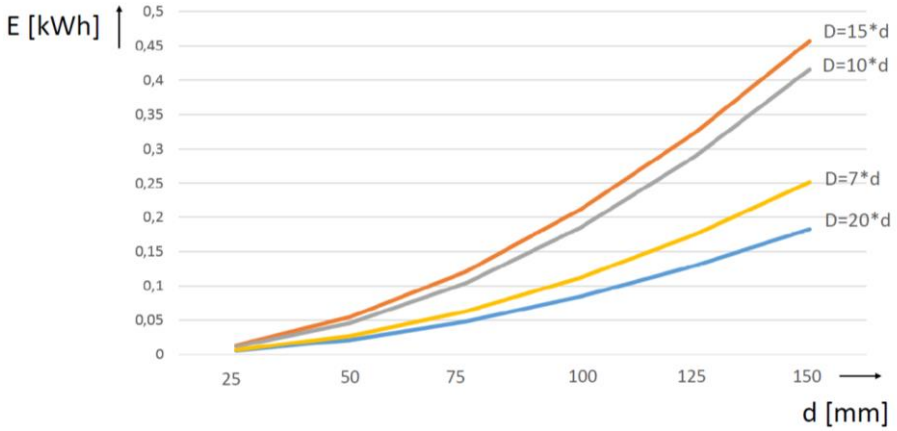

Figure B13 Relation between the wire thickness 'd' and the potential energy storage 'E' for a single compression spring for different D/d ratio's

In Figure B-13 it is notable that the blue 'D=20*d' curve shows a rather small amount of potential energy storage. This can be explained by the fact that the in-between spacing of the coils corresponding with the assumed L_n/(N*d) ratio of 5 is much smaller than the theoretical maximum change in length 'u_{max}' which follows from the 'D/d' ratio of 20. As the change in length goes to the power two in the energy equation, this practical issue has a rather large influence.

Multiplying the amount of potential energy storage of a single spring (Figure B-13) with the amount of springs which could physically be installed in a certain amount of space, we find a relation between the wire thickness 'd' and the total potential energy storage 'E' for different outer diameters as shown in Figure B-11. In these graphs, it is assumed that the springs are installed in a storage shaft with a diameter of 3 [m]. Furthermore, typical spring material Music Wire ASTM A228 with a shear modulus of G = 80.000 [N/mm^2] and an allowable torsional stress of τ_w = 650 [N/mm^2] is assumed in these calculations.

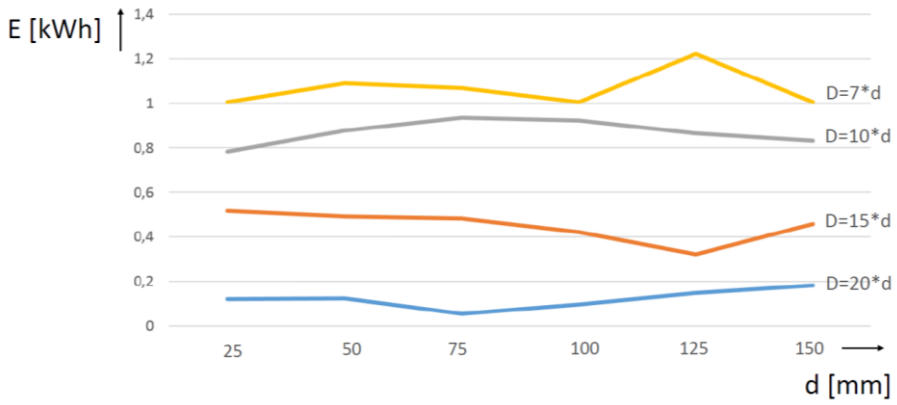

Figure B-14 Relation between the wire thickness 'd' and the potential energy storage 'E' for the amount of springs fitting in a storage shaft with a diameter of 3 [m] for different D/d ratio's

From Figure B-14, we find that using a large amount of springs with a small diameter would result in the largest potential storage capacity. We should however, also consider the maximum compression length which is possible with these springs, as this might determine the stroke and thus the amount of movable water of the energy storage system. A small stroke as a result of the use of small diameter springs is therefore not desirable. A schematic view of a spring system inside a storage shaft is shown in Figure B-15. In this figure, the stroke is assumed to be about 4/5th of the neutral length of the spring.

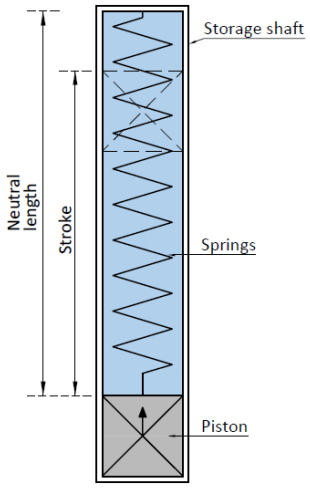

Figure B-15 Schematic view of the neutral length and stroke of a compression spring inside a storage shaft

Using above formula for u_{max}, we find the following relationship curves between the D/d factor and the stroke of the spring with respect to its neutral length for different L_n/(N*d) ratio's. For the desired stroke of 4/5th of the neutral length as implied in Figure B-15, the corresponding D/d ratio is about 14 [-] for a L_n/(N*d) ratio of 5 [-] as can be seen in Figure B-16. This means that if a larger D/d ratio is

used, the theoretical extension length of the spring 'u_{max}' and not the in-between spacing becomes normative for determining the stroke of the spring. The corresponding tipping points for the other L_n/(N*d) ratios are also shown in this figure.

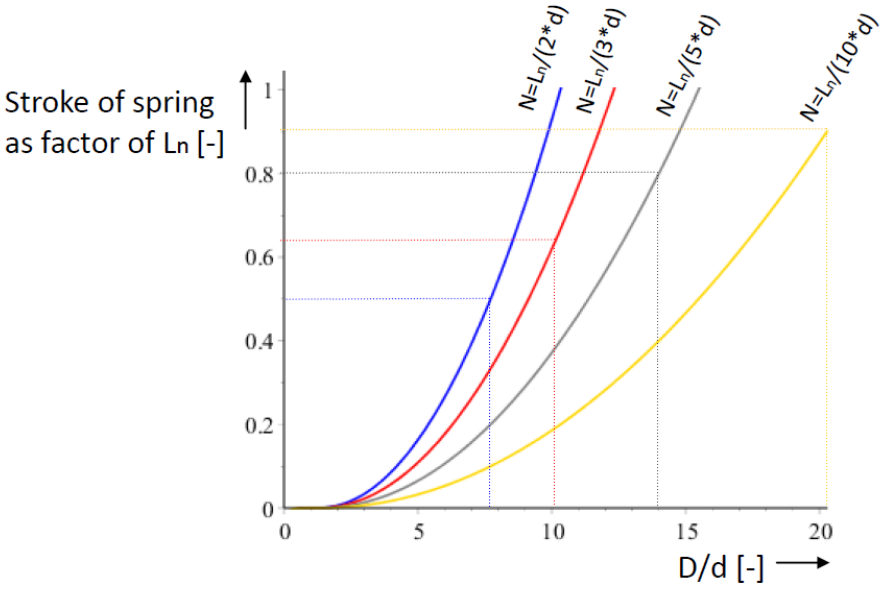

Figure B-16 Relationship curves between the D/d factor and the stroke of the compression spring with respect to its neutral length for multiple L_n/(N*d) ratios

If we look at the L_n/(N*d) ratio alone, we find the following relation between the wire thickness 'd' and the potential energy storage 'E' for different L_n/(N*d) ratio's as shown in Figure B-17. The neutral length is set at 14.000 [mm], the D/d ratio to 15 [-] and the wire thicknesses vary from 25 to 150 [mm] in these graphs.

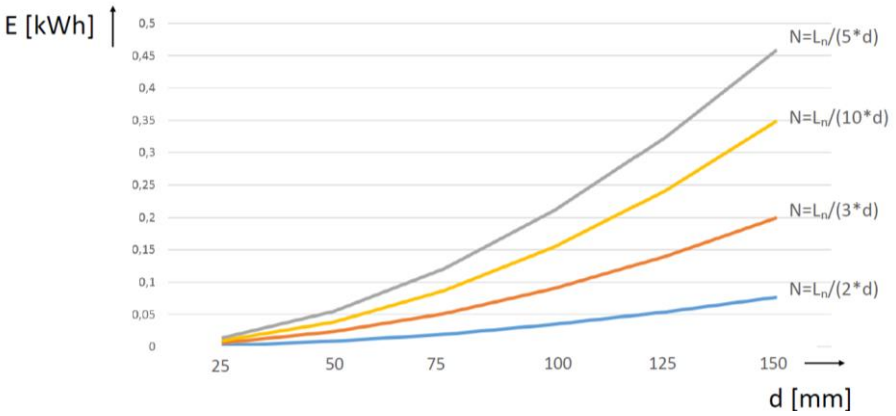

Figure B-17 Relation between the wire thickness 'd' and the potential energy storage 'E' for a single compression spring for different L_n/(N*d) ratio's

In Figure B-17 it is notable that the yellow 'N= L_n/(10*d)' curve shows a smaller amount of potential energy storage than one might expect. This can however be explained by the fact that for this L_n/(N*d) and D/d ratio, the maximum stroke of the springs is very limited. As the change in length goes to the power two in the energy equation, this has a rather large influence.

Example calculation compression springs

Assume a storage shaft with a diameter of 3 [m], a height of 20 [m] and a watertight piston with a negligible weight (Figure B-19). Four compression springs with a large wire thickness of d =75 [mm] and an outside diameter of D =15*75 =1125 [mm] are connected to the piston in the following pattern:

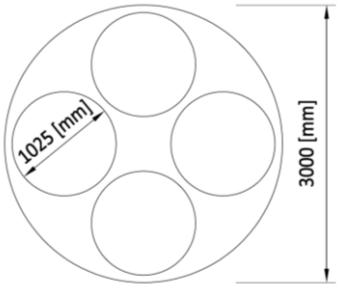

Figure B-18 Top view with the pattern of the four compression springs inside a 3 [m] storage shaft

The neutral length L_n is 14.000 [mm] (multiple springs are connected together), which makes the number of active coils N = 14000/(5*75) = 37 [-]. Furthermore, the springs have the following material values:

Material	:	Music Wire ASTM A228
Shear modulus	:	G = 80.000 [N/mm^2]
Allowable torsional stress	:	τ_w = 650 [N/mm^2]

The 'k' factor now becomes (5*80.000*75^2)/(21952*14000) = 7,32 [N/mm] = 7,32 * 10^3 [N/m] and 'u_{max}' = (2744*π*14000*650)/(75*80.000) = 13074 [mm] = 13,07 [m]. Physically, it is only possible to compress the springs up to 36*4*75 = 10800 [mm] = 10,8 [m]. Using the optimal energy equation, we find a total amount of potential energy storage for the four springs of E = 4*½*7,32*10^3*10,8^2 = 1,71 [MJ] Assuming the power will be delivered for four hours, we find P = (1,71*10^6)/(4*60*60) = 0,12 [kW] and the capacity of one storage cycle is 0,47 [kWh].

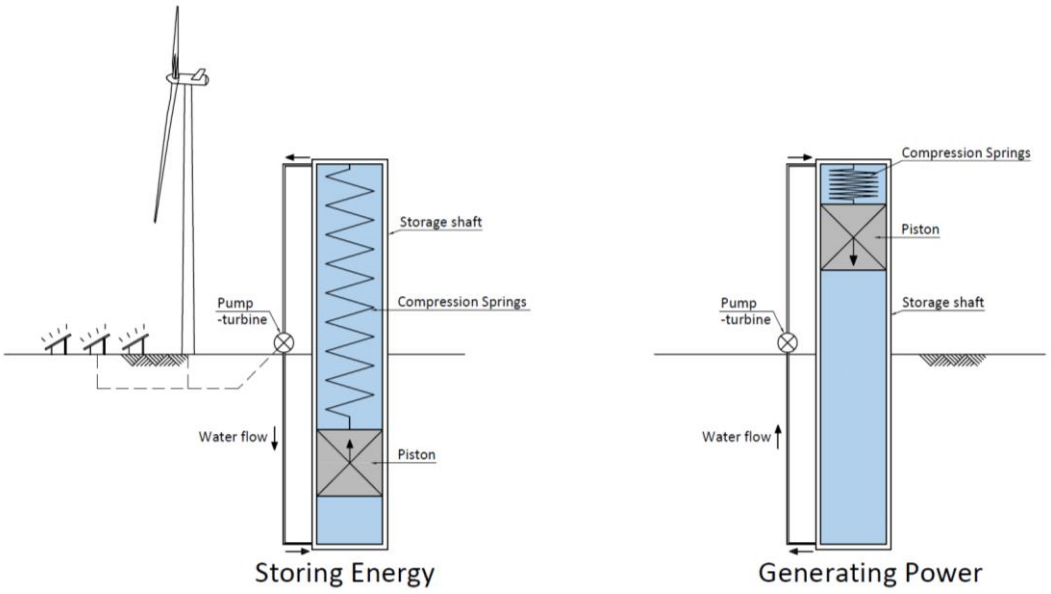

Figure B-19 Schematic view of an compression spring power system in a storage shaft

B3 Result

Taking above into account, we assume a D/d ratio of 15 and a $L_n/(N*d)$ ratio of 5 [-] which make that the outer diameter D = 15*d and the number of active coils N= L_n/d (extension spring) and N= $L_n/5d$ (compression spring) for the following example calculations. With this assumptions, we find the following formula's for 'k' and 'u_{max}', only depending on 'd' and 'L_n':

Extension spring:

$$k = \frac{1}{\left(3\frac{D}{d^2} - 3\frac{D^2}{d^3} + \frac{D^3}{d^4} - \frac{1}{d}\right)} * \frac{G}{8*N} = \frac{1}{21952} * \frac{G*d^2}{L_n}$$

$$u_{max} = \left(3d - 3D + \frac{D^2}{d} - \frac{d^2}{D}\right) * \frac{\pi * N * \tau_w}{G} = \frac{2744}{15} * \frac{\pi * L_n * \tau_w}{G}$$

Compression spring:

$$k = \frac{1}{\left(3\frac{D}{d^2} - 3\frac{D^2}{d^3} + \frac{D^3}{d^4} - \frac{1}{d}\right)} * \frac{G}{8*N} = \frac{5}{21952} * \frac{G*d^2}{L_n}$$

$$u_{max} = \left(3d - 3D + \frac{D^2}{d} - \frac{d^2}{D}\right) * \frac{\pi * N * \tau_w}{G} = \frac{2744}{75} * \frac{\pi * L_n * \tau_w}{G}$$

To determine the amount of potential energy that can be stored, one should multiply the spring constant 'k' with the square of the maximum displacement of the spring 'u_{max}^2'. Since the spring constant 'k' depends on the chosen neutral length of the spring 'L_n' to the power one and on the wire thickness 'd' to the power two, choosing a larger wire thickness will significantly increase the 'k' factor. The maximum displacement length does only depend on the chosen and constant neutral length of the spring 'L_n' and is therefore independent of the wire thickness 'd'. The relationship curves between k and d, u_{max}^2 and the sum of the two is shown in the figure below:

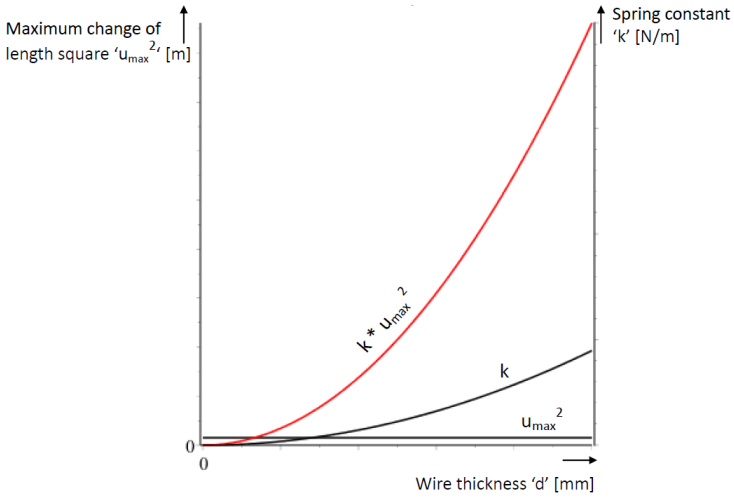

Figure B-20 Relationship curves between k and u, u_{max}^2 and the sum of the two

Conclusion

The wire thickness of a spring has a large influence on the potential energy storage capacity of a single spring. The larger the wire thickness, the more potential energy could be stored. When multiple springs are used however, we find that a large number of smaller springs would potentially store about the same amount of energy as fewer large springs which would fit in the same area. The D/d ratio is therefore more determinative with respect to the potential energy storage of a system of springs. A small D/d ratio makes that the springs each have a smaller footprint so more springs could be installed in a certain area. This increases the potential energy storage capacity of the system of springs fitting in this area. However, an unwanted result of using a small D/d ratio is that the maximum change in length of the spring 'u_{max}' decreases, which causes a smaller stroke and results in less movable water if applied in a storage shaft. Furthermore, taking above example calculations in account, we find that the total amount of potential energy storage of a spring with a realistic wire thickness is relatively low. We can therefore conclude that spring power energy storage is not beneficial for this application.

Appendix C – Thin-walled pressure vessels

C1 stress in thin walled pressure vessel

A vessel can be considered thin-walled if the diameter is at least 10 times greater than the wall thickness. A cylinder body of a thin-walled pressure vessel is shown in the following figure:

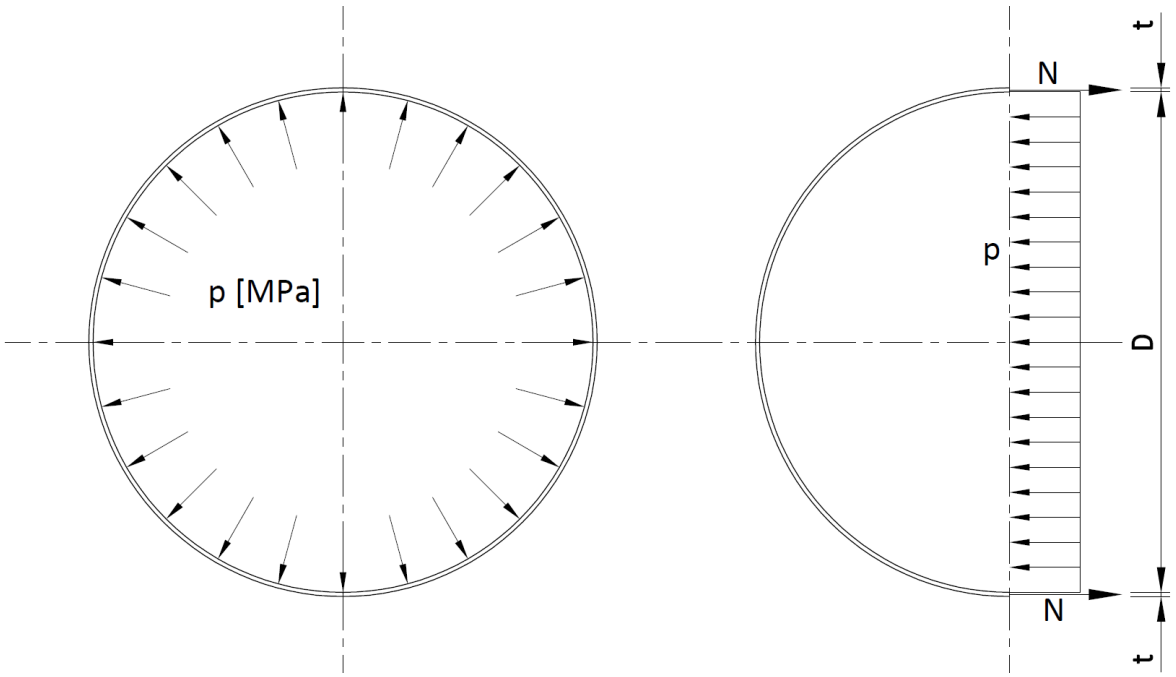

Figure C-1, A thin-walled cylinder body with an inside pressure

The inside pressure force acts perpendicular on the cylinder wall. To make calculation easier, the cylinder is cut in half and the pressure is modelled as a distributed load. One should note that the value of this load is the same as the value of the pressure p. Because of equilibrium it now follows that '2N = p * D'. Where N is the resulting force in the wall. Because of the relatively small wall thickness 'e', we assume an equal stress distribution. It follows that 'N = σ* e'. Combining both formula's we find that the following applies to the radial stress of the vessel:

$$\sigma_\theta = \frac{p * D}{2e}$$

Where:

σ_θ *is the stress in radial direction* $[N/mm2]$
p *is the internal pressure* $[MPa]$
D *is the inner diameter of the cylinder* $[mm]$
e *is the wall thickness* $[mm]$

For an infinitely long cylinder where the wall thickness is constant and the material and thus the yield stress σ_y is known and no longitudinal stresses are present, a relation between the diameter and the maximum internal pressure can be derived. We find:

$$p = \frac{\sigma_y * 2e}{D}$$

The volume of the cylinder per meter length can be found by:

$$V = \frac{\pi * D^2}{4}$$

To determine the amount of energy which can be stored in a system, the air pressure inside the cylinder needs to be multiplied with the volume. Since the volume is dependent of the diameter to the power two, and the pressure is only dependent to the diameter to the power one, a larger diameter would potentially store more energy. The relationship curves between p and D, V and D and the sum of the two is shown in the figure below:

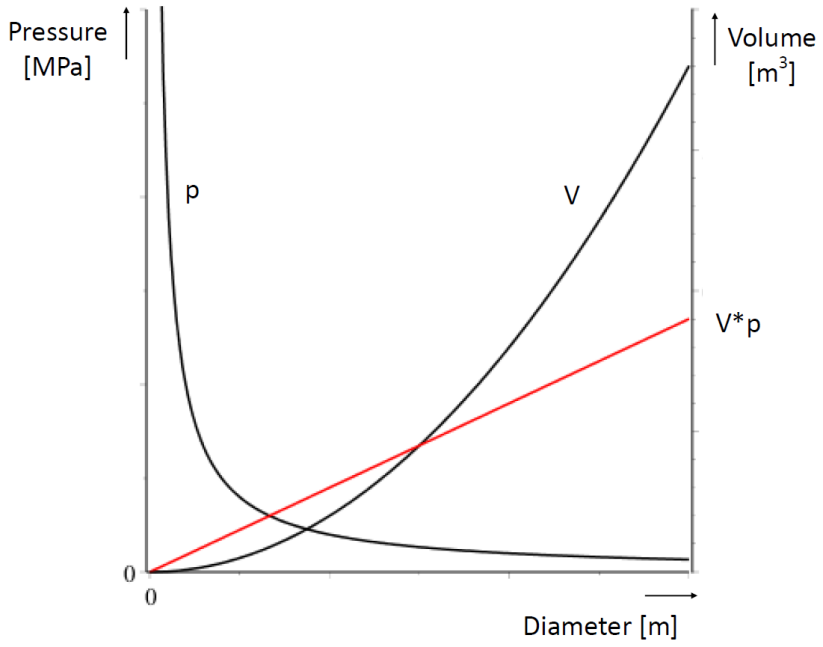

Figure C-2, The relationship curves between p and D, V and D and the sum of the two

Translating this to the amount of potential energy which could be stored using $E=p_2*V_1/e$, we find a linear relationship between the amount of energy storage 'E' and the diameter of the shaft 'D as shown in the figure below. Here, the wall thickness, yield stress and the shaft height are set as constants with e = 25 [mm], σ_y = 235 [N/mm^2] and H = 20 [m]. No maximum air pressure is taken into account in this figure. If a maximum tolerated pressure would be set at 50 [MPa] for instance, a lower energy storage would be the result for smaller diameters up to 1.5 [m].

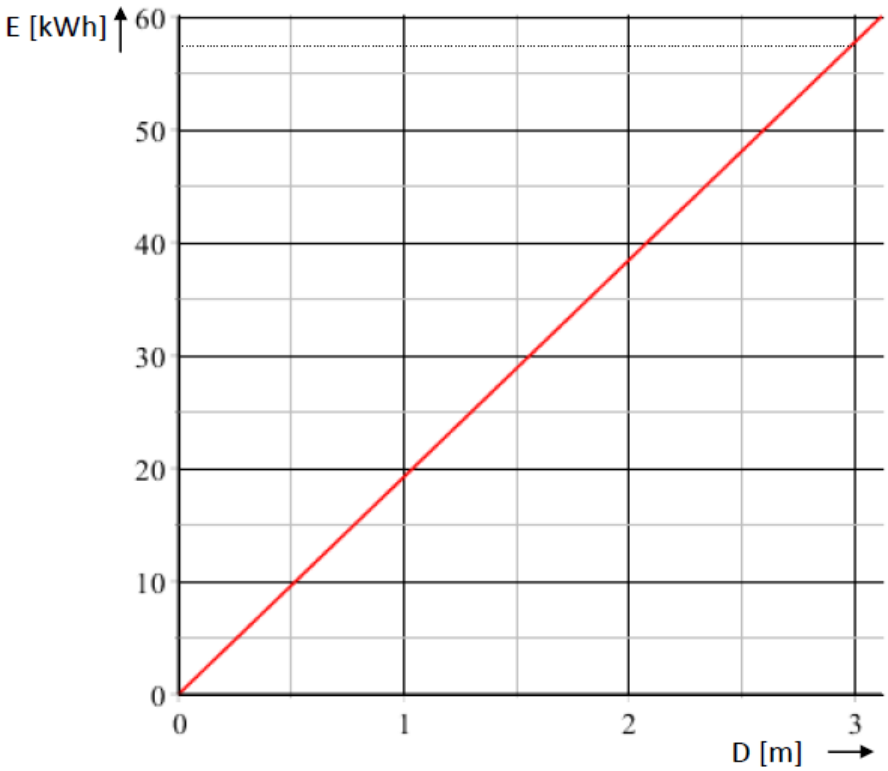

Figure C-3, The relationship curve between E and D

Appendix D – Delivery and instalment costs of steel piles

The delivery and instalment costs of the steel piles is expected to be one of the largest expenses of the designed energy storage system. In this appendix, these costs are estimated.

D1 Production range

In order to make realistic and affordable design choices, one may take the production range of various suppliers into account. Using non-standard pile dimensions may drastically increase the costs, or might even be impossible to make. To get an impression, the common production sizes of ArcellorMittal are shown in figure D-1.

Weight (kg/m pipe)

Wall thickness (mm & inch)

Outside diameter (mm & inch)

mm	inch	10	11	12	13	14	15	16	17	18	19	20	21	22	23	24	25
mm	inch	0,39	0,43	0,47	0,51	0,55	0,59	0,63	0,67	0,71	0,75	0,79	0,83	0,87	0,91	0,94	0,98
864	34	211	231	252	273	293	314	334	355	375	396	416	436				
914	36	223	245	267	289	311	333	354	376	398	420	441	463	484			
965	38	236	259	282	305	328	352	375	398	420	443	466	489	512			
1.016	40	248	273	297	322	346	370	395	419	443	467	491	515	539	563	587	611
1.067	42	261	286	312	338	363	389	415	440	466	491	516	542	567	592	617	642
1.118	44	273	300	327	354	381	408	435	461	488	515	541	568	594	621	648	674
1.168	46	286	314	342	370	399	427	455	483	511	539	566	594	622	650	677	705
1.219	48	298	328	357	387	416	445	475	504	533	562	591	621	650	679	707	736
1.270	50	311	342	372	403	434	464	495	525	556	586	617	647	677	707	737	768
1.321	52	323	355	387	419	451	483	515	547	578	610	642	673	705	736	768	799
1.372	54	336	369	402	436	469	502	535	568	601	634	667	699	732	765	798	830
1.422	56	348	383	417	452	486	521	555	589	623	658	692	726	760	794	828	862
1.473	58			432	468	504	539	575	611	646	681	717	752	787	823	858	893
1.524	60			447	484	521	558	595	632	669	705	742	778	815	851	888	924
1.575	62			462	501	539	577	615	653	691	729	767	805	842	880	918	956
1.626	64			478	517	556	596	635	674	714	753	792	831	870	909	948	987
1.676	66			493	533	574	615	655	696	736	777	817	857	898	938	978	1.018
1.727	68			508	550	592	633	675	717	759	800	842	884	925	967	1.008	1.049
1.778	70			523	566	609	652	695	738	781	824	867	910	953	995	1.038	1.081
1.829	72			538	582	627	671	715	760	804	848	892	936	980	1.024	1.068	1.112
1.880	74			553	598	644	690	735	781	826	872	917	963	1.008	1.053	1.098	1.143
1.930	76			568	615	662	709	755	802	849	896	942	989	1.035	1.082	1.128	1.175
1.981	78			583	631	679	727	775	823	871	919	967	1.015	1.063	1.111	1.158	1.206
2.032	80			598	647	697	746	795	845	894	943	992	1.041	1.091	1.140	1.188	1.237
2.083	82			613	664	714	765	816	866	917	967	1.017	1.068	1.118	1.168	1.219	1.269
2.134	84			628	680	732	784	836	887	939	991	1.042	1.094	1.146	1.197	1.249	1.300
2.184	86			643	696	749	803	856	909	962	1.015	1.068	1.120	1.173	1.226	1.279	1.331
2.235	88			658	712	767	821	876	930	984	1.038	1.093	1.147	1.201	1.255	1.309	1.363
2.286	90			673	729	784	840	896	951	1.007	1.062	1.118	1.173	1.228	1.284	1.339	1.394
2.337	92			688	745	802	859	916	973	1.029	1.086	1.143	1.199	1.256	1.312	1.369	1.425
2.388	94			703	761	820	878	936	994	1.052	1.110	1.168	1.226	1.283	1.341	1.399	1.457
2.438	96			718	778	837	896	956	1.015	1.074	1.134	1.193	1.252	1.311	1.370	1.429	1.488
2.489	98			733	794	855	915	976	1.036	1.097	1.157	1.218	1.278	1.339	1.399	1.459	1.519
2.540	100			748	810	872	934	996	1.058	1.120	1.181	1.243	1.305	1.366	1.428	1.489	1.551
2.591	102			763	826	890	953	1.016	1.079	1.142	1.205	1.268	1.331	1.394	1.456	1.519	1.582
2.642	104			778	843	907	972	1.036	1.100	1.165	1.229	1.293	1.357	1.421	1.485	1.549	1.613
2.692	106			793	859	925	990	1.056	1.122	1.187	1.253	1.318	1.383	1.449	1.514	1.579	1.645
2.743	108			808	875	942	1.009	1.076	1.143	1.210	1.276	1.343	1.410	1.476	1.543	1.609	1.676
2.794	110			823	892	960	1.028	1.096	1.164	1.232	1.300	1.368	1.436	1.504	1.572	1.639	1.707
2.845	112			838	908	977	1.047	1.116	1.186	1.255	1.324	1.393	1.462	1.532	1.601	1.670	1.739
2.896	114			853	924	995	1.066	1.136	1.207	1.277	1.348	1.418	1.489	1.559	1.629	1.700	1.770
2.946	116			868	940	1.012	1.084	1.156	1.228	1.300	1.372	1.443	1.515	1.587	1.658	1.730	1.801
2.997	118			883	957	1.030	1.103	1.176	1.249	1.322	1.395	1.468	1.541	1.614	1.687	1.760	1.832

Legend:
up to X70
up to X52

all intermediate dimensions are available on demand

| 5

Figure D-1 Spirally welded steel pipe production dimension (ArcelorMittal, 2016)

These pipes are available in steel qualities S235, S275, S355, S420 and S460 and can be produced up to 53 [m]. Longer lengths can be achieved by welding pipes together. An impression about the production process is shown in figure D-2.

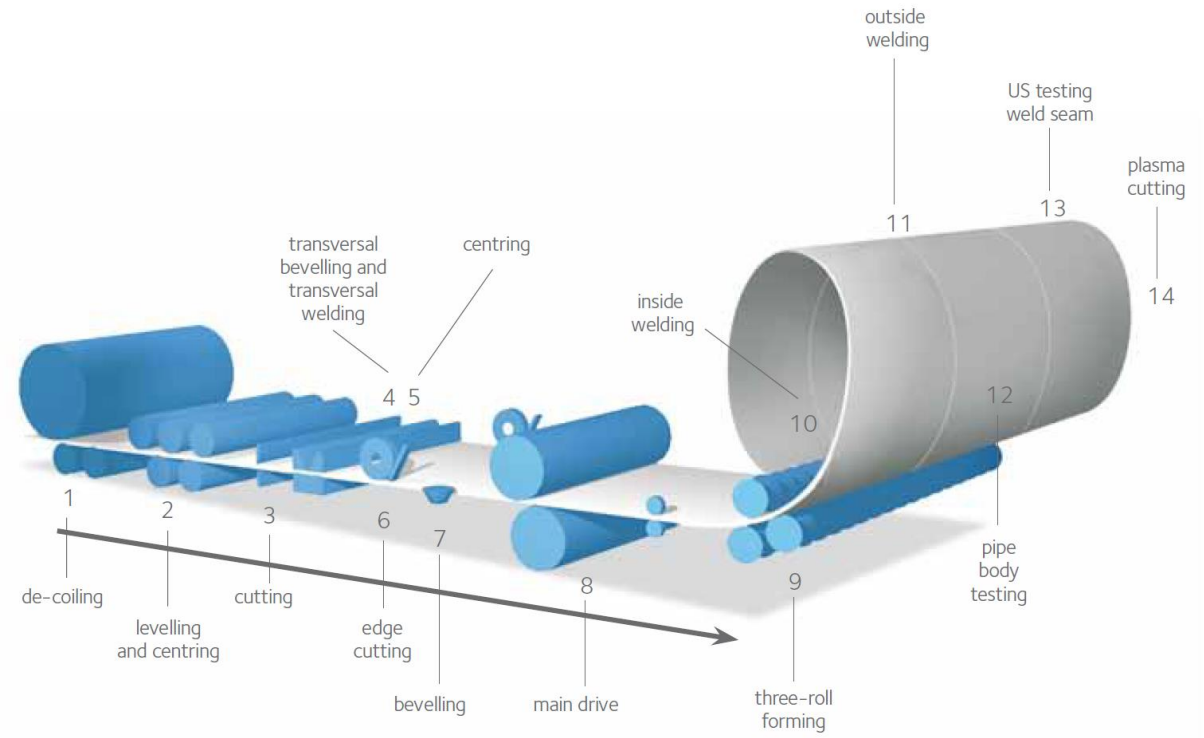

Figure D-2 Impression of the production process of spirally welded steel pipes (ArcelorMittal, 2016)

D2 Execution methods

A very crucial part for designing a steel pile foundation, is taking the execution method into account. For smaller piles, rather standard execution methods can usually be used in order to drive the piles in position. Installing piles with larger diameters usually requires special, non-regular equipment. Below, different execution methods are stated and the construction costs are estimated.

Internally driven

One way to install a steel pile is by using a free-fall drop hammer inside the pile. The hollow pile is provided with a welded base plate. During pile driving, a few buckets of gravel stones are often thrown to the bottom of the pile in order to drive it without punching through the base plate. Typical diameters vary from 168 to 508 [mm] (Waalpaal, 2016). Slightly larger diameters are sometimes possible on demand but it will depend on the soil properties if these piles can still be installed internally driven. The advantages of this execution method are that it is relatively cheap, easy and the shaft does not need to be dug out afterwards. An impression of this execution method is shown below:

Figure D-3 Impression of a steel pile being installed by a free-fall drop hammer inside the pile (Vroom, 2016)

A cost estimation of the delivery and instalment of a single steel pile with a diameter of 508 [mm], a wall thickness of 20 [mm] and a length of 20 [m] is shown in table D-1.

Tabel D-1 Cost estimation of a steel pile with a diameter of 508 [mm], a wall thickness of 20 [mm] and a length of 20 [m] (excluding VAT)

Item	Units	Price per unit	Price
Delivery steel pile	2450 [kg]	€ 0,85	€ 2.100,-
Mobilization/demobilization equipment	[-]	€ 3.000,-	€ 3.000,-
Instalment	32 [m^2]	€ 15,-	€ 500,-
Subtotal:			€ 5.600,-
Further detailing	20%	€ 5.600,-	€ 1.100
Overhead costs	25%	€ 6.700,-	€ 1.700,-
Contingency costs	10%	€ 8.400,-	€ 840,-
Total costs:			**€ 9.240,-**

Pile drilling

A drilled pile is a pile with a drilling head attached to it. The pile is screwed into the ground by applying an axial pressure and a torque moment. After reaching the desired depth, the pile may be considered installed. Typical diameters vary from 168 to 762 [mm] (Fundex, 2016). This method is vibration free and can be applied in a various range of soil properties. Furthermore, in contrast with the internally driven piles, the drilled piles can be installed under a slope. An impression of a drill head is shown in figure D-4.

Figure D-4 Impression of multiple drill heads attached to a pile

An estimation of the costs can be found in the table below:

Tabel D-2 Cost estimation of a steel pile with a drill head, a diameter of 762 [mm], a wall thickness of 20 [mm] and a length of 20 [m] (excluding VAT)

Item	Units	Price per unit	Price
Delivery steel pile	3700 [kg]	€ 0,85	€ 3.200,-
Attaching drill head	[-]	€ 500,-	€ 500,-
Mobilization/demobilization equipment	[-]	€ 3.000,-	€ 3.000,-
Instalment	48 [m^2]	€ 30,-	€ 1.500,-
Subtotal:			€ 8.200,-
Further detailing	20%	€ 8.200,-	€ 1.650
Overhead costs	25%	€ 9.850,-	€ 2.450,-
Contingency costs	10%	€12.300,-	€ 1.200,-
Total costs:			**€ 13.530,-**

Large diameter pile driving by vibrating and hydraulic hammering

Larger diameter steel piles are usually installed without a base plate. The steel piles, typically in the range from 1016 to 3000 [mm] are vibrated into the soil as far as possible. Subsequently, a hydraulic hammer can install the pile to its final position (Voorbij, 2016). Afterwards, the soil inside the pile needs to be excavated and a underwater concrete floor can be poured. A steel plate can then be welded to the pile in order to make it a 100 percent watertight. An impression of the instalment of such a pile can is shown in figure D-2.

Figure D-5 Impression of a large diameter steel pile being installed by a hydraulic hammer (Voorbij, 2016)

A 'normal' non-modified pile driving machine and vibration hammer would be able to drive piles in the range up to roughly 1.6 [m]. When the diameter becomes bigger and the piles become heavier, the equipment which is needed to install the piles needs to be larger and sometimes even specially modified. A pile with a diameter of 2020 [mm], a wall thickness of 25 [mm] and a length of 20 [m] for instance weights almost 25 tons. This, together with the huge vibration hammer which is needed, may cause the need for a very large and thus more expensive crane in order to install the pile. An impression of such a size pile and special vibration hammer is given in figure D-6 and figure D-7.

Figure D-6 Securing a steel pile with a diameter of 2400 [mm] in the port of Rotterdam (Gebr.deKoning, 2016)

Figure D-7 Impression of the modified vibration hammer, used to install the piles with a diameter of 2400 [mm] (Gebr.deKoning, 2016)

An estimation of the costs can be found in the tables below:

Tabel D-3 Cost estimation of a steel pile with a diameter of 1600 [mm], a wall thickness of 25 [mm] and a length of 20 [m] (excluding VAT)

Item	Units	Price per unit	Price
Delivery steel pile	9800 [kg]	€ 0,85	€ 8.300,-
Mobilization/demobilization equipment	[-]	€ 10.000,-	€ 10.000,-
Instalment	1 [day]	€ 3.000,-	€ 3.000,-
Excavation	40 [m^3]	€ 12,-	€ 500,-
Underwater concrete	2 [m3]	€ 300,-	€ 600,-
Pumping dry	[-]	€ 1500,-	€ 1500,-
Delivery steel plate	500[kg]	€ 0,85	€ 400,-
Welding steel plate (1 men + crane)	[-]	€ 1.200,-	€ 1.200,-
Subtotal:			€ 25.500,-
Further detailing	20%	€ 25.500,-	€ 5.100,-
Overhead costs	25%	€ 30.600,-	€ 7.700,-
Contingency costs	10%	€ 38.300,-	€ 3.830,-
Total costs:			**€ 42.130,-**

Tabel D-4 Cost estimation of a steel pile with a diameter of 3000 [mm], a wall thickness of 25 [mm] and a length of 20 [m] (excluding VAT)

Item	Units	Price per unit	Price
Delivery steel pile	36700 [kg]	€ 0,85	€ 31.200,-
Mobilization/demobilization equipment	[-]	€ 25.000,-	€ 25.000,-
Instalment	1 [day]	€ 6.500,-	€ 6.500,-
Excavation	141 [m^3]	€ 12,-	€ 1.700,-
Underwater concrete	7 [m3]	€ 300,-	€ 2.100,-
Pumping dry	[-]	€ 1.500,-	€ 1.500,-
Delivery steel plate	1650[kg]	€ 0,85	€ 1.400,-
Welding steel plate (2 men + crane)	[-]	€ 1.600,-	€ 1.600,-
Subtotal:			€ 71.000,-
Further detailing	20%	€ 71.000,-	€ 14.200,-
Overhead costs	25%	€ 85200,-	€ 21.300,-
Contingency costs	10%	€ 106.500,-	€ 10.600,-
Total costs:			**€ 117.150,-**

D3 Result

Taking above production ranges and execution methods into account, we find the following graph of the estimated construction costs of a single steel pile with respect to its diameter:

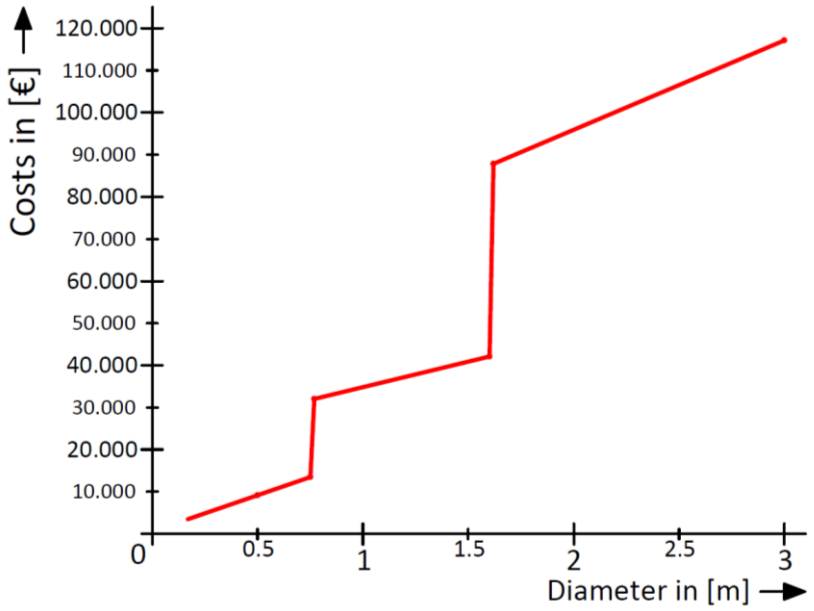

Figure D-8 Estimated construction costs of a single steel pile with respect to its diameter

Appendix E –Water Turbines

The water turbine which is used in a hydropower system determines the power output which can be delivered. Water turbines can be divided into two categories, namely impulse- and reaction turbines. Impulse turbines are spinning due to a water jet hitting the turbine blades. The potential energy of the water is converted into kinetic energy by a nozzle focused on the turbine. The most common type of impulse turbine is called a 'Pelton Turbine'. Reaction turbines are spinning as the water pushes through and past its blades. A reaction turbine does not change the direction of the water flow as drastically as an impulse turbine. Commonly used reaction turbines are Francis- or Kaplan Turbines.

E1 Pelton Turbines

A Pelton turbine describes an impulse turbine mainly used for high head hydro power facilities. The water, which is under pressure, is transported in a penstock pipe towards the rotor or so called 'Pelton Wheel'. A basic diagram of a Pelton turbine is shown in Figure E-1.

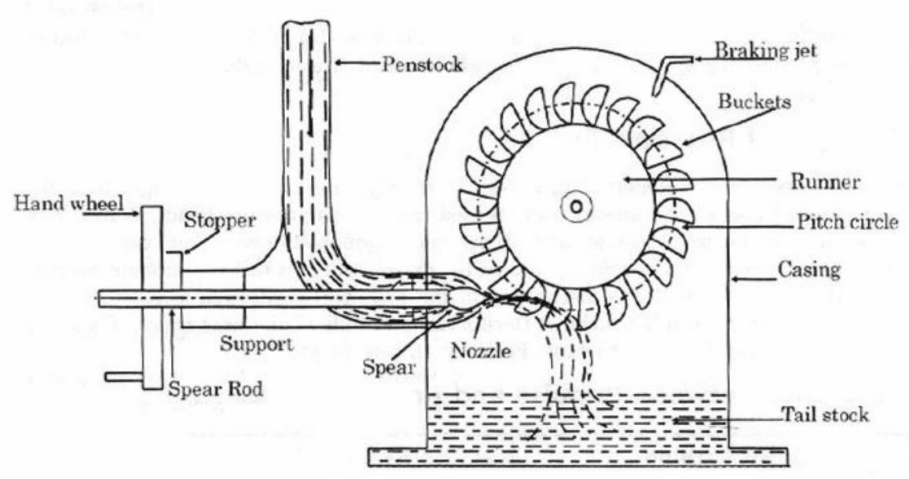

Figure E-1 Basic diagram of a Pelton turbine

In Figure E-1 a penstock pipe transports the water on the left hand side. Before the water makes contact with the buckets on the Runner or so called 'Pelton Wheel', it passes an adjustable nozzle called a spear-jet. The spear-jet adjusts the flow area and thereby the flow rate by moving back and forth which moves the head of the spear into and away from the nozzle. Once through the spear-jet, the water hits the curved spoon shaped buckets of the Pelton Wheel, making it spin. The buckets are designed to minimize all losses and maximize the transfer of kinetic energy (motion of water) into rotational energy of the rotor. Firstly the water jet is split into two equal jets on each side of the buckets. Then, the shape of the bucket is designed in such a way that the turn of the jet of water is almost 180 degrees. This shape maximizes the energy transfer, minimizes the amount of splashing and leaves just enough energy for the water jet to fully exit the rotor so hardly any water hits the next bucket. Once the water jets leave the buckets, the water falls down and is transported into the water tank. A figure of the Pelton Wheel and its typical curved spoon shaped buckets is shown in Figure E-2.

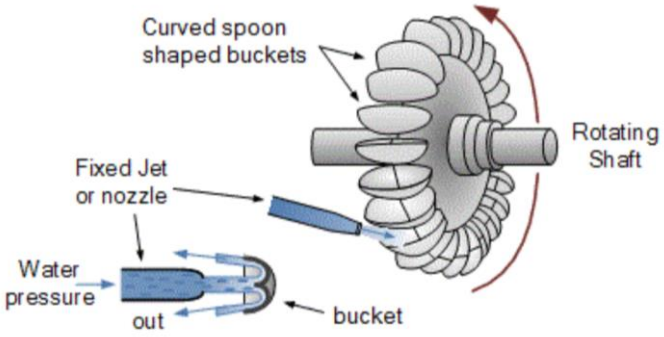

Figure E-2 'Pelton Wheel' with typical curved spoon shaped buckets

Pelton turbines can reach up to 95% efficiency, and even on 'micro' scale 90% peak efficiency is achievable (RenewablesFirst, 2015). Furthermore, Pelton Turbines show a behavior where a rather high efficiency is maintained even for flow rates that are a fraction of its maximum or design flow rate. This can mainly be devoted to the low-loss design of the spear-jet. A typical efficiency curve for a Pelton turbine is shown in Figure E-3. In this figure, a curve for a single spear-jet Pelton turbine is shown in red. When multiple spear jets are applied, the Pelton turbine would operate at high efficiency over an even wider flow range. The blue curve in this figure represents the efficiency curve when two spear-jets are applied on a Pelton Turbine.

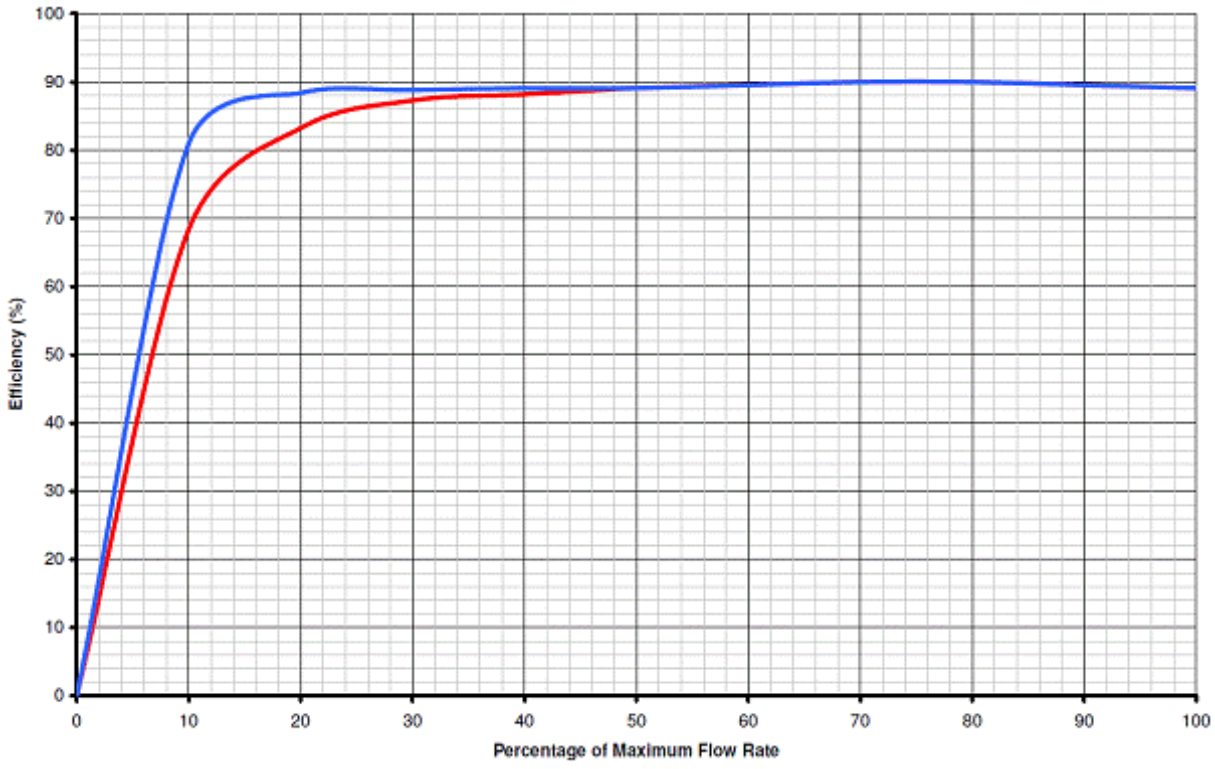

Figure E-3 Typical efficiency curves for a single- (red) and twin (blue) spear-jet Pelton turbine (RenewablesFirst, 2015)

Pelton turbines rotate at relatively high speeds. This is an advantage, since it is often possible to design them such that the operating speed of the turbine and the generator are the same. As a consequence, the turbine and the generator can be directly coupled, leaving no need for a belt or gearbox which may cause extra losses. Figure E-4 shows a turbine which does need a belt to connect the turbine to the generator. Not only does this belt-drive add extra components and thereby additional costs, it also

causes (friction) losses which can be between 2% to 7% (RenewablesFirst, 2015). The other figures give a good idea about the range of Pelton system application. In Figure E-5, a large multi-megawatt system with twin rotors and a directly-coupled generator is installed. Figure E-6 shows a Pelton turbine with a maximum output of 11 [kW] being installed. Figure E-7 shows a cross section of a Pelton turbine with two nozzles and Figure E-8 shows a detail of a Pelton Wheel.

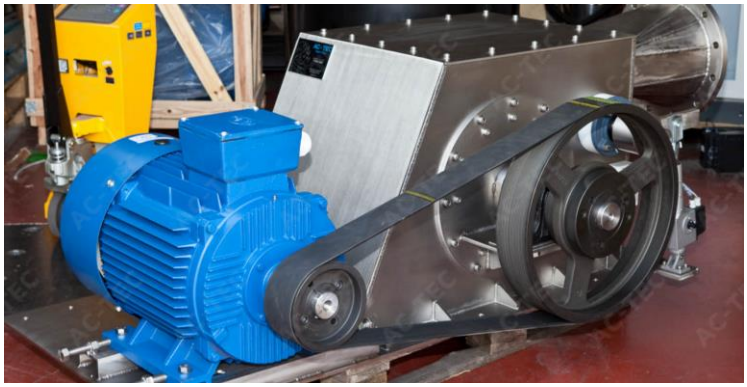

Figure E-4 A turbine coupled to its generator using a rubber belt (AC-TEC, 2015)

Figure E-5 A large utility-scale Pelton turbine installation (RenewablesFirst, 2015)

Figure E-6 A 11 [kW] Pelton turbine installation (RenewablesFirst, 2015)

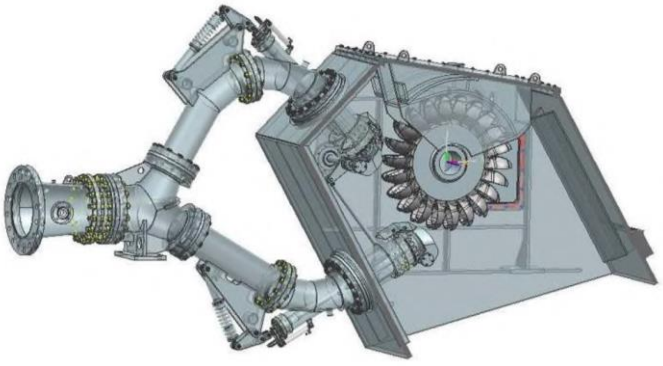

Figure E-7 A cross section of a Pelton turbine with two nozzles (BulgariaSerbia, 2014)

Figure E-8 A Pelton Wheel (BulgariaSerbia, 2014)

E2 Kaplan Turbines

A Kaplan turbine describes a reaction turbine in the form of a propeller inside a tube which mainly used for low head and high flow hydro power facilities. The water is transported through the inlet guide-vanes, which can be opened and closed in order to regulate the amount of flow that can pass through the turbine. The turbine itself is a axial-flow turbine, which means that the flow direction does not change as it crosses the rotor. A basic diagram of a Kaplan turbine is shown in Figure E-9.

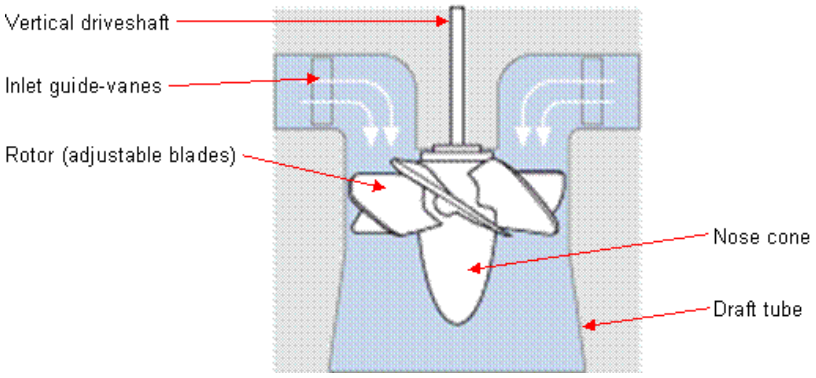

Figure E-9 Basic diagram of a Kaplan turbine (RenewablesFirst, 2015)

The rotor blades of the turbine can be made adjustable, which ensures that the water, depending on the flow rate, hits the blades at the most efficient angle for the highest efficiency. The nose cone on a Kaplan turbine is an important hydro-dynamical part which reduces losses and prevent the formation of a core 'rope vortex'. The draft tube below the rotor has a carefully designed geometry, as it has to extract any remaining kinetic energy from the flow by reducing the water pressure after the rotor.

Typically, Kaplan turbines are used on sites with net head from 1.5 to 20 [m] and peak flow rates from 3 [m^3/s] to 30 [m^3/s] (RenewablesFirst, 2015). Such sites would have power outputs ranging from 75 [kW] up to 1 [MW]. The efficiency achieved by Kaplan turbines can go over 90% (Waterturbines, 2016), mainly due to the variable geometry of inlet guide-vanes and turbine blades. When the turbines are equipped with non-adjustable rotor blades, the range of a proper efficiency becomes rather small, as Figure E-10 clearly shows. In this figure, a turbine with adjustable rotor blades and regulated guide-vanes has a much wider range to achieve a high efficiency than a turbine which has non-adjustable rotor blades.

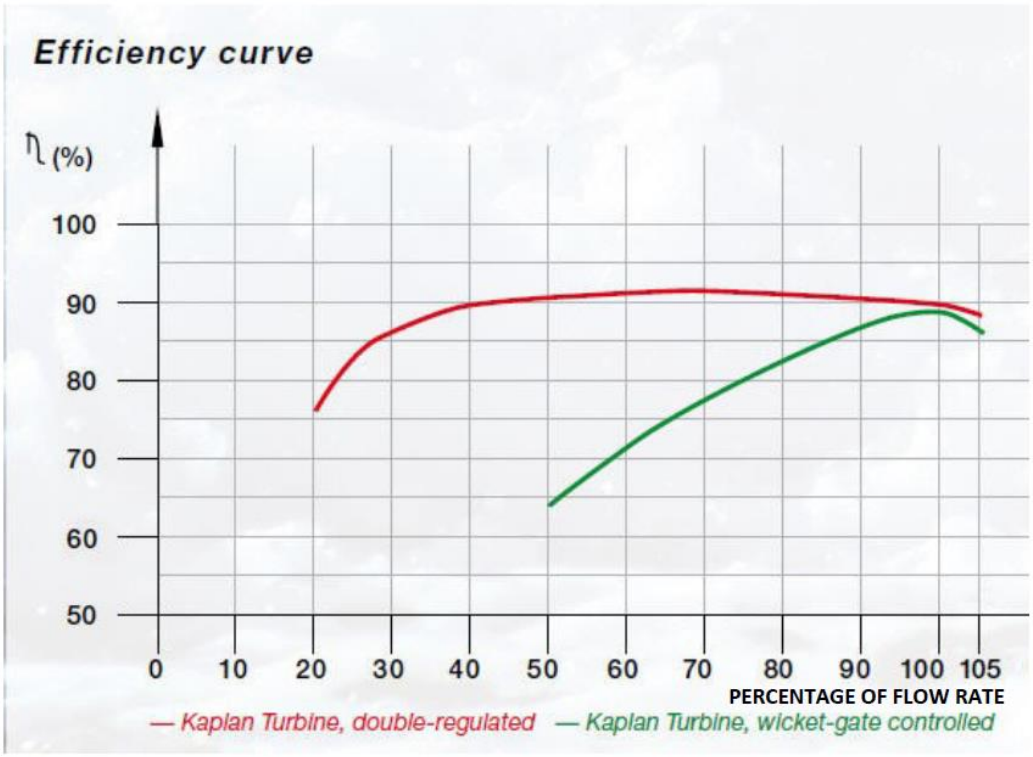

Figure E-10 Typical efficiency curves for a double-regulated- (red) and an only guide-vanes controlled (green) Kaplan turbine (Water21, 2014)

Figure E-11 shows a Kaplan turbine with a cross section of the snail shell shaped inlet volute which distributes the water equally around the whole rotor. The draft tube is often casted in concrete during the construction phase.

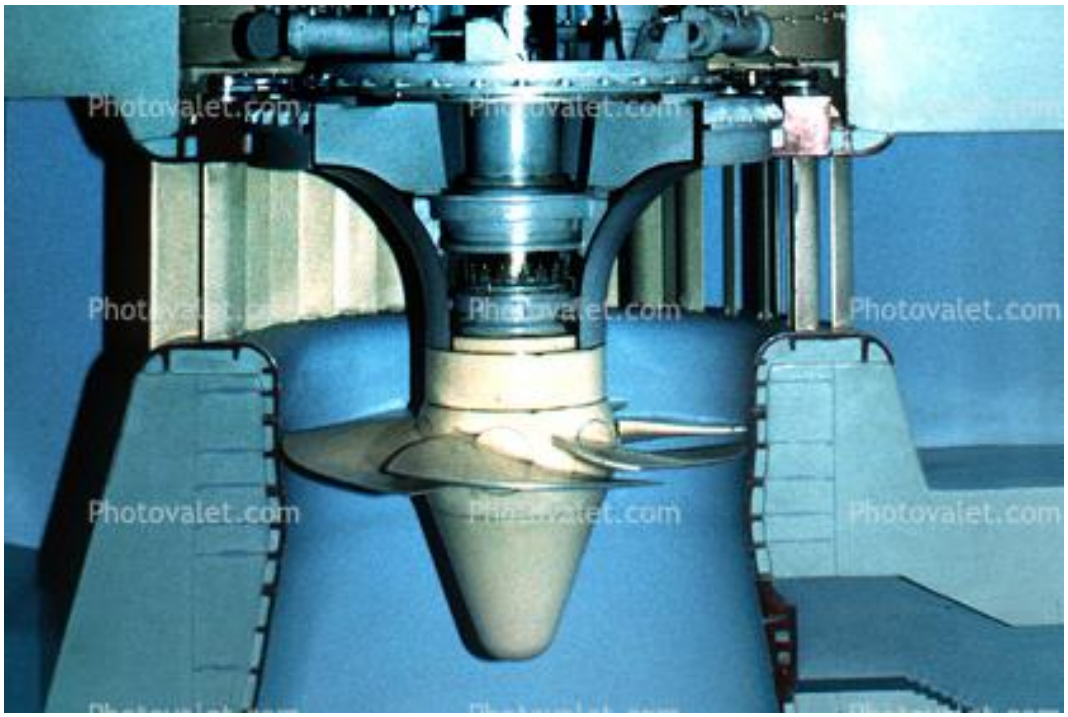

Figure E-11 A Kaplan turbine build into a concrete structure (Waterturbines, 2016)

E3 Francis Turbines

A Francis Turbine describes a reaction turbine where water changes pressure as it moves through the runner and transfers its energy. The water is transported through a snail shell shaped spiral casing which moves the water around the runner, where it enters horizontally and exits vertically down through the centre of the turbine. A basic diagram of a Francis turbine is shown in Figure E-12. The characteristic shape of the runner of a Francis turbine is shown in Figure E14.

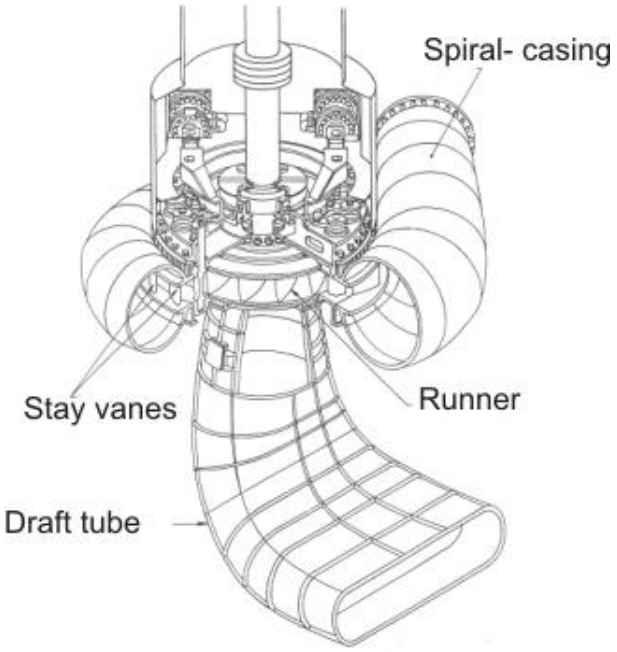

Figure E-12 Basic diagram of a Francis turbine (Waterturbines, 2016)

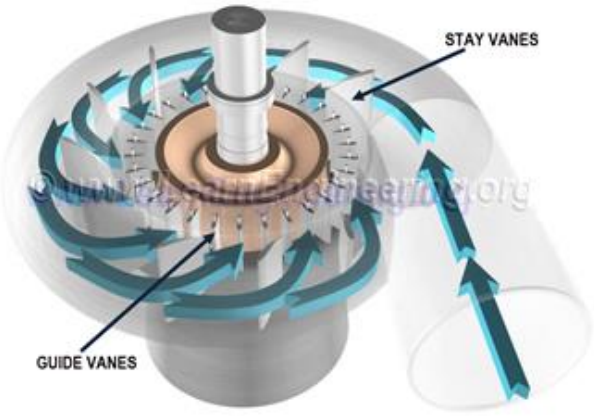

Figure E-13 Water being transported through the snail shell shaped spiral casing of a Francis turbine (Waterturbines, 2016)

Figure E-14 Runner of a Francis turbine (Waterturbines, 2016)

In Figure E-13 it is shown that the spiral casing and the stay vanes guide the water into the runner. The cross section of the spiral casing is continuously decreasing, resulting in an equal distribution of water into the guiding vanes and into the runner. The runner itself converts the energy in the water into rotational motion and torque. It is connected to a generator, via a shaft, for electricity production. The draft tube describes a channel with increasing cross section. Its purpose is to convert the kinetic

energy at the runner outlet to pressure energy at the draft tube outlet. Francis turbines are often used and typically operate in a water heads varying from 45 to 400 [m] with flow rates varying from 10 to 700 [m^3/s] (Learnengineering, 2011). The turbines are individually designed for each site to operate with the given water supply and water head at the highest possible efficiency, typically over 90% (Waterturbines, 2016). A relationship curve of the turbine's efficiency with respect to a percentage of the turbine flow is shown in Figure E-15.

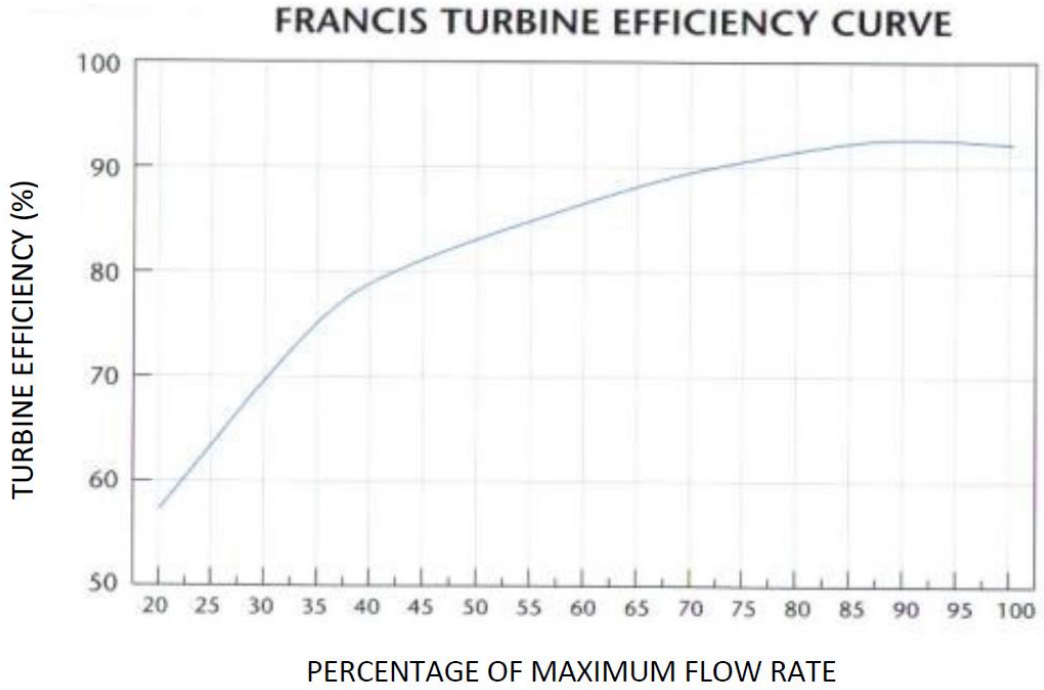

Figure E-15 Typical efficiency curve for Francis turbines (Strathclyde, 2002)

Francis turbines are often used for pumped storage pants, as the turbine can be set in reverse to function as a water pump. This is a big advantage with respect to Pelton- or Kaplan turbines, where a separate pump station would be needed in order to pump the water back in the upper basin.

In a pumped storage plant, power is gained from water running through a turbine, which is attached to a generator. From the generator, the power is transformed from direct- to alternating current using a transformer after which it is delivered to the grid as shown in Figure E-16.

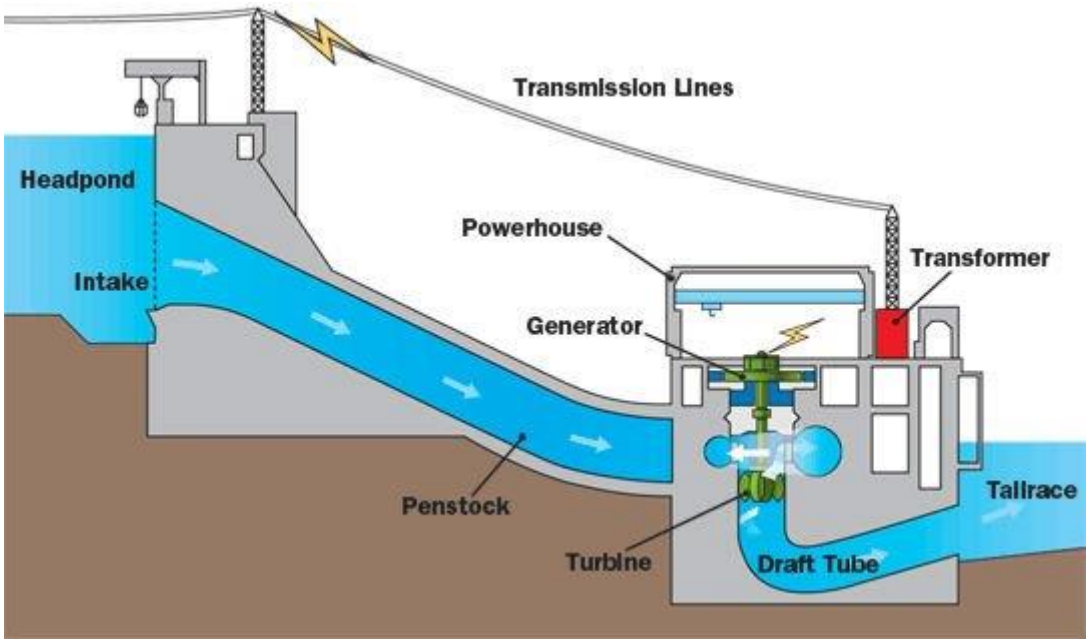

Figure E-16 A Pumped Storage Plant using a Francis turbine (Waterturbines, 2016)

E4 Selection

When selecting a type of turbine for a hydropower system, the water column height or 'head' and the considered flow rate of the system should be taken into account. The three turbine types elaborated in this appendix have their own specific operating range as can be seen in Figure E-17, where the small hydro application range from the supplier Andritz Hydro is shown.

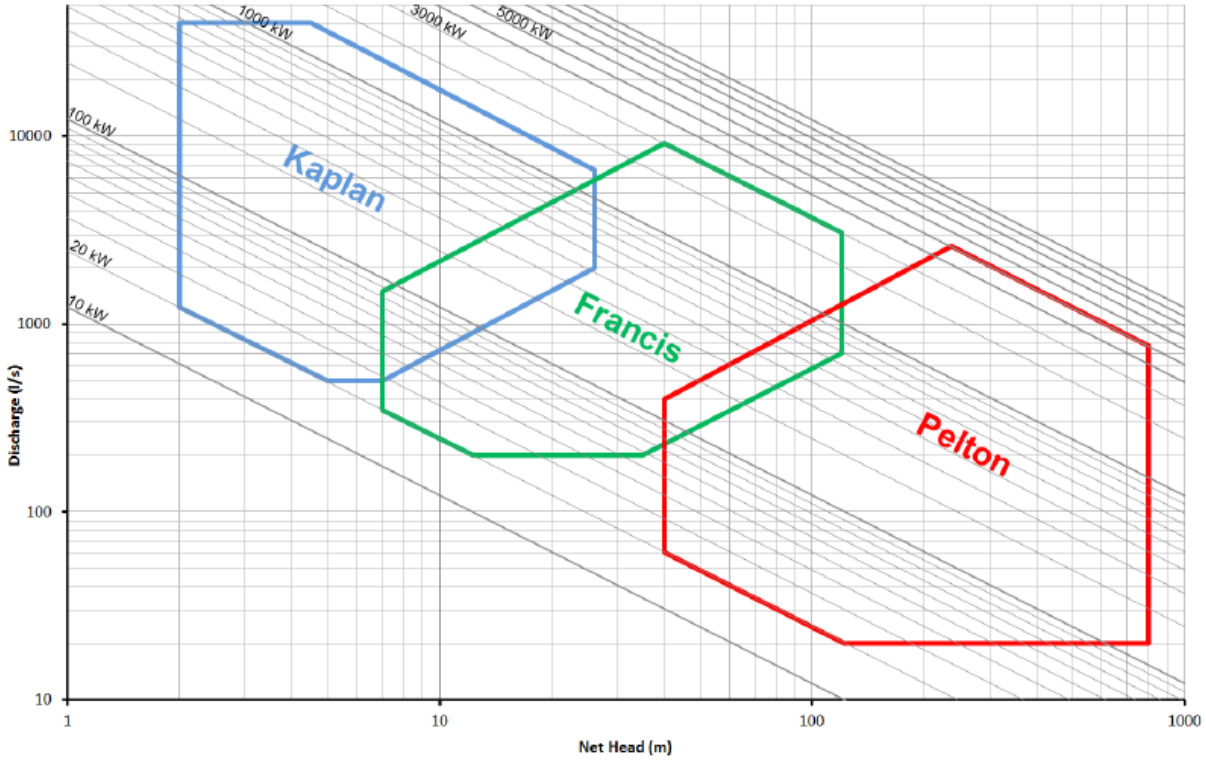

Figure E-17 Application range for Kaplan-, Francis- and Pelton turbines (AndritzHydro, 2015)

In this research, we are focussing on a local energy storage system with a power output in the range of 3 to 30 [kW]. The functional water head of the system depends on the amount of air pressure which is used. The capacity of the considered system goes hand in hand with the time this power can be delivered and therefore with the amount of movable water. The less water is used, the less space is needed to store this water. It is therefore that preference is given to a Pelton turbine, which can generate the most power using a low flow rate, but a large water head. A preferable discharge would be between 5 and 20 litres of water per second and a preferable pressure would correspond with a net water head between 150 and 800 meters.

Reference project

To give a feeling of how such a Pelton turbine would look like, a reference project is shown. An Italian company called 'AC-TEC' installed two hydropower installations which used a Pelton turbine for a small river in the mountainous area of Tirol, Austria. The first turbine has a net head of 157,8 [m], a flow rate of 5,5 [l/s] and a power output of 6 [kW]. The second turbine has a net head of 389,7 [m], a flow rate of 10 [l/s] and a power output of 28 [kW]. Images of the Pelton turbine are shown in Figure E-17 to E-20.

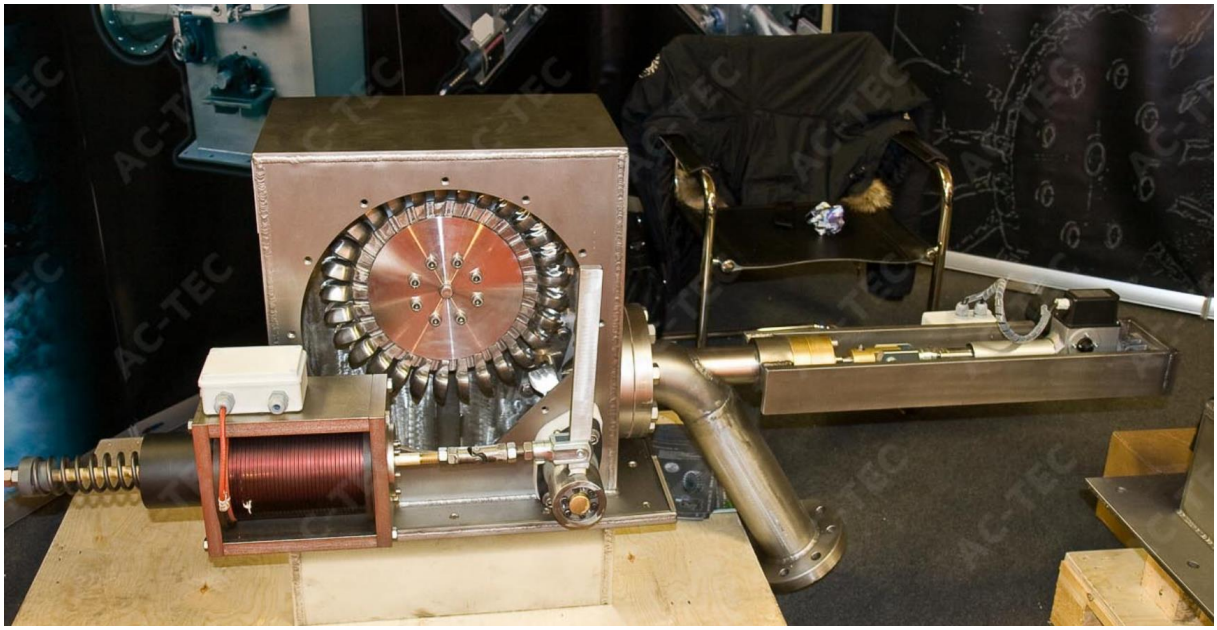

Figure E-18 Pelton turbine 1: 157,8 [m], 5,5 [l/s] and 6 [kW] (AC-TEC, 2015)

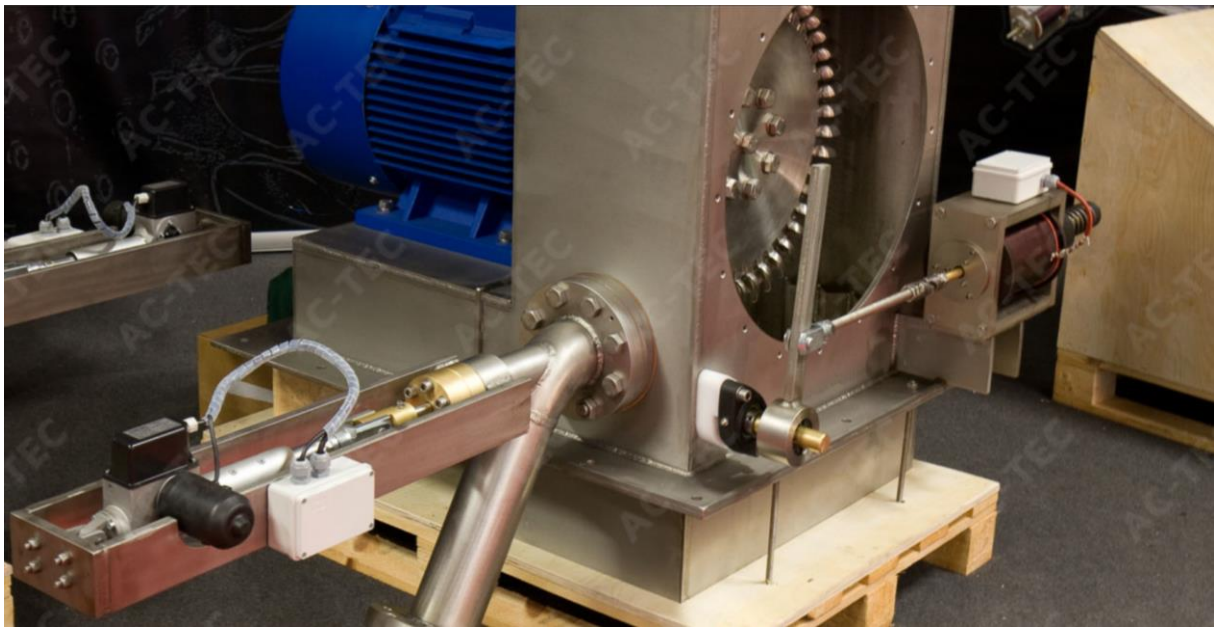

Figure E-19 Pelton turbine 2: 389,7 [m], 10 [l/s] and 28 [kW] (AC-TEC, 2015)

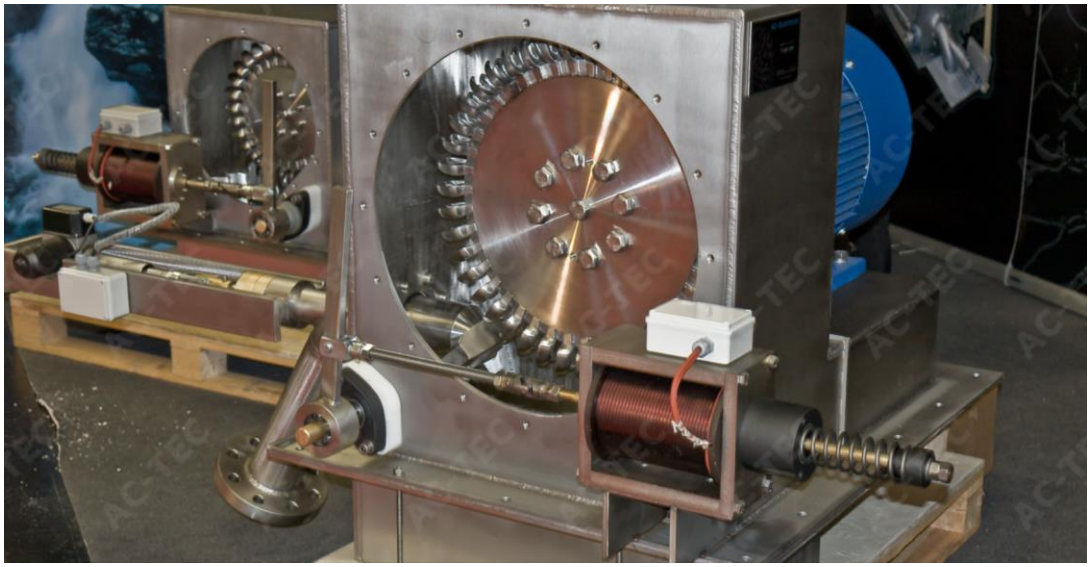

Figure E-20 Both turbines placed on a pallet for transportation (AC-TEC, 2015)

Figure E-21 Both turbines placed on their final position (AC-TEC, 2015)

Appendix F –Water Pumps

The water pump which is used in a pumped hydro system determines the flow rate and the hydraulic height which can be reached by the water. Basically, there are two types of water pumps, namely centrifugal pumps and positive displacement pumps.

F1 Centrifugal pumps

The Centrifugal pump is a very commonly used type of pump. It creates an increase in water pressure by transferring mechanical energy from a motor to the water through a rotating impeller. The water flows from the inlet, which is situated at the centre of the impeller, along the blades towards the outside of the impeller. The centrifugal force increases the water velocity and transforms the kinetic energy of the water into water pressure. The water pressure then results in a certain flow. A basic diagram of such a centrifugal pump is shown in Figure F-1.

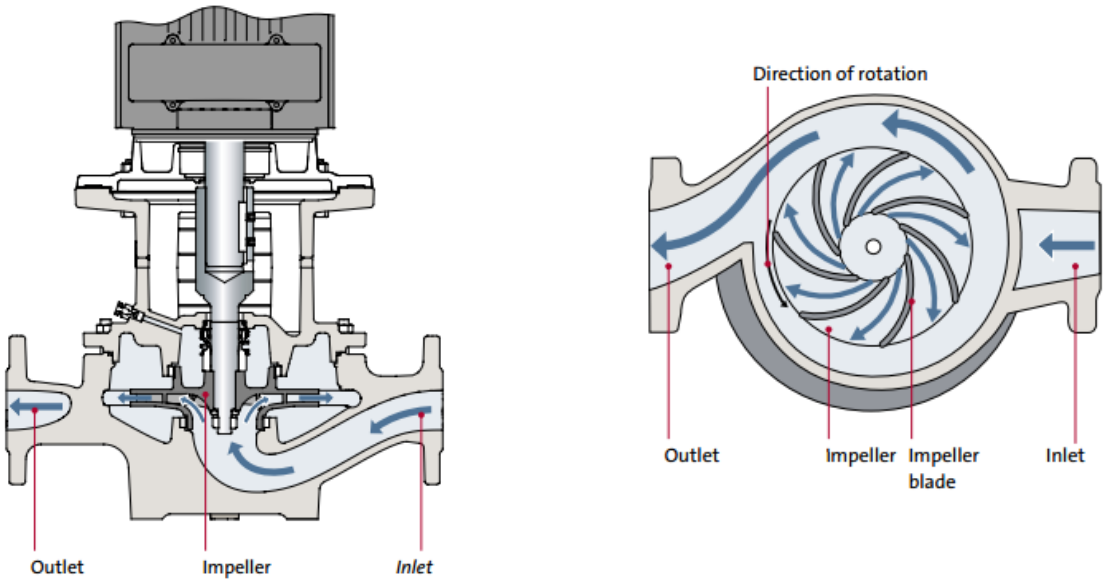

Figure F-1 Basic diagram of a centrifugal pump (Allpumps, 2016)

The performance of a centrifugal pump can be shown by a set of performance curves:

The system- and QH-curve

The system curve is displaying the amount of resistance which the system will give at a certain flow rate. This includes the (constant) static head of the system as well as the resistance or friction head which depends on the flow rate. The QH-curve shows the amount of pressure, measured in head difference 'H', that a certain pump is able to perform at a given flow rate 'Q'. Here, the head is measured in meter water column and the flow rate in [m3/h]. A typical system- and QH-curve for a centrifugal pump are shown in Figure F-2.

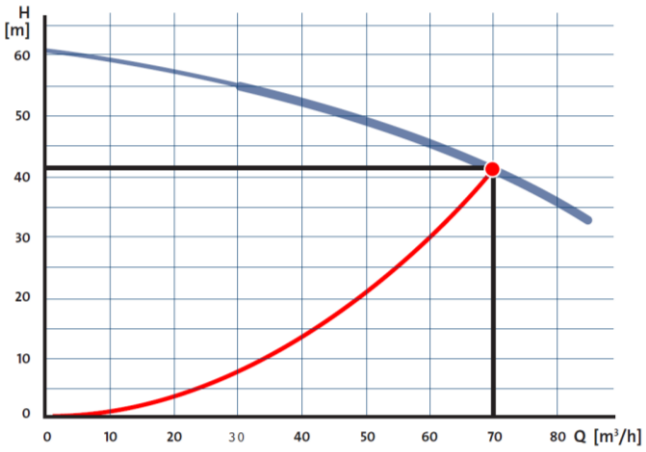

Figure F-2 A typical system- (in red) and QH-curve (in blue) for a centrifugal pump (Ecademy, 2016)

The efficiency curve

The efficiency of a pump is determined by the power the pump delivers to the water and the power input it needs. Centrifugal pumps typically have a certain 'best efficiency point' where the maximum efficiency is reached. This point, depending on the flow rate and head difference, is important when choosing a particular pump. An efficiency curve of a typical centrifugal pump is shown in Figure F-3. Note that this curve does not include the efficiency of the motor which is driving the pump.

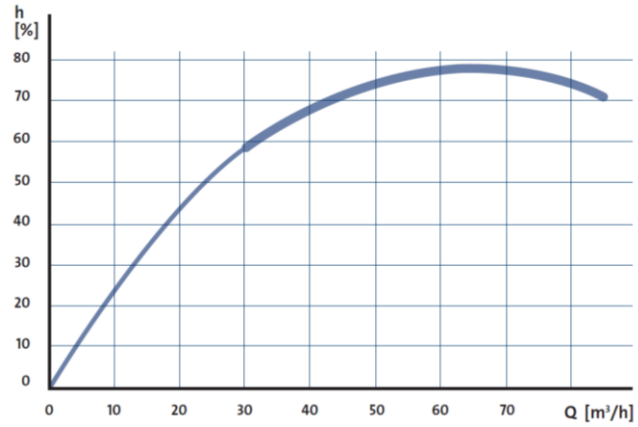

Figure F-3 The efficiency curve of a typical centrifugal pump (Ecademy, 2016)

The power consumption curve

The amount of power that a pump is consuming also depends on the desired flow rate of the water. At larger flow rates, more power is being consumed by the pump. A relationship curve between the flow rate and the power consumed is shown in Figure F-4. Here, the power value increases when the flow increases.

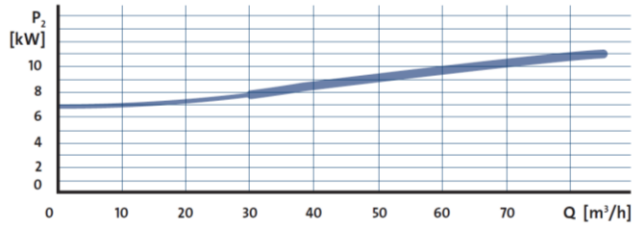

Figure F-4 The power consumption curve of a typical centrifugal pump (Ecademy, 2016)

Net Positive Suction Head (NPSH) curve
The NPSH value of a pump depends on the flow rate and displays the minimum pressure that must be present at the suction side of the pump to avoid cavitation. NPSH values are measured in [m]. When the flow rate increases, the NPSH value also increases as is shown in Figure F-5.

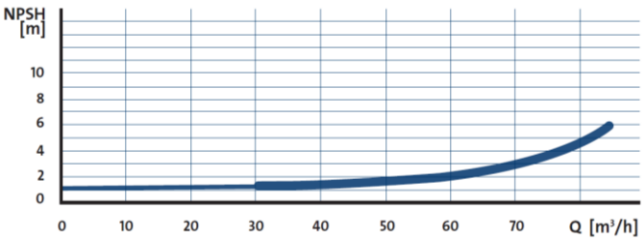

Figure F-5 The NPSH curve of a typical centrifugal pump (Ecademy, 2016)

An impression of a centrifugal pump is shown in Figure F-6.

Figure F-6 An impression of a centrifugal pump (Allpumps, 2016)

F2 Positive displacement pumps

Positive displacement pumps operate by forcing a fixed volume of water from the inlet section into the discharge zone of the pump. There are many kinds of positive displacement pumps, including gear pumps, piston pumps and vane pumps.

F2.1 Gear pumps

Gear pumps use one or two rotating gears which take the water in at the suction side of the pump, to create a vacuum, and force the water to the discharge side. The spaces between the gear teeth transport the water along the outer perimeter of the housing towards the outlet. The gears then come in contact, forcing the water out under a high pressure. A basic diagram of a gear pump is shown in Figure F-7.

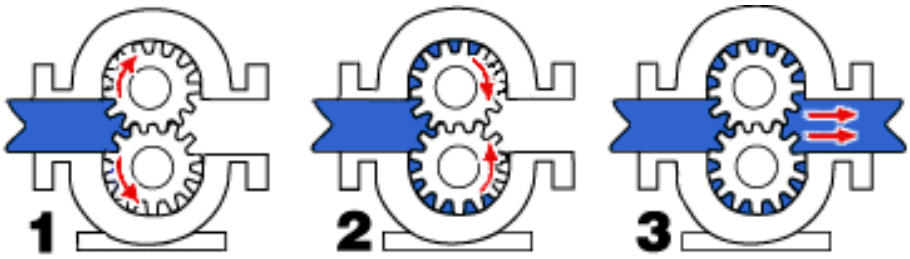

Figure F-7 Basic diagram of a gear pump (Pumpschool, 2014)

Gear pumps can come with spur, helical and herringbone gears. The latter two typically offer a smoother flow than spur gears, making them very suitable for large-capacity gear pumps. The gears have small tolerances and shaft support of both sides of the gears. This makes that they are rather silent pumps and well suitable for creating high pressures. Typically, gear pumps have an overall efficiency, which is little influenced by pressure change, of around 85% (Machinerylubrication, 2016). This overall efficiency includes the volumetric efficiency, based on the internal leakage, and the mechanical efficiency, which is determined by the mechanical and water friction. The efficiency of the motor that is driving the pump is not taken into account. Figure F-8 shows a gear pump with helical gears where one gear is driven. This gear drives the other one when it rotates.

Figure F-8 An impression of a gear pump with helical gears (BoschRexroth, 2016)

F2.2 Piston pumps

Piston pumps typically use rotary shaft motion converted into axial motion of a piston to produce water flow. As the piston extends, partial vacuum created in the pump chamber draws water through the inlet or suction valve into the chamber. The volume of water drawn into the chamber is then forced out the pump through the discharge valve by the piston. As the piston retracts, the suction of the water closes the discharge and opens the suction valve, letting the same amount of water run into the chamber again. A basic diagram of a piston pump is shown in Figure F-9.

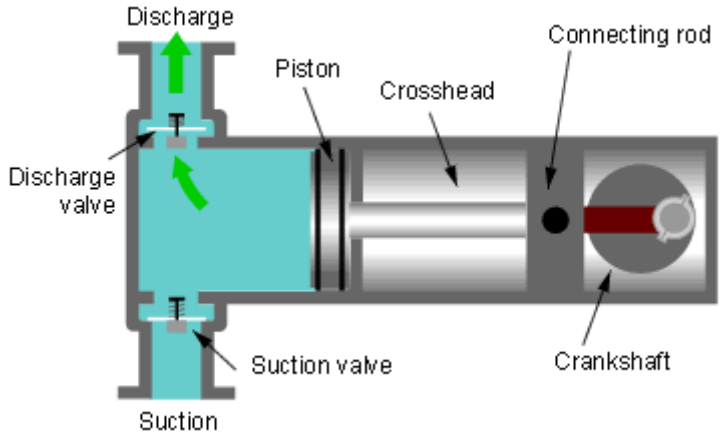

Figure F-9 Basic diagram of a piston pump (Stackexchange, 2016)

Piston pumps can be provided with multiple pistons. Modifications such as radial or bent-axis piston pumps are also possible. For this latter one, the plane of rotation of the pistons is at an angle, making the distance between each one of the multiple pistons and the valving surface change continually during rotation. Each piston moves away from the valving surface during one half of the rotation, and during the other half it moves towards it. Bent-axis pistons are one of the most efficient piston pumps with an overall efficiency reaching up to 92% (Machinerylubrication, 2016). An impression of a bend-axis piston pump is shown in Figure F-10.

Figure F-10 An impression of a bend-axis piston pump (Hydrotech, 2007)

F2.3 Vane pumps

Vane pumps typically use a slotted rotor to create water flow. The rotor is eccentrically supported in a circular shell and sealed waterproof by two side plates. Vanes or blades that fit within the slots of the rotor are used to push the water and create flow. As the rotor rotates and water enters the pump, the vanes eject out of their slots and move the water. The tight seals of the vanes, rotor, shell, and side plates are the key to the good suction characteristics common to the vane pumping principle. The shell forces the water into the pumping chamber, where the rotor vanes are ejected from the water inlet to its discharge valve. As the rotor continues rotating, the vanes sweep the water into the discharge valve after which the vanes are pushed back into the rotor. A Basic diagram of a vane pump is shown in Figure F-11.

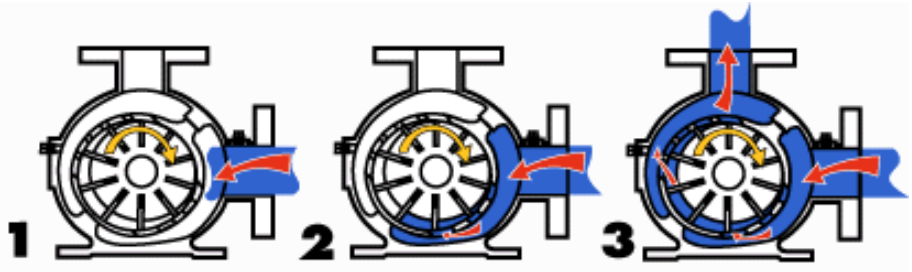

Figure F-11 Basic diagram of a vane pump (Pumpschool, 2014)

Vane pumps are often used for applications within the LPG, refined fuels and chemical industry. The easy maintenance, high reliability and relatively low cost are a great advantage of this type of pump. The maximum pressure which can be reached is, however, relatively low (order of magnitude: 20 [bar] (Vikingpump, 2015)) and the overall efficiency can reach up to 85% (Machinerylubrication, 2016). An impression of a vane pump is shown in Figure F-12.

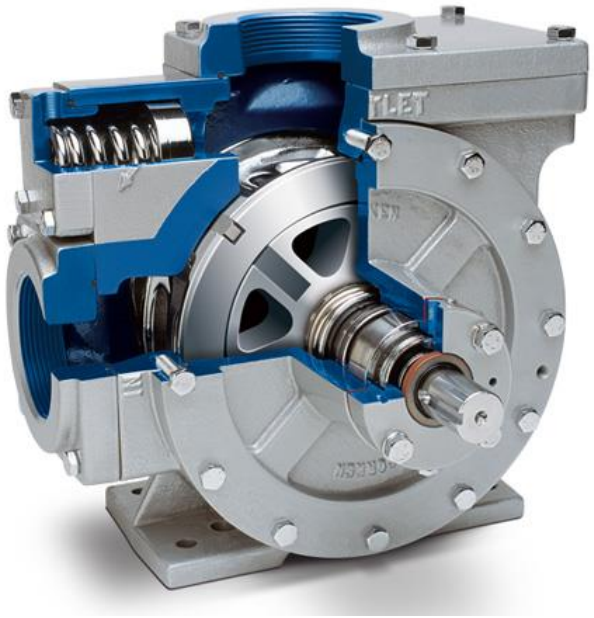

Figure F-12 An impression of a vane pump (Corken, 2016)

F3 Selection

Before selecting a type of pump for the pumped hydro system, an overview of the main differences between centrifugal- and positive displacement pumps is given.

Pressure dependence on flow rate

Centrifugal- and positive displacement pumps show a very different behaviour related to the pressure dependency on the flow rate. A centrifugal pump has varying flow depending on pressure or head, whereas the positive displacement pump has more or less constant flow regardless of the pressure. Typical performance curves of a centrifugal and a positive displacement pump are shown in Figure F-13.

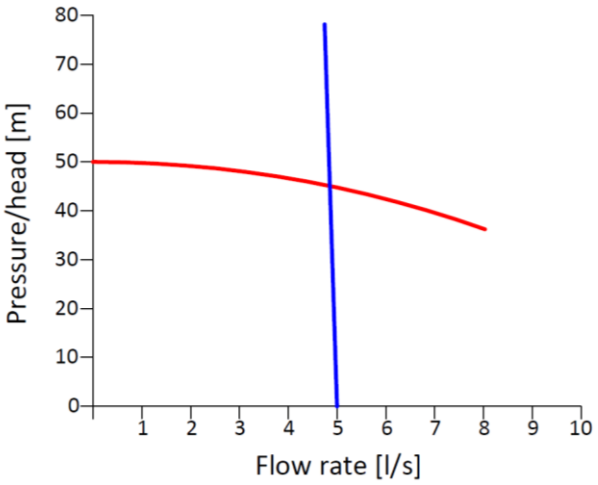

Figure F-13 Performance curves of a typical centrifugal (in red) and a typical positive displacement pump (in blue), based on (Pumpschool, 2014)

Efficiency dependence on pressure

The behaviour when considering mechanical efficiency is very different for centrifugal pumps as it is for positive displacement pumps. Changes in pressure have little effect on positive displacement pumps but a drastic effect on centrifugal pumps. Typical efficiency curves of a centrifugal and a positive displacement pump are shown in Figure F-14.

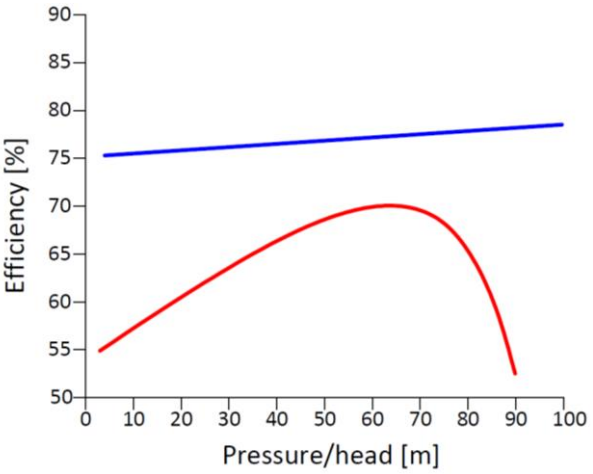

Figure F-14 Efficiency curves of a typical centrifugal (in red) and a typical positive displacement pump (in blue), based on (Pumpschool, 2014)

Inlet conditions

Another consideration is creation of suction. Centrifugal pumps cannot create suction, which means the water must run in the pump inlet by itself for the pump to work. Positive displacement pumps are able to create suction at the inlet valve. As the considered design in this research involves large pressure differences and underground water tanks where suction of water by the pump would be beneficial, a positive displacement pump will be used. These pumps can function very well under large

pressures and pressure changes. Therefore, the variant of a bend-axis piston pump has the preference, as this particular pump has a rather high efficiency and can operate under high pressures. A catalogue of the American manufacturer Parker shows a number of bend-axis piston pumps which would work for the LHES system. Three of Parker's F11-010 pumps are chosen to operate. These pumps have a combined capacity of 5 [l/s] and can easily reach the desired pressure of 60 [bar]. An impression of such a bend-axis piston pump is shown in Figure F-15. These pumps are rather small as Figure F-16 shows. Further details of these pumps are shown in Figure F-17

Figure F-15 Impression of a F11-010 pump (Parker, 2016)

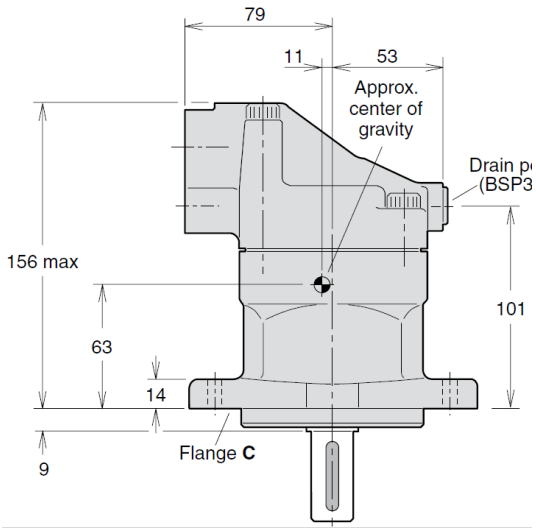

Figure F-16 Dimensions of a F11-010 pump (Parker, 2016)

Catalogue HY30-8249/UK
Specifications

Hydraulic motor/pump
Series F11

Frame size F11	**-005**	**-006**	**-010**	**-012**	**-014**	**-019**
Displacement [cm³/rev]	4.9	6.0	9.8	12.5	14.3	19.0
Operating pressure						
max intermittent[1] [bar]	420	420	420	420	420	420
max continuous [bar]	350	350	350	350	350	350
Motor operating speed [rpm]						
max intermittent [1]	14 000	11 200	11 200	10 300	9 900	8 900
max continuous [3]	12 800	10 200	10 200	9 400	9 000	8 100
min continuous	50	50	50	50	50	50
Max pump selfpriming speed [2]						
L or R function; max [rpm]	4 600	–	4 200	3 900	3 900	3 500
Motor input flow						
max intermittent[1] [l/min]	69	67	110	129	142	169
max continuous [l/min]	63	61	100	118	129	154
Drain temperature[3], max [°C]	115	115	115	115	115	115
min [°C]	-40	-40	-40	-40	-40	-40
Theoretical torque at 100 bar [Nm]	7.8	9.5	15.6	19.8	22.7	30.2
Mass moment of inertia						
($x10^{-3}$) [kg m²]	0.16	0.39	0.39	0.40	0.42	1.1
Weight [kg]	4.7	7.5	7.5	8.2	8.3	11

1) Intermittent: max 6 seconds in any one minute.
2) Selfpriming speed valid at sea level. Find more info on page 11

Figure F-17 Table with characteristics of Parker's F11 bend axis piston pump series (Parker, 2016)

Appendix G – Drawings

To give a better understanding of how the LHES system works, the technical drawings, P&ID and 3d drawings are shown in this appendix. Figure G-1 shows the pile- and installation plan of the LHES system, Figure G-2 shows the piping and instrumental diagram and Figure G-3 to Figure G-7 show a 3D impression of the system.

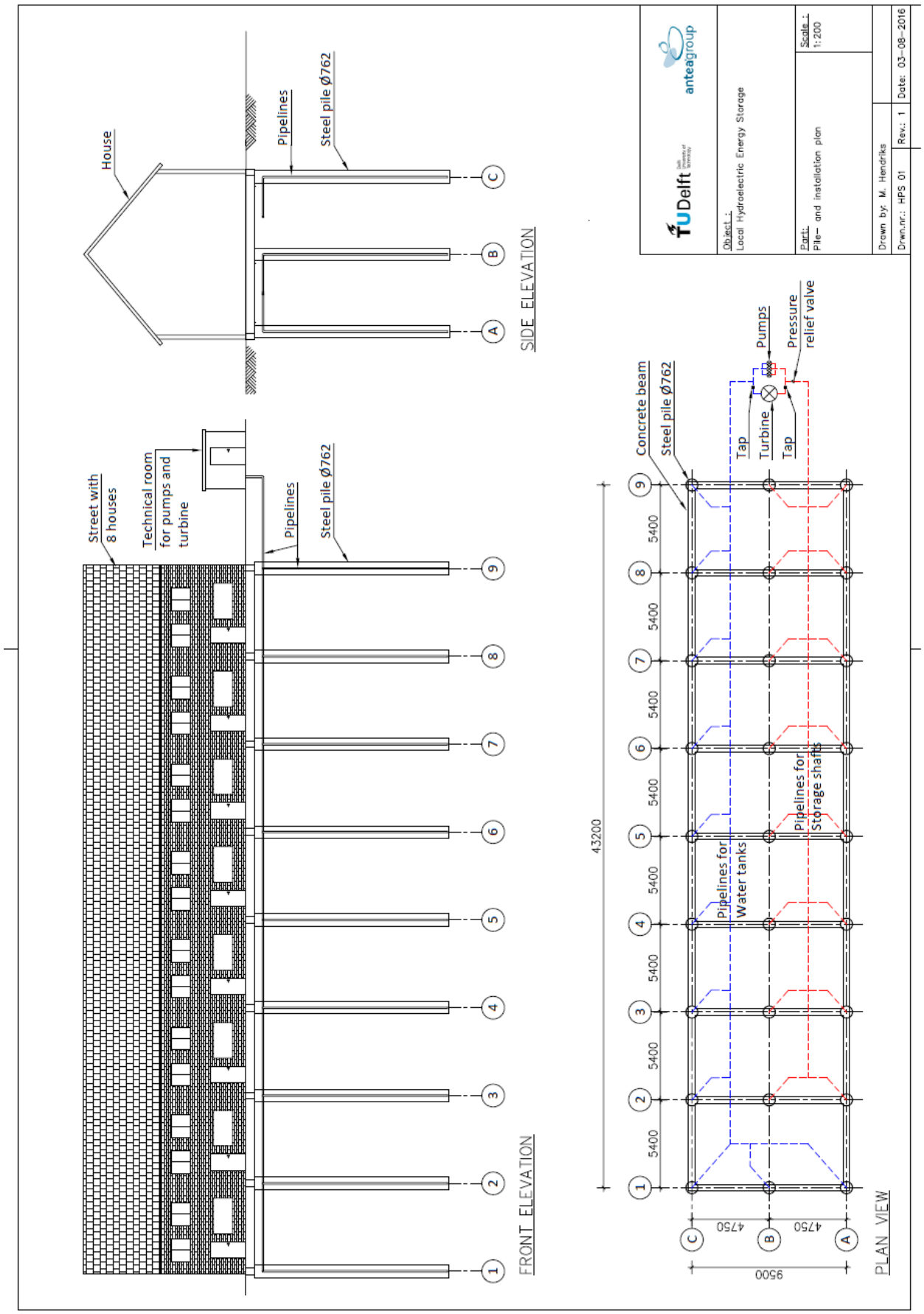

Figure 0G-1 Pile- and installation plan of the LHES system

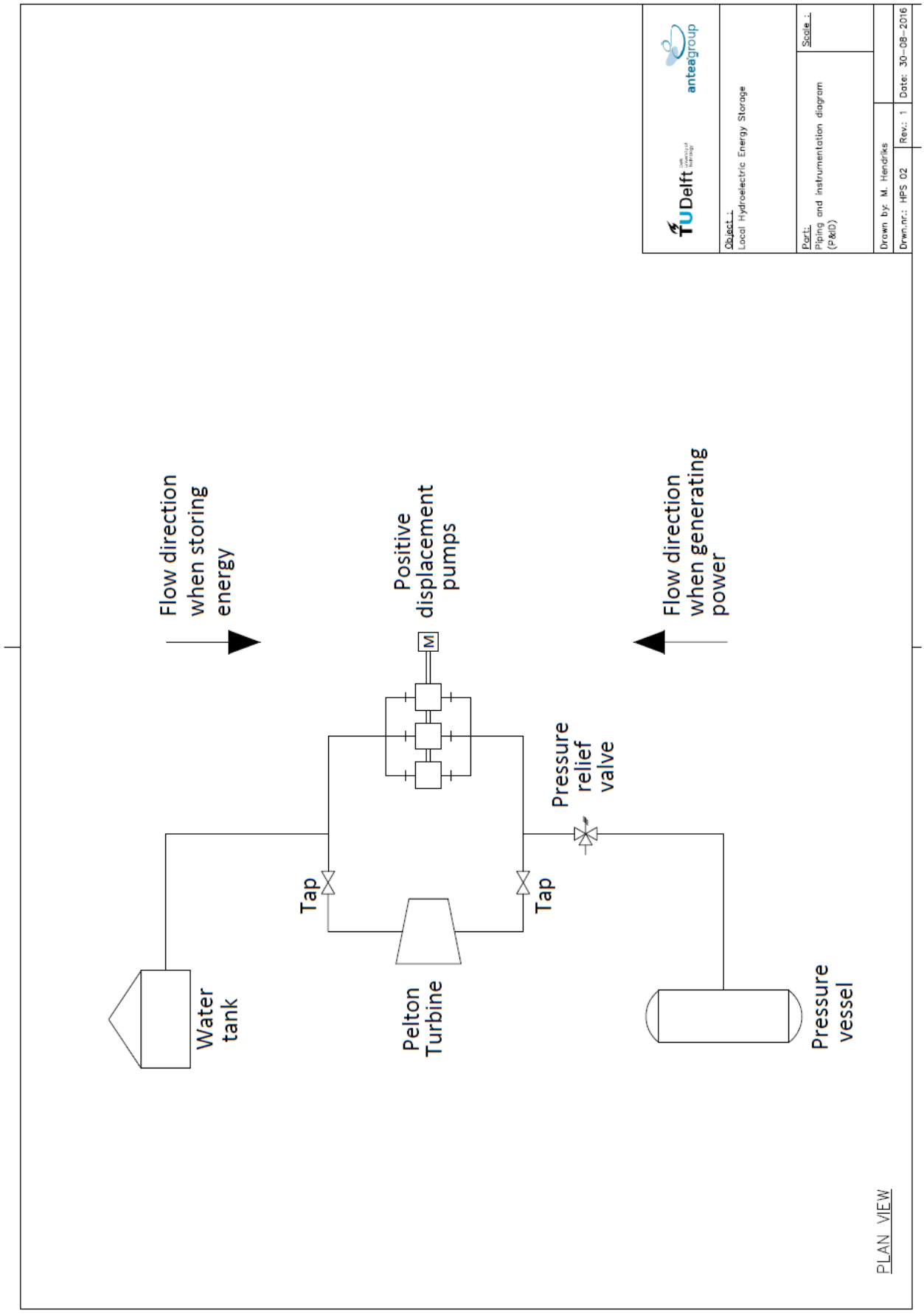

Figure 0G-2 Piping and Instrumental Diagram of the LHES system

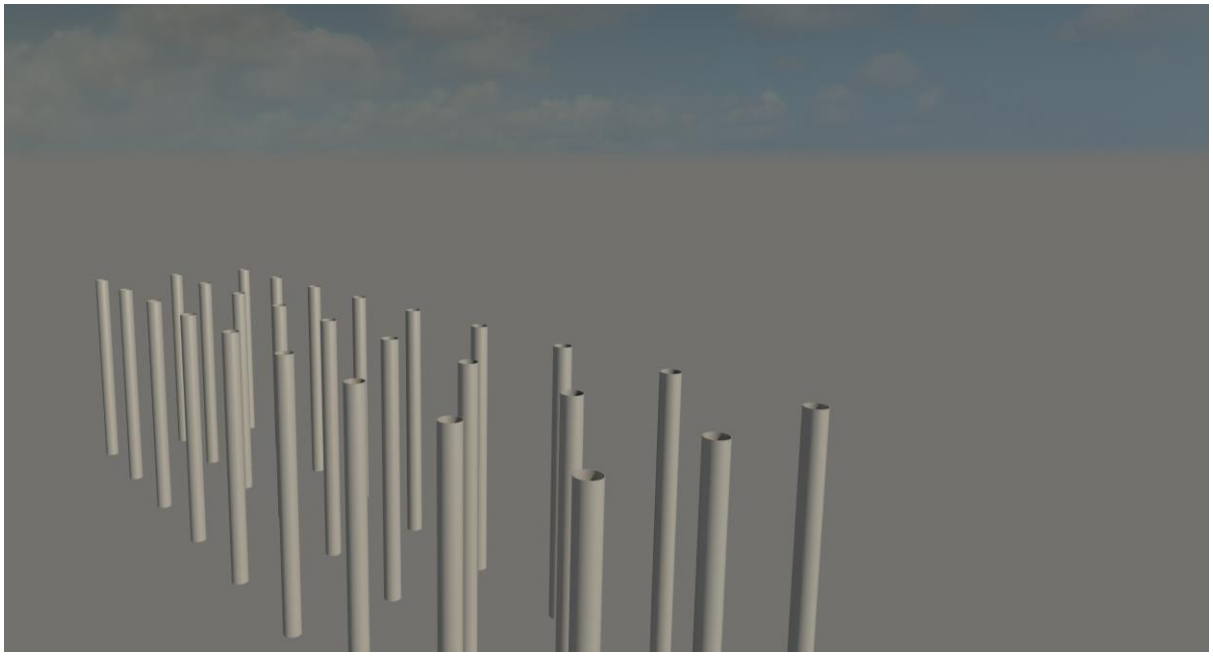

Figure 0G-3 Impression of the 27 piles being installed

Figure 0G-4 Impression of the piping and installations being installed

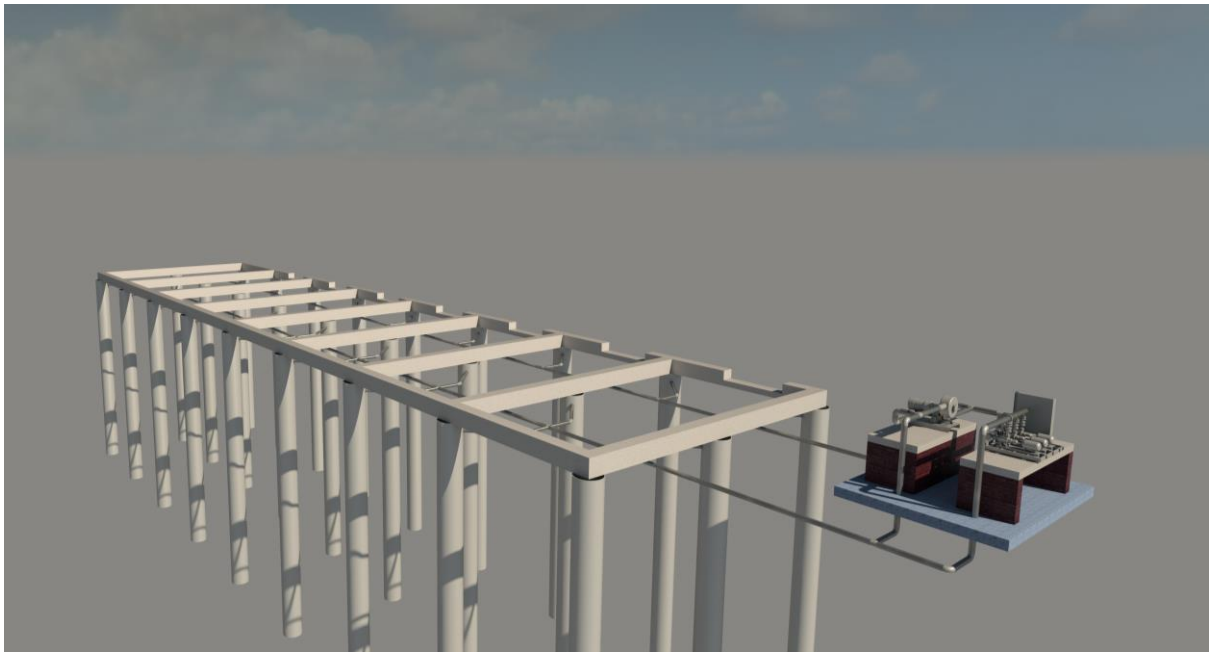

Figure 0G-5 Impression of the concrete beams on top of the piles

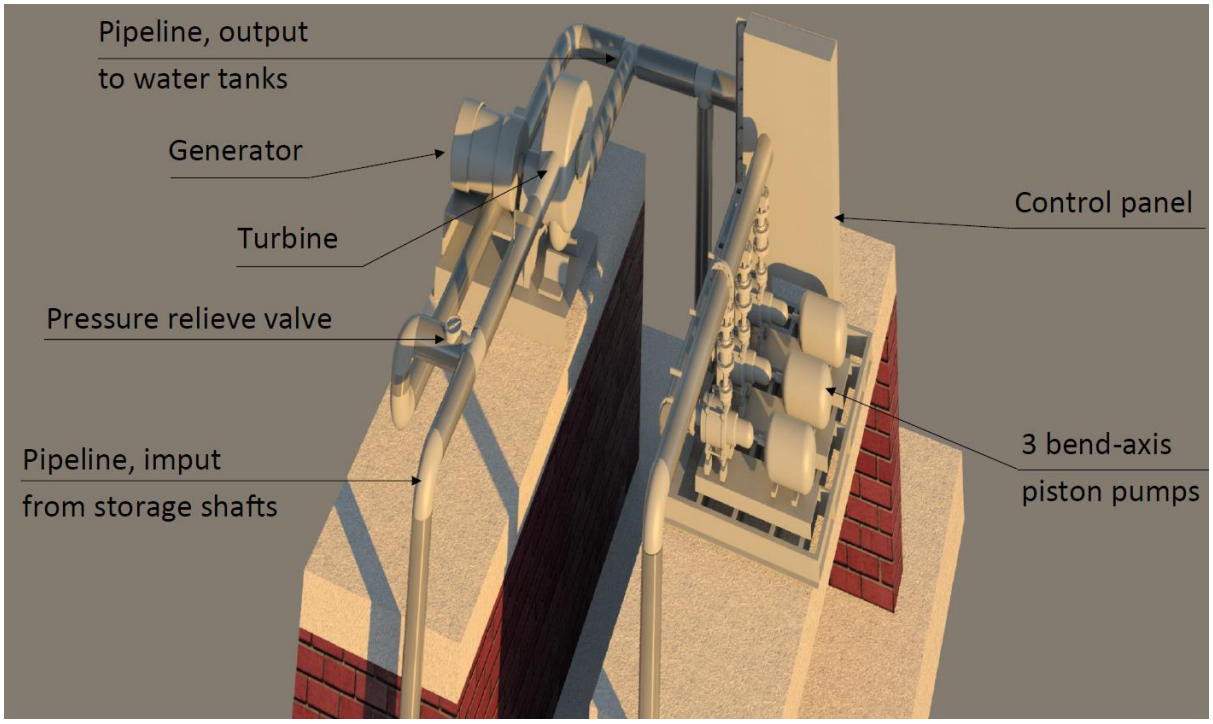

Figure 0G-6 Detailed 3D impression of the installations

Figure 0G-7 Impression of the LHES system with 8 houses on top

Appendix H – Other applications

The number of variations to apply a Local Hydroelectric Energy Storage (LHES) system would be endless. Besides the applications mentioned in Chapter 4.3 of this research, a number of other applications is briefly shown in this appendix. The goal of this appendix is to give an idea about the various ways a LHES system could be applied. One may think of an application to minimize supply fluctuations of wind turbine (Figure H-1) or an application in a so called Tidal Bridge (Figure H-2 and H-3), which is a concept where Antea Group is working on. The dimensions and (water) volumes shown below are estimated using the capacity calculations of this research.

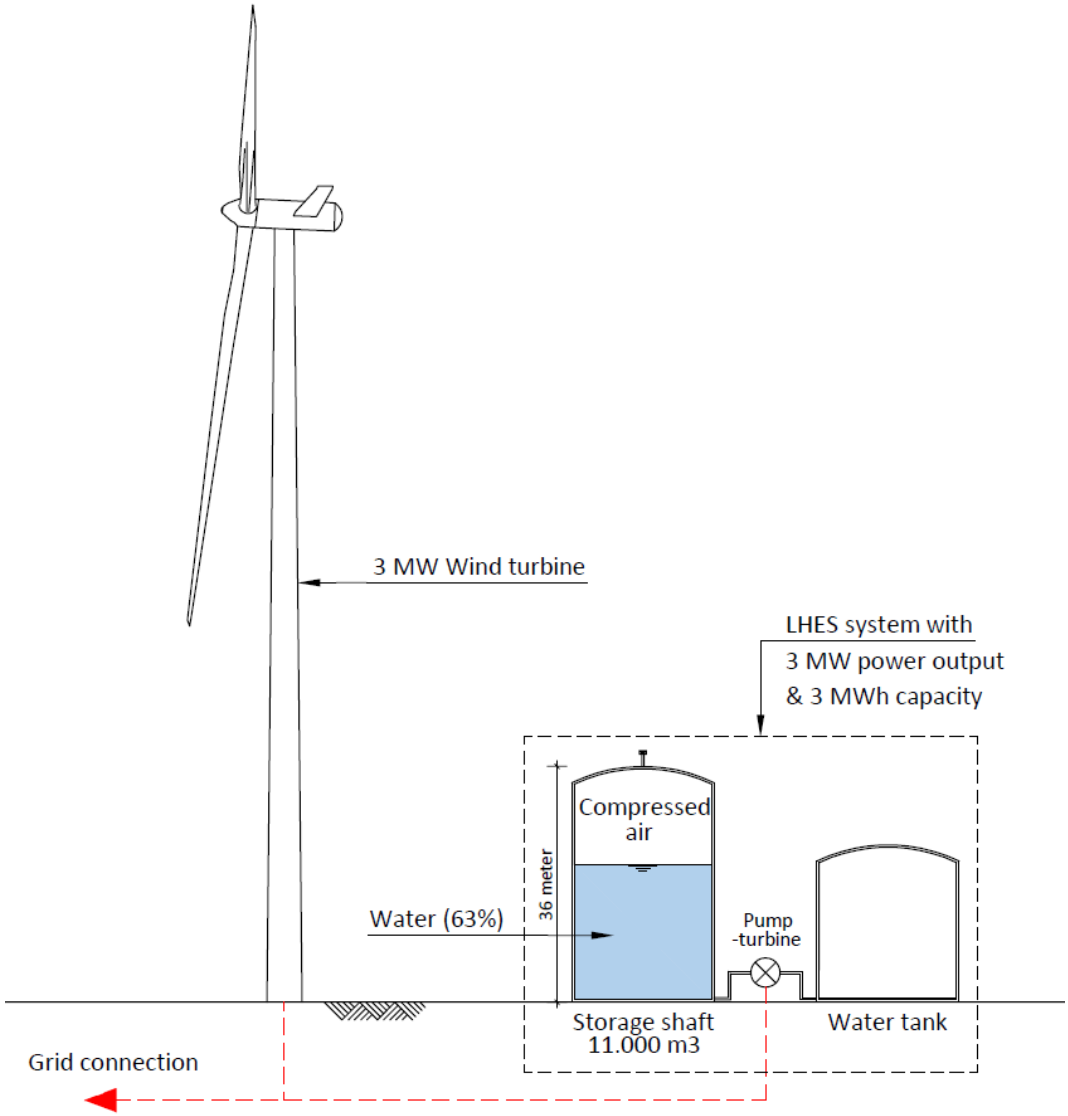

Figure 0H-1 Impression of a LHES system applied to store wind powered energy

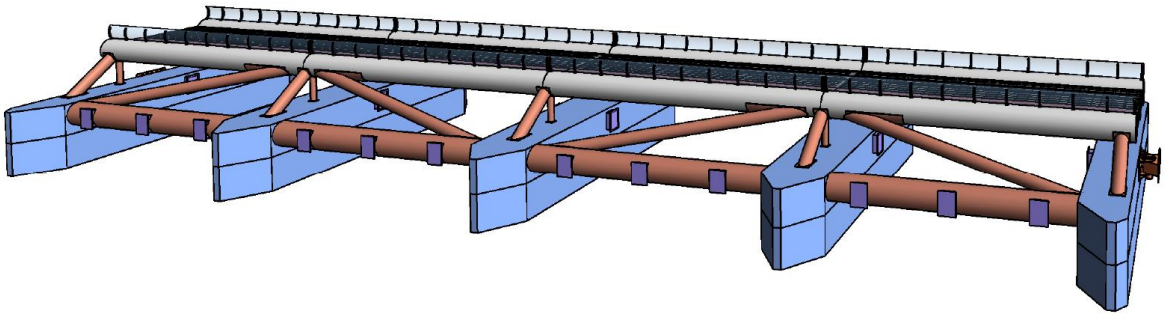

Figure 0H-2 Impression of a (floating) tidal bridge (Antea Group)

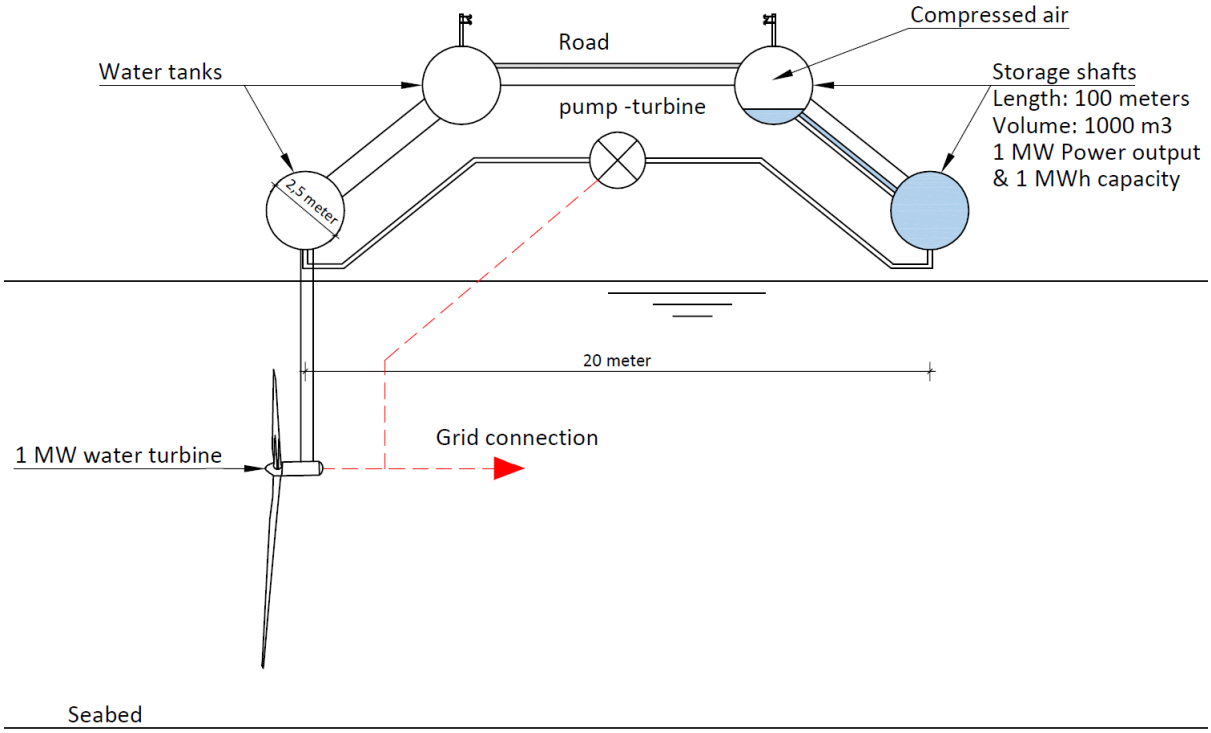

Figure 0H-3 Cross section showing a LHES system integrated in a tidal bridge